Utilisation of geothermal energy

Aalborg University
Study Board of Energy
M.Sc thesis
Lea Bandholtz Jørgensen
June 1st 2017

Board of Studies of Energy

Title:	Utilisation of geothermal energy
Semester:	10^{th}, Spring Semester 2017
Semester theme:	Master thesis
Project period:	01.02.17 to 1.06.17
ECTS:	30
Supervisors:	Kim Sørensen and Thomas Condra
Project group:	TEPE4-1010

Lea Bandholtz Jørgensen

Copies:	5
Pages, total:	86
Appendices:	3
Supplements:	0

SYNOPSIS:

This project concerns modelling a geothermal power plant which can be used in most places around the world in geothermal areas with high enough temperatures for electricity generation.
Three types of units was modelled. The binary cycle, the single flash and the double flash. The units was modelled in such a manner that it can be utilised independent of geothermal field.
A parameter optimisation of the three unit was conducted. The pressures in the units was optimised to find the configurations which would give the highest electrical power output. For the binary cycle unit this was found to be 20 bar in the evaporator and 4.65 bar in the condenser which gave 8.64 MW_e. For the single flash the power output was 14.3 MW_e, where the separator pressure was 3.21 bar and the condenser pressure was 0.1 bar. The double flash optimisation gave a power output at 52.4 MW_e at a HP separator pressure at 12.7 bar, a LP separator pressure at 2.67 bar and the HP and LP condenser pressure was 0.1 bar.
The optimised unit configurations was used to design at power plant. This was done with one binary cycle, one single flash with a bottom binary cycle and a double flash with a bottom binary cycle. District heating was also added to this model. The results for the power plant model was 91.8 MW_e and 610 MW_{th}. This is 21.4 MW_e higher than if the units was not combined.

By signing this document, each member of the group confirms that all participated in the project work, and thereby all members are collectively liable for the content of the report. Furthermore, all group members confirm that the report does not include plagiarism.

Executive Summary

Geothermal power is a renewable energy source with a high potential for utilisation in areas with both high underground temperature gradient, but also with a lower temperature gradient. There are different ways to utilise the geothermal energy. The most common is the hydrothermal geothermal resource. In this report a power plant model for this type of resource is investigated. There is many ways to design a power plant for this type of resource, but mostly there are three type of units used, the binary cycle, the single flash and the double flash. The designs of the units and how they are combined depends on the geothermal field where the power plant is placed.

A state-of-the-art was conducted to investigate how the utilisation of geothermal energy has progressed from 1980 to 2015. It was found that over this period of time the utilisation of geothermal energy has increased every year. It was also found that more and more countries are utilising geothermal energy for electrical power, with USA as the country which utilises most geothermal electrical power. Furthermore ten power plants was investigated to give an insight of how geothermal power plants are design around the world. It was found that the designs consist of the units, but the unit design varied from geothermal field to geothermal field.

The system in this report is a hypothetical geothermal field which is placed in the Hengil mountains in Iceland. The geothermal field consist of 26 wells which is utilised in three different units, a binary cycle unit where eight wells is directed to, a single flash unit where ten wells is directed and a double flash unit where eight wells are directed to. The components used in the units was investigated and modelled to be able to formulate the units.

There has been formulated three model for the units, one for each type. The models has been made simple to ensure that the unit can be utilised around the world. A parameter optimisation was conducted to find the largest possible power output, the pressures was optimised to accomplish this. In the binary cycle unit the evaporator and condenser pressure was optimised. This resulted in a power output at 8.64 MW_e at the pressure of 20 bar and 4.65 bar respectively. In the single flash unit the separator and condenser pressure was optimised and this resulted in a power output of 14.3 MW_e at a pressure of 3.21 bar and 0.1 bar respectively. The last model optimised was the double flash unit, in which four pressures was optimised. These were the HP separator, the LP separator, the HP condensers and the LP condensers. When optimised the total power output was 52.4 MW_e at the pressures at 12.7 bar, 2.67 bar, 0.1 bar and 0.1 bar respectively.

As the configurations of the units was found these was used to design a combined power plant consisting of three binary units (one for low temperature, one bottom unit for the single flash and one bottom unit for the double flash), one single flash and one double flash. District heating was included in this model to replace some of the cooling towers. The power plant model was found to have a total power output of 91.8 MW_e and 610 MW_{th}. The electrical power output was 21.4 MW_e larger than if the units did stand alone.

It was investigated whether geothermal energy could be used as an electricity source in Denmark, as geothermal energy presently is utilised for district heating, three places in Denmark. It was found that there was a possibility, as the temperature gradient in Denmark is between 22°C/km and 35°C/km, and there are possible reservoirs under

Denmark in depths that would give a geothermal fluid which could be utilised. However it is uncertain if the permeability is high enough at the needed depths to be able to extract the geothermal fluid.

Preface

This report is written by a 4. semester master student studying *Thermal Energy and Process Engineering* at Aalborg University. The project investigates the utilisation of geothermal energy. This project focuses on a model that can be utilised in different geothermal fields.

The report will include background knowledge of theory, model development, simulation and optimisation results. It will contain the following:

- Introduction
- State-of-the-art
- System presentation
- Model
  - Binary cycle unit
  - Single flash unit
  - Double flash unit
  - Power plant
- Project analysis and future work

Reading Instructions

In the beginning of the report there is a nomenclature for the variables and the respective units following a list of abbreviations. In the report, the literature utilised is listed at the end of the report on page 75. In the text, the references are listed by the Harvard method, where it is shown as (Author, Year). The references in the bibliography are given in the following manner:

Author, Title, Publisher, Journal, Year, URL

All the equations, figures and tables are numbered in correspondence with their respective chapter number. This means that the first figure in Chapter 2 is numbered 2.1 and the next figure is numbered 2.2. Explanatory captions can be found beneath the figures and tables. When a figure, created by others than the authors of this project, has been altered, the reference will include the word *adapted*. Several appendices are included in the report and are listed after the bibliography.

The numbered subscripts indicated stages in the components and the models. Furthermore, when referring to a billion in this report the short scale is used, where a billion is equal to 10^9.

Nomenclature

Symbol	Description	Unit
A	Area	m^2
B	Width	m
b	Fin height	m
c_p	Specific heat at constant pressure	J/(kg K)
D	Distance	m
d	Diameter	m
f	Friction factor	-
h	Enthalpy	J/kg
L	Length	m
ℓ	Fin spacing	m
$\dot{m}$	Mass flow	kg/s
N	Number	-
P	Pressure	Pa
p	Tube pitch	-
$\dot{Q}$	Heat transfer rate	W
Re	Reynolds number	-
s	Entropy	J/(kg K)
T	Temperature	K
U	Overall heat transfer coefficient	$W/(m^2\ K)$
$\dot{V}$	Volumetric flow	m^3/s
v	Velocity	m/s
W	Power	W
x	Steam quality	kg/kg

Subscripts

Symbol	Description
amb	Ambient
air	Air
CT	Cooling Tower
CW	Cooling Water
c	Critical
cond	Condenser
e	Electrical
f	Fluid
fan	Fan
fin	Fins
i	In
LMTD	Logarithm mean temperature difference
o	Out
p	Pump
req	Required
s	Isentropic
spec	Specific

t	Turbine
t/r	Tubes per row
th	Thermal
tot	Total

Superscripts

Symbol	Description
g	Gas
l	Liquid

Greek Letters

Symbol	Description	Unit
η	Efficiency	-
η_{II}	Second efficiency	-
ρ	Density	kg/m^3
τ	Thickness	m

Abbreviations

Abbreviation	Description
BC	Binary Cycle
DF	Double Flash
DH	District Heating
DS	Dry-Steam
DHGE	Deep Hydrothermal Geothermal Energy
FC	Fluid Collector
G	Generator
HDR	Hot Dry Rock
HGR	Hydrothermal Geothermal Resource
HP	High Pressure
LP	Low Pressure
NCG	Non-Condensable Gasses
PH	Power House
ORC	Organic Rankine Cycle
S	Separator
SC	Steam Collectors
SF	Single Flash
TF	Triple Flash

Contents

CHAPTER 1

Introduction

The worldwide climate changes forces the worlds population to think of new directions regarding energy sources. Today renewable or so-called green energy is being utilised more often. According to REN21 (2016) the worldwide capacity of renewable energy has increased over the last few years. In 2015 the capacity was 1,848 GWe of power and 435 GW_{th} of thermal energy. This is an increase from 2014 at 8.6% and 6.0% respectively. The increase in renewable energy over the past 10 years gives research scientists and goverment an incitement to increase the capacity of renewable sources even more. The prospects for the future energies predict an increase in the renewable energy capacity, for both the optimistic and the most conservative predictions (Marinot, 2013).

Due to a worldwide increase in energy demand from 6.18 TW in 1971 to 12.49 TW in 2014, a larger renewable energy capacity is needed (International Energy Agency, 2016). The increase in the energy demand has been steady for the entire period, 1971-2014, except for 2008 where the financial crisis hit, but in 2009 the demand increased again.

The main renewable energies that is utilised on a global basis is hydropower and windpower, which represents 1,497 GW in 2015. According to REN21 (2016), all the different renewable energy sources have had an increase in capacity from 2014 to 2015. The percentage increase can be seen in table 1.1.

Energy source	**2014 [GW]**	**2015 [GW]**	**Percentage increase**
Hydro power	1,036	1,064	2.70%
Bio power	101	106	4.95%
Geothermal Power	12.9	13.2	2.33%
Solar PV	177	227	28.25%
Concentrated solar power	4.3	4.8	11.6%
Wind Power	370	433	17.03%

Table 1.1: The increase in renewable energies from 2014 to 2015 (REN21, 2016)

As seen from table 1.1 the geothermal energy has lowest growth rate from 2014 to 2015. This could be due to the long time frame for building a geothermal power plant. The time from the first exploration of the geothermal area, including a surface exploration drilling, the completion and start-up of a geothermal power plant is minimum six years, depending on the size and place of the power plant (Dickson and Fanelli, 2003).

The low growth rate could indicate that there is a higher potential in geothermal energy as this area has not been exploited as much as others. The potential of geothermal energy worldwide is estimated to be 3.83 TW_e for high temperature reservoirs and 44 MW_e for low temperature reservoirs (Dickson and Fanelli, 2003). These potentials are the electrical power potentials, and with other technologies, such as heat pumps the low reservoirs can be utilised in a more suitable way, such as being used for heating.

1.1 Background for geothermal energy

Geothermal energy is one of the oldest renewable energy sources that have been utilised by humans. In the United States there is evidence that 10,000 years ago the hot springs in

North America were used for warmth and spiritual cleansing. In other places around the world, the geothermal water was used in this way (Ene, 2014). The first time geothermal energy was used on an industrial basis was in 1904 in Larderello in Italy, but a geothermal power plant was not build until 1938 (DiPippo, 2012a). The second power plant was not build until 1958 in New Zealand, the Wairakei Power Plant (DiPippo, 2012a).

The geothermal energy is utilised using the temperature gradient which occurs through the earth due to the 4700 °C hot core in the centre of the earth. Most of the earth surface area has a relatively low temperature gradient, regarding utilising geothermal energy, which is around 25-30°C/km (Marshak, 2012). In other areas of the earth, mostly near trenches and ridges, the temperature close to the surface of the earth is much higher (DiPippo, 2012a). A good prospective for utilising the geothermal energy, is that the temperature gradient has to be at least seven times the normal temperature gradient (DiPippo, 2012a). These ridges and trenches are found all over the world, see figure 1.1, and most of the geothermal power plants which produce electricity in 2003 are placed close to or on one of these ridges or trenches (Dickson and Fanelli, 2003).

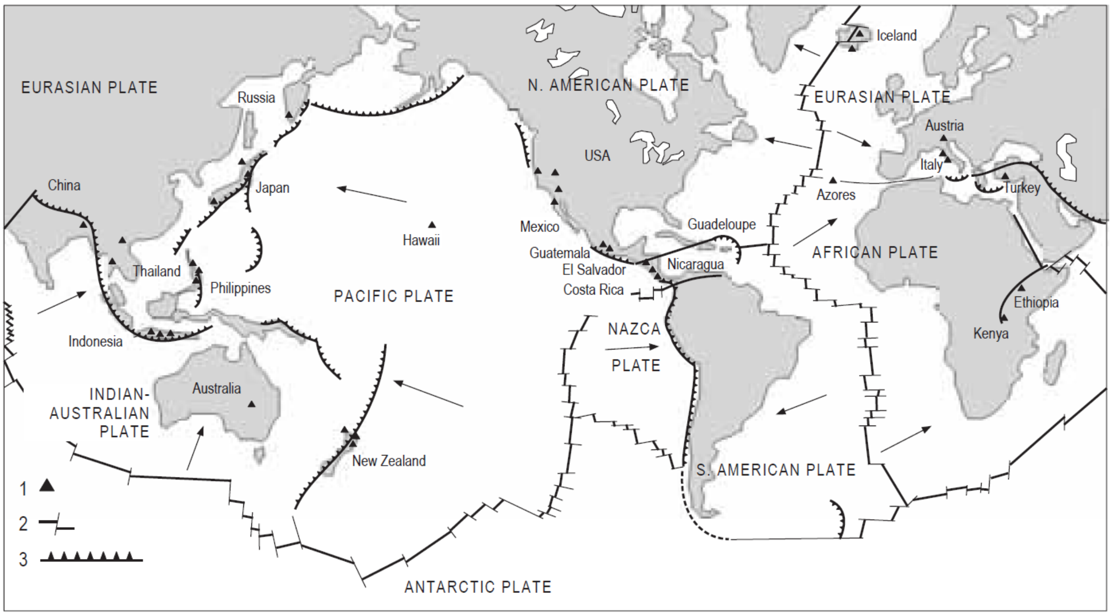

Figure 1.1: Worlds ridges and trenches. **(1)** Geothermal fields producing electricity **(2)** Mid-oceanic ridges crossed by transform faults **(3)** Subduction zones, where the subducting plate bends downward (Dickson and Fanelli, 2003)

For the last 5-7 years, geothermal energy has been utilised more and more for direct use (district heating, farmhouses etc.), and therefore geothermal power plants today are found outside the ridges and trenches areas. Some good examples are the geothermal power plants in Sweden, which use geothermal heat pumps to heat 20% of the houses in the country, and Tunesia which uses geothermal energy for heating 244 ha of greenhouses (Lund and Boyd, 2016).

When utilising geothermal energy, the most used resource is a *hydrothermal geothermal resource, HGR* (DiPippo, 2012a). A HGR can be used when five conditions are present, which are;

- *A hot heat source*, this could be magma or just a higher geothermal temperature due to ridges or trenches.

- *A water supply*, to ensure that the well will not run dry.
- *A recharge system*, this could be a reinjection well or water from the surface which seeps through the ground to ensure that the water supply persist.
- *A reservoir which is permeable*, this is needed to ensure that water can flow to the fractures or well.
- *A impermeable layer of rock*, to ensure the heated water does not escape before it reaches the fracture or the well.

If any of the above conditions are missing, it will not be profitable exploiting the geothermal field any further (DiPippo, 2012a). It makes a lot of sense that if there is not a sufficient heat source there will most likely not be hot water. It also makes sense that if there is no permability, it will not be possible to extract any fluid or steam and thereby will not be possible to feed the fracture or well with water. Thereby if there is no water to feed the fraction or well it will run dry and long time production from the area is not possible. The impermeable layer is important to ensure that the fluid stays in the ground and thereby the pressure will rise. If this layer was not there the geothermal fluid would emerge at the surface in a large area and the pressure will dissipate (DiPippo, 2012a). The HGR is the most normal resource to utilise and will here after be named as *geothermal energy*.

The process of a HGR can be seen in figure 1.2. The HGR is normally utilised in the depth of 900-3000 m (Thorhallsson, 2016).

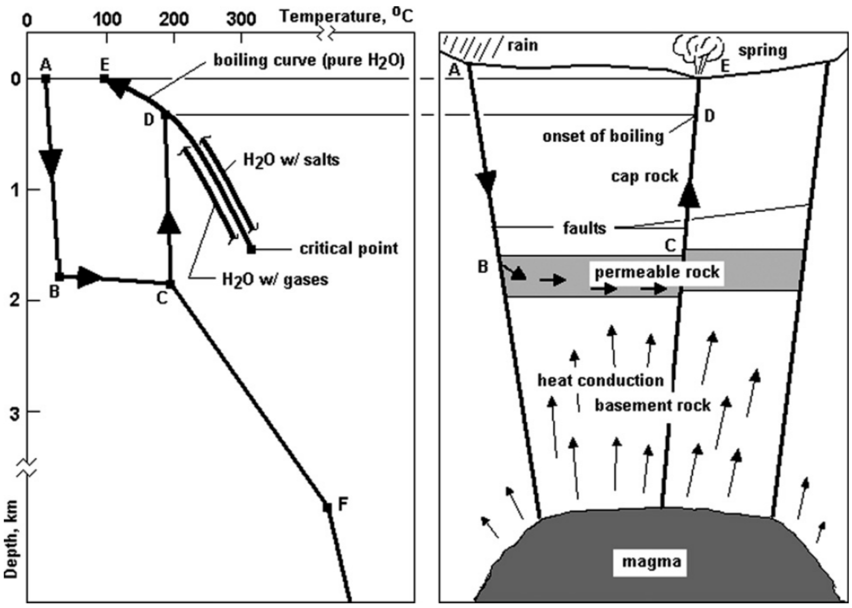

Figure 1.2: Hydorthermal geothermal process. **(A)** Rain falls and acts as the recharge system, as the water seeps through the fraction. **(B)** The water reaches the permeable rock and flows through the least resistant path. **(C)** The water reaches another fraction where the rock above become permeable again and the fluid will ascend to the surface. **(D)** The fluid rises and thereby the pressure is falling, until it reaches the boiling temperature and the steam flashes **(E)** The geothermal fluid reaches the surface and emerges as a mud hole, a fumarole or steam seeping out. (DiPippo, 2012a).

The HGR process seen in figure 1.2, is a cycle process, from surface rain, the permeable rock layer and back to the surface spring. There has to be a heat source for the HGR process to exist. The rainwater will seep down through the ground, but will not be heated very much as the heat source does not exist there. When the water reaches a permeable rock layer, the water will not descend much further into the ground, but instead the water will be heated from the ground around it, this is seen as process B to C in figure 1.2, due to the impermeable rock layer above the permeable layer the heated water, with a lower density, cannot ascend to the surface as it would have otherwise (DiPippo, 2012a). The heated water cannot escape to the surface until it reaches a fault and the impermeable layer is now permeable. As the water ascend towards the surface, the pressure becomes lower until it reaches the boiling point for the given pressure. When the water properties reaches the boiling curve it will flash into steam, which will be seen on the surface as a fumarole, mud pot, hot spring etc, see figure 1.3, 1.4 and 1.5 for examples (DiPippo, 2012a). The HGR process can also be human-induced for power plants, using reinjection wells, which acts like the rainwater and production wells as the faults.

Other ways of utilising the geothermal energy which although not commonly used is *hot dry rock, HDR*, where a hot but dry formation exist. To utilise HDR, water has to be pumped into the ground to crack fractures so that the heat can be utilised (DiPippo, 2012a). During the 1970's and 1980's HDR was highly investigated but over the last years this method has not been utilised on a big scale, as well as not investigated very much any more. However in China a project is ongoing regarding utilising HDR (Zhu et al., 2015).

Another area which is under investigation is *deep hydrothermal geothermal energy, DHGE*, which is essentially the same as hydrothermal geothermal energy but the wells are deeper. The wells in DHGE are 2500 m and deeper. No geothermal power plant has been utilising these wells yet, but in Iceland a project is ongoing with an aim to reach supercritical conditions (IDDP, 2000).

Geopressure is another source, but it is still a concept. The potential of geopressure has been found due to oil and gas drilling. When drilling, water was found which have a very high pressure, and thereby oil and natural gas could not be drilled. It is being investigated whether it could be used for geothermal power generation (DiPippo, 2012a).

Magma energy is a source which is still on the concept state. To utilise magma energy the idea is to drill directly into the magma chamber and injecting water under high pressure, hoping this will solidify and crack so that permeability exits and then use the magma as a direct heat source and not heated rocks as now (DiPippo, 2012a).

1.1.1 Geothermal field

A geothermal field is most of the time visible from the surface, as the ground most likely will have mud holes, be discoloured, steam will escape the ground and in some cases the ground will be hot. Examples of this can be seen in figure 1.3, 1.4 and 1.5.

Figure 1.3: Mud holes and discolouration of the surface at the geothermal area Kafla in Iceland (Jørgensen, 2016).

Figure 1.4: A fumarole at geothermal field Gunnuhver in Iceland (Jørgensen, 2016).

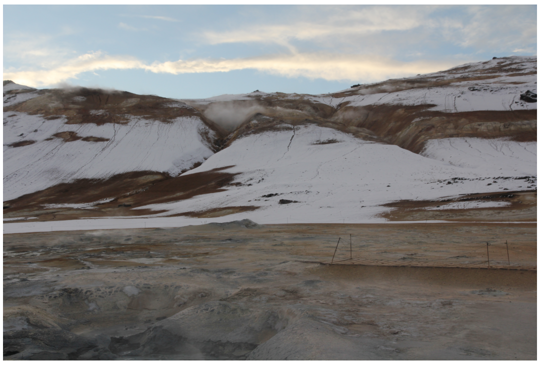

Figure 1.5: The hot ground has melted the snow, and steam is coming up of the ground in the geothermal field Hverir in Iceland (Jørgensen, 2016).

The temperature gradient in a geothermal field can vary quite a lot (Steingrímsson, 2016). This is also visible in figure 1.3 and 1.5, as there can be seen green landscapes in the background in figure 1.3 suggesting the surface temperature is lower as plants can grow there. In figure 1.5 the snow is only melted in some places showing the ground is warmer in these places. Due to these temperature differences in the geothermal field, an exploration of the geothermal field is crucial as the bottom of the wells will have to be placed in the areas with the highest temperature.

To ensure that the production reaches as close to the potential as possible an exploration program is formed. A successful exploration program should be able to locate and estimate the areas and volume of the hot reservoir. Furthermore it should be able to predict what type of reservoir it is, dry, liquid or two-phase as well as the chemical composition of the fluid. In the end it should be able to estimate the potential power generation of the field and thereby if it profitable to construct a power plant, this process is further described in chapter 4.

1.1.2 Geothermal power plants

A geothermal power plant can be designed in different ways. The design of the energy conversions mostly depends on the temperature of the geothermal field but also depends on if the field has been utilised before (Dickson and Fanelli, 2003). There are basically five types of conversions systems that are utilised in the the world. These are *Dry-Steam* (DS), *Single Flash* (SF), *Double Flash* (DF), *Triple flash* (TF), and *Binary Cycle* (BC) (DiPippo, 2012a). The classifications of the types and the respective temperatures can be seen in table 1.2. The most used conversion system is the SF, and the BC (DiPippo, 2012a). These power plants types will be described further in detail in chapter 5, and in chapter 2 where different power plant designs will be shown. The BC is mostly used in low temperature areas, while SF is used in moderate and high temperature areas, the DF is also used in moderate and high temperature areas, but often after a SF has been installed to check how the production is as the DF has a higher installation cost (Dickson and Fanelli, 2003).

	Temperature	**Type of power plant**
Non electrical	<100 °C	Direct use
Very low temperature	100°C to <150 °C	BC
Low temperature	150 °C to <190 °C	BC, SF and combination
Moderate temperture	190 °C to <230 °C	SF, DF, and combinations
High temperature	230 °C to <300 °C	SF, DF, TF and combinations
Ultra high temperature	300 °C to 374.1 °C	SF, DF, TF and combinations
Steam field	From 240 °C	DS

Table 1.2: Classifications of geothermal reservoirs (Sanyal, 2005).

Another factor that is important to take into account is the area the power plant is built on. This is important as a geothermal power plant will have a large visual impact on the surrounding nature. If the visual impact is to large, with for example large cooling towers or separators, or the pipe and road network is too large and thereby have a major impact on the nature surroundings, residents in this area might protest against the power plant (Dickson and Fanelli, 2003). In many countries laws has been made to ensure that the nature does not suffer at the expense of utilising power. Therefore when designing a power plant one has to consider the type of cooling towers, see chapter 5 for different types, and how the piping network is designed (Dickson and Fanelli, 2003).

CHAPTER 2

State-of-the-art

A literature study has been conducted to give a state-of-the-art of geothermal development worldwide as well as for the design and capacity of geothermal power plants world wide. To enlighten the state-of-the-art for capacity and design, ten articles describing this for ten different power plants has been investigated. Five reviews has been studied which states the geothermal energy development through the years 1985 to 2015. The reviews that has been studied is: Dipippo (1985), Huttrer (1995), Huttrer (2001), Bertani (2011), Bertani (2015). All of these reviews only focused on electrical power generation, and not heat, which is also often utilised.

Dipippo (1985) addresses the state-of-the-art for the electrical power production by geothermal power plants for the year 1980 to 1985. The power generation for this is given in larger locations, *Europe*, *America*, *Africa*, *Asia* and *Oceania*. The countries this areas include can be seen in table 2.2. Dipippo (1985) states that Africa had a slow development, the first power plant opened in 1981, compared to the other areas in regards of utilising geothermal energy, Africa did not utilise geothermal power until 1981 where the other continents have utilised geothermal energy on larger scale since the 1970's. America is the area which had the highest power generation in the five years this study covers, see figure 2.1. The worldwide percentage increase per annum in geothermal power generation for the years 1980-1985 were 101.1 %. The electrical power generation for the continents and the total world generation can be seen on figure 2.1 for the power generation by continent for the years 1980-2015.

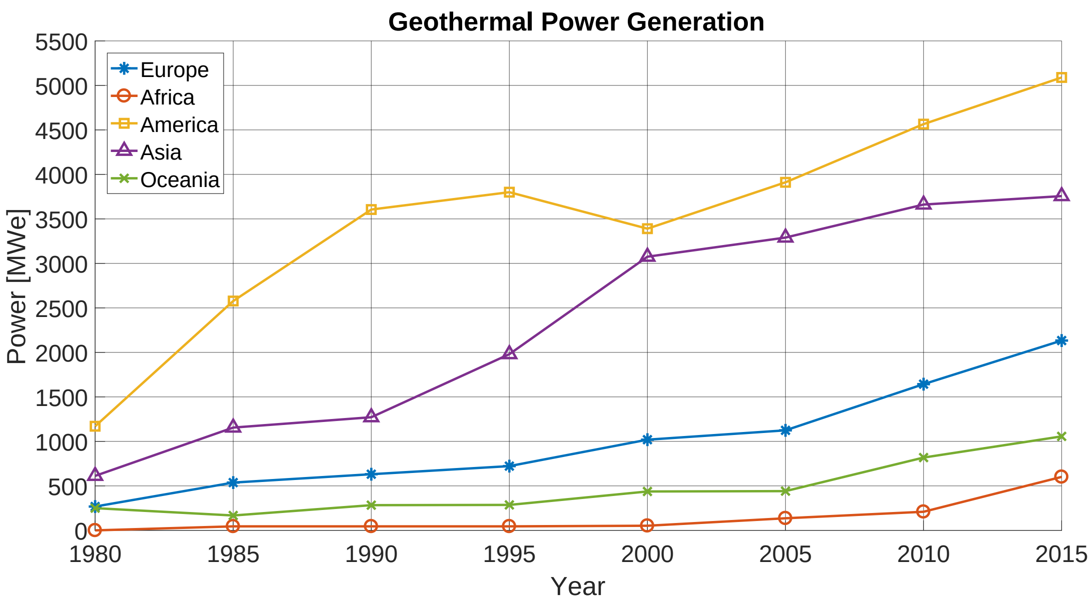

Figure 2.1: Geothermal power per area from year 1980 to 2015 (Huttrer, 2001) (Bertani, 2011) (Bertani, 2015).

Huttrer (1995) followed up on the world geothermal power generation in the years 1990-1995. The review concentrates on the changes for each individual country regarding geothermal power generation. The main aspects of the review, as well as the news in geothermal energy in the years 1990-1995 compared to the past years, is that Australia built the first operating geothermal power plant along with Portugal. The Philippines had become the second largest producer of geothermal energy after the United States, see table A.2 in appendix A. The United States grow rate has decreased in the four years compared to the years before. In Greece, the geothermal power generation were stopped in these four years due to resistance from residents on Milos where the power plant was placed. The rest of the countries that have a geothermal power production has either increased their capacity or held it steady over the years 1990-1995. The number of countries which are exploring the potential to produce electrical geothermal energy has also increased.

In 2001 Huttrer (2001), made a new review which should enlighten how the status of the geothermal energy has developed over the years 1995-2000. This status uses a lot of the same information as (Huttrer, 1995), but some aspects have changed in the 5 year period. Argentina stopped producing geothermal electricity but Ethiopia and Guatamala has started producing geothermal energy. The United States was the only country that had decreased the production, the other countries, which still utilised geothermal power had increased the geothermal production or kept it steady. However, even though most countries increased the production over the five years, the total percentage grow rate is lower for these five years than the previous five years, with 16.7% for 1995-2000 compared to 17.1% for 1990-1995. This is mainly due to fall in production in the United States geothermal field, The Big Geyser, because of decline in both quality and quantity. The growth rates for the period 1980-2015 can been seen in table 2.1.

Years	**Growth rate**
1980 - 1985	101.1 %
1985 - 1990	29.6 %
1990 - 1995	17.1 %
1995 - 2000	16.7 %
2000 - 2005	11.7 %
2005 - 2010	22.4 %
2010 - 2015	16.0 %

Table 2.1: Growth rates for five year periods from 1980 - 2015

The next review of the world wide electrical geothermal power production came in 2011 for the years 2005-2010 with the review from Bertani (2011). In the period from 2005 to 2010 three new countries have started producing of geothermal electrical power, these countries are Austria, Germany and Papua New Guinea. The number of countries starting to investigate the geothermal potential has also increased to 22 countries compared to 12 countries in 1995, so both the number of producing counties and developing counties have increased over the last 15 years. Most of the countries have increased or kept the production steady, but two has decreased the production. These are China and the Philippines. Another thing Bertani (2011) showed was that the grow rate has increased compared to the previous 25 years, with a grow rate at 22.4 %.

In 2015 Bertani (2015) investigated the development of the electrical geothermal power for the latest state-of-the-art; the review was revised in late 2015. The review found that the increase in geothermal electrical energy continued in the years 2010-2015 as it has since 1980. In 2015, 26 countries had power plants which utilised geothermal energy. These countries can be seen in table 2.2 and the capacity for these can be seen in table A.2, in appendix A. The growth rate for 2010-2015 decreased to 16.0 %, but there has been a continuous increase in geothermal energy from 1980 and the number of both power plants worldwide, countries with power production and countries that are exploring geothermal potential increases each year. The total growth in the worldwide geothermal capacity can be seen in figure 2.2. The top five countries regrading installed capacity are: the United States, the Philippines, Indonesia, Mexico and New Zealand, whereas the top five countries with the highest percentage growth in 2015 are: Turkey, Germany, Kenya, Nicaragua and New Zealand. The variance these countries can be due to the fact that the five countries with the largest capacity have been expanding the fields for many years and therefore the growth is lower. However the countries with the largest growth rate is new within the geothermal market or has not expanded for a long time, such as Kenya, and therefore will have a large percentage growth. According to Bertani (2015) the prospects for the number of countries with geothermal power production will increase to 51 countries from around the world.

	Countries with geothermal power generation		
Europe	Austria France Germany	Iceland Italy Portugal	Romania Russia Turkey
America	Costa Rica El Salvador	Guatemala Mexico	Nicaragua USA
Africa	Etiopia	Kenya	
Asia	China Indonesia	Japan Philippines	Taiwan Thailand
Oceania	Australia	Papua New Guinea	New Zealand

Table 2.2: Countries with electrical geothermal power generation (Bertani, 2015).

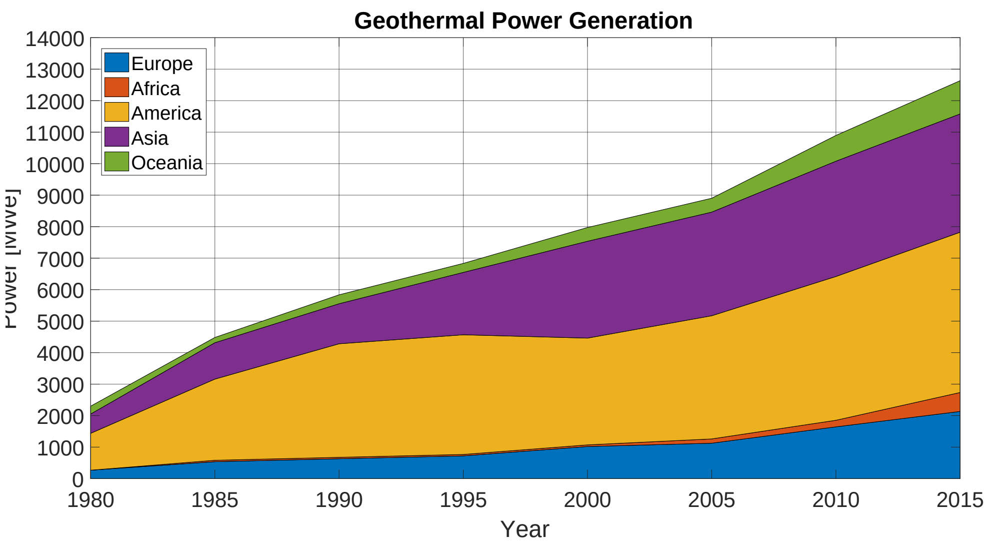

Figure 2.2: Total growth in geothermal power from 1980 - 2015 (Huttrer, 2001) (Bertani, 2011) (Bertani, 2015).

For understanding of the-state-of-the-art within development and design of geothermal power plants throughout the world and how it has changed over the years, ten articles has been investigated along with DiPippo (2012a) for all the power plants. The power plants that has been chosen can be seen in table 2.3. The power plants has been divided into types of power plants described in chapter 1, DS, SF, DF, TF and BC.

Larderello Geothermal power plant in Italy, was the worlds first power plant and is a dry steam power plant, one of three power plant which is only dry steam. A dry steam power plant uses that the wells produced saturated steam instead of liquid or a two phase fluid (DiPippo, 2012a). The first units in Larderello used direct intake, meaning that the steam from the wells was used directly in the turbines (DiPippo, 1978). Some of the units used condensers to re-inject the fluid, other units do not and emitted the steam into the atmosphere after the turbine; a back pressure turbine. However, all of these have been decommissioned, for more modern units (DiPippo, 1978). The newer units were not designed to specific conditions but standardised. These unit designs can be seen in figure 2.3. Larderello Power Plant has over the years had 53 units but only 22 units are producing today, the last unit added was in 2009, none of these units have utilised heat (DiPippo, 2012a).

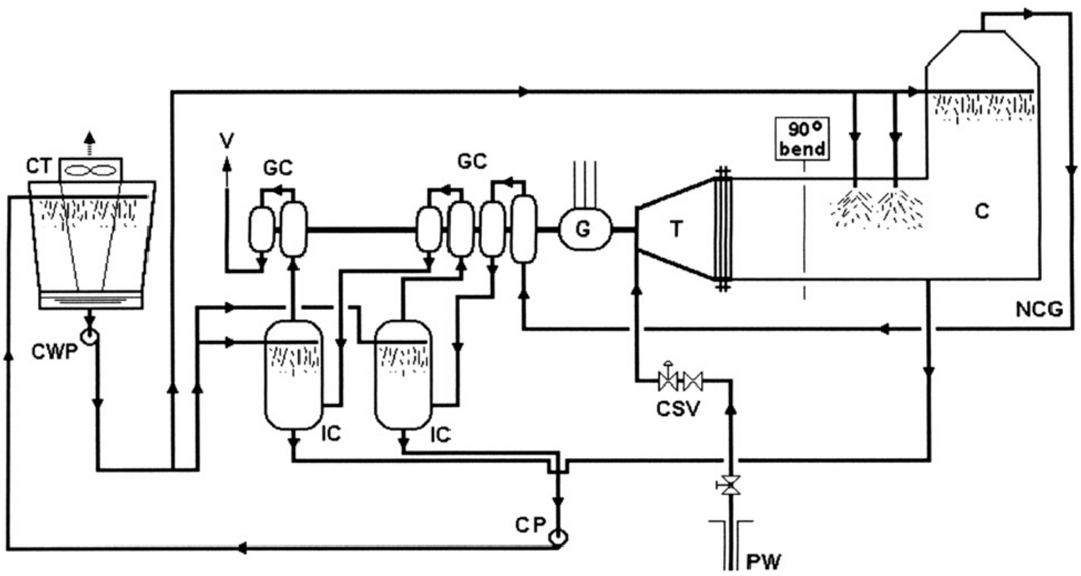

Figure 2.3: Design of the standardised units in Larderello(DiPippo, 2012a) [1].

Wairakei Geothermal Power Plant in New Zealand, was the second power plant in the world to utilise geothermal power in 1959. Wairakei power plant consists of two stations placed approximately 5 km apart. Wairakei Power Station A had four SF, two DF and four TF in 1963. Today the SF units has been decommissioned or moved (Thain and Carey, 2009) (DiPippo, 2012a). Wairakei Power Station B has three DF units, the units for both Power Station A and B can be seen in figure 2.4. The last unit added was in 2005. Wairakei does not utilise heat (Thain and Carey, 2009).

The Big Geyser geothermal field in USA, is the geothermal field which produces most power in the world and it is also one of the three areas in which dry steam power plants are used (Sanyal and Enedy, 2011). The production in the Big Geyser has not been steady and 23 separated power plants has been build, the latest was added in 1989 (DiPippo, 2012a). Since the Big Geyser covers a large area, many companies has utilised energy

Author, year	Power Plant	Plant type	Capacity MWe	No. of units	Location	Year of first production
DiPippo (1978)	Larderello	DS	594.5	22	Tuscany, Italy	1913
Thain and Carey (2009)	Wairakei	SF, DF, TF	254.9	17	North island, New Zealand	1958
Sanyal and Enedy (2011)	Big Geyser	DS	1477	26	Califonia, USA	1960
Garcia-Gutierrez et al. (2015)	Cerro Prieto	SF, DF	720	13	Baja California, Mexico	1973
Thorolfsson (2005)	Svartsengi	SF, BC, DS	76.7	5	Reykjanes, Iceland	1976
Menzies et al. (2010)	Tiwi	SF	220	4	Bicol Region, Philippines	1979
Wesula (2011)	Olkaria I	SF	45	3	Olkaria, Kenya	1981
Gunnarsson et al. (1992)	Nesjavellir	SF	120	4	Southern Region, Iceland	1990
Murakami (2001)	Wayang Windu	SF	227	2	West Java, Indonesia	1999
Quick et al. (2010)	Landau	BC	3	1	Rheinland-Pfalz, Germany	2007

Table 2.3: The ten power plants that is being investigated

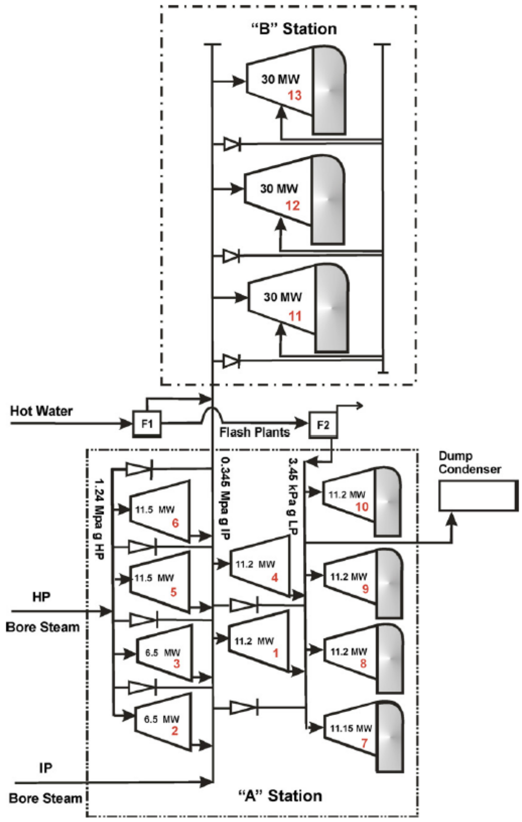

Figure 2.4: Wairakei Power Station A and B (Thain and Carey, 2009).

and therefore power plants varies a lot in designs (DiPippo, 2012a). All the power plants in Big Geyser are dry steam.

Cerro Prieto in Mexico, is the largest liquid dominated geothermal field and the largest field in Mexico. It was also the first to utilised geothermal power in Mexico in 1979 (Garcia-Gutierrez et al., 2015). The Cerro Prieto has four power stations in the large field, CP1 with five SF units, CP2 with two DF units, CP3 with two DF units and CP4 with four SF units, the design of SF units can be seen in figure 2.5 and the DF design can be seen in figure 2.6. All the units in Cerro Prieto are still operating and the last power station was added was CP4 in 2000. Cerro Prieto does not utilised energy for heating purpose.

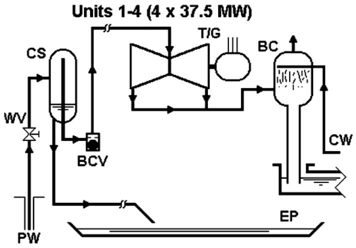

Figure 2.5: SF unit design for the power stations CP1 and CP4 in Cerro Prieto (DiPippo, 2012a).

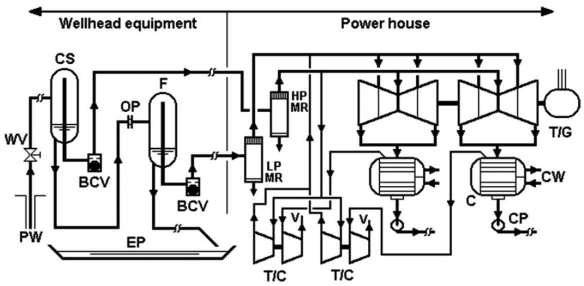

Figure 2.6: DF unit design for the power stations CP2 and CP3 in Cerro Prieto (DiPippo, 2012a).

Svartsengi in Iceland has operated since 1976 and has five units, the latest added in 2007, a dry steam unit (DiPippo, 2012a). Unit 1 and 2 has a low electrical capacity. The reason is that these units was primarily build for geothermal heat, the heat capacity of these units are 50 MW_{th} and 75 MW_{th} respectively, these units are a SF unit. Unit 3 is a SF, back pressure unit. Unit 4 is a *Organic Rankine Cycle*, ORC, unit which is placed after the back pressure turbine, see figure 2.7. Unit 5 was intentionally a renewal of unit 1, however it was decided to maintain both units. Unit 5 is a SF and dry steam placed after each other and has a capacity of 60 MW_e and 150 MW_{th} (Thorolfsson, 2005).

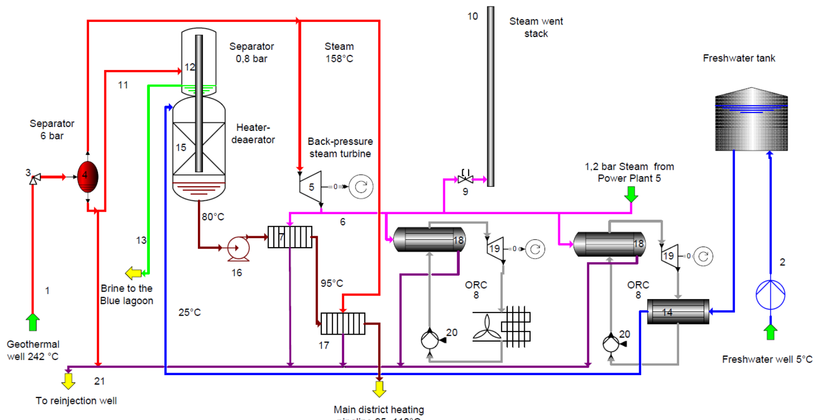

Figure 2.7: Design of unit 3 and 4 in the Svartsengi powerplant (Thorolfsson, 2005).

The Tiwi geothermal power plant in the Philippines, consist of four units all of a SF with capacity of 55 MW_e (DiPippo, 2012a). Initially there were six units, but due to operational reliability, as oil and gas increase (sic: decrease) in price, unit 3 and 4 was shut down so they could be started if another unit failed (Menzies et al., 2010). As Tiwi is placed in the Philippines this is more necessary as they are often hit by a typhoons resulting in a lot of damage (Menzies et al., 2010).

The Olkaria I power plant in Kenya, was the first power plant in Africa, it was commissioned in 1981 with the first unit. Today Olkaria I has three units the last added in 1985. The units are SF with 15 MW_e each (DiPippo, 2012a). The SF units is standard units and the designs is like CP1 and CP4 in Cerro Prieto, see figure 2.5, but with a

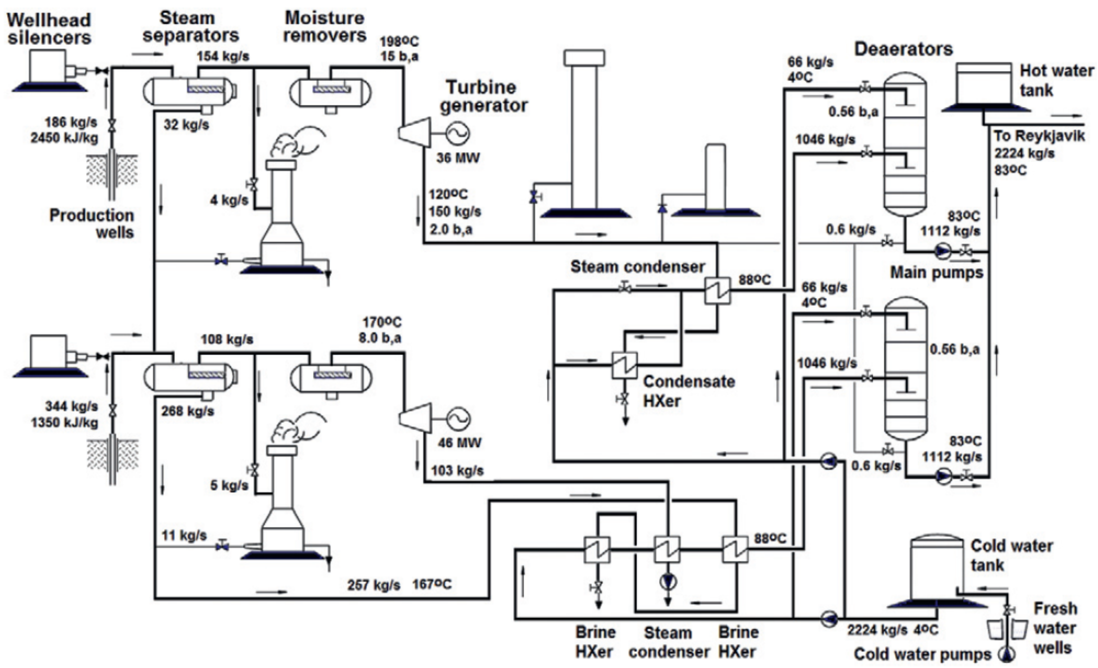

Figure 2.8: Design of two units in the Nesjavellir power plant (Gunnarsson et al., 1992).

single output turbine (Wesula, 2011). In 2000 and 2003 two new power plants were build, Olkaria II and Olkaria III.

Nesjavellir in Iceland, power plants is located just north of the volcano Hengill and therefore is in a high temperature area (Gunnarsson et al., 1992). The power plant was commissioned in 1998 and the last of four units added in 2005. The Nesjavellir power plant was initially built to supply heat to the Reykjavik area and has 290 MW_{th} and 120 MW_e. The units in Nesjavellir are SF units with a capacity of 30 MW_e each. The heat is utilised after the condensers, see figure 2.8, and is sent to the Reykjavik area. The units are interconnected to be able to maximise the use of the geothermal fluid heat the most.

The Wayang Windu power plant in Indonesia, is one of the power plants with the largest turbine capacity per unit (Murakami, 2001). The power plant has two units each with a SF system. Unit 1 was commissioned in 1999 and has a capacity of 110 MW_e and unit 2 which started producing in 2009 has capacity of 117 MW_e (DiPippo, 2012a). The units in Wayang Windu power plant is simple as seen in figure 2.9. The Wayang Windu power only provides electricity to the population close to the power plant (Murakami, 2001).

The newest geothermal power which was investigated was the Landau geothermal power plant in Germany which was commissioned in 2008. This is a low temperature power plant, 160°C, and therefore the Landau power plant is a binary power plant using an ORC (Quick et al., 2010).

The state-of-the-art within the area geothermal power generation has now been presented. It was found that worldwide the geothermal power production has increased from 1980-2015 and the numbers of countries utilising geothermal power is also increasing. It was found that the designs of geothermal power plants varies depending on the geothermal area. High temperature areas often uses a flash system mostly either single or double, however one plant has TF units. ORC is mostly used in low temperature areas or after

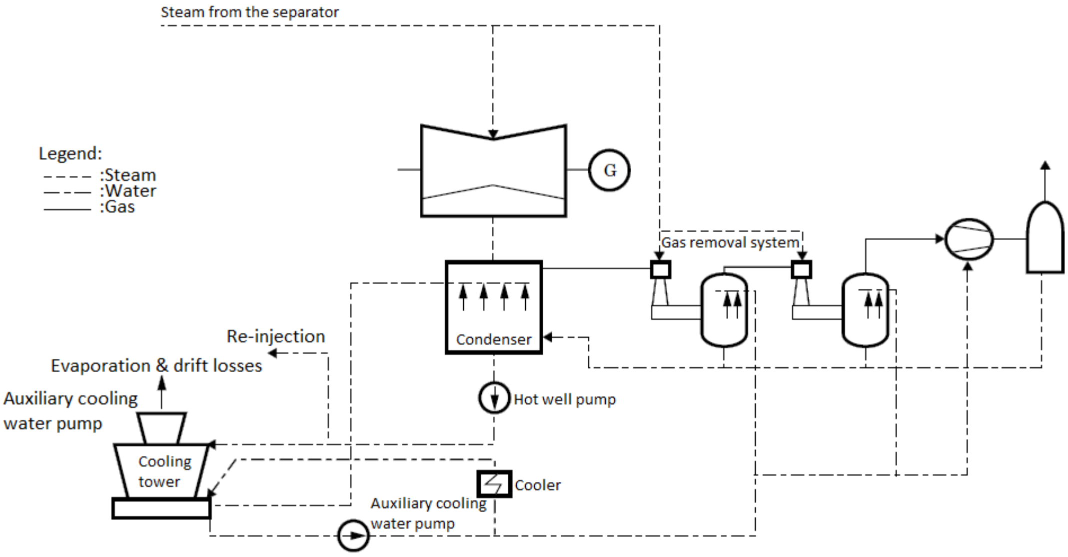

Figure 2.9: Design of a unit in the Wayang Windu power plant (Murakami, 2001).

the flash unit to extract more energy. It was found that a dry steam plant has the highest capacity, it is however also the two power plants with most units. The dry steams systems is estimated to be only 5% of all geothermal systems and most of these are already utilising geothermal power (DiPippo, 2012a). The most common power plant type represented in this state-of-the-art is the SF system, and this is also representative for the study literature (DiPippo, 2012a) (Bertani, 2015).

CHAPTER 3

Problem statement

In chapter 1 it was found that the potential for utilising geothermal power is high all over the world, but the power output of the power plant would depend on the geology and temperature gradient through the underground at the place the power plant is built. Different resources can be used to utilise geothermal energy, the most common and most used is the hydrothermal geothermal resource. As the potential for geothermal energy is world wide it has been decided to design a power plant that will match the criteria for a hydrothermal geothermal resource and it should be able to fit into all geothermal systems which generate electricity. In chapter 2 a state-of-the-art was conducted in regards to worldwide development and power plants designs which utilise hydrothermal geothermal resources, here it was found that most of the geothermal power plants are not interconnected and that the temperature differences of the geothermal fluid from different wells is gathered together and sent to a power plant.

Main purpose

Designing a system that is applicable all over the world if the well temperatures is known. Furthermore the design should take the different well temperature into account, so that the geothermal fluid from low temperature wells is not gathered together with the geothermal fluid from the high temperature wells.

Project limitations

The project limitations is following:

- The main object is to design a electrical power plant and therefore the heat capacity is not taken into account when the plant is optimised.
- The design is assumed to work in a steady state even though there might be dynamic elements.
- The components are ideal or with fixed losses described in the respective chapter
- Wells with supercritical conditions are not considered in the plants designed.

CHAPTER 4

The geothermal development process

When a potential geothermal field is discovered, there are seven phases which has to be covered before a geothermal power plant is operating. These phases are formulated to ensure that the financial losses are minimum if the geothermal field it not suitable for production (Harvey and GeothermEx Inc, 2013). The seven phases are:

1. Preliminary study
2. Exploration
3. Test drilling
4. Project review and planning
5. Field development
6. Power plant construction
7. Commissioning and operation

The time perspective for a geothermal project is normally seven years until production is possible. The early stage (preliminary studies, exploration and test drilling) takes around four years, the middle stage (project review and planning and field development) takes around four years as well and the late stage (power plant construction) takes around three year (Gehringer and Loksha, 2012). The phases overlap to save as much time as possible and thereby minimising the costs. For a more detailed timeline for a geothermal project see appendix B.

4.1 Phase 1 - Preliminary study

According to Harvey and GeothermEx Inc (2013), the preliminary study is mostly about gathering information. One of the important steps is to do a literature study, to investigate if there is already geothermal production in the area or country. The literature study should also include regulations for the country which could restrict the exploration, such a national parks, areas which special flora and fauna, geological hazards or cultural sites which are to be preserved.

The preliminary study should also make an assessment of the environmental impact and the issues a geothermal power plant could give rise to in the surrounding area. These should include the pipe and road network as well as what the power plant buildings will consist of. This assessment is important so that if it is necessary to build bridges and other infrastructure it can be taken into considerations when the planning is done. In the first phase it is also important to obtain and retain the legal rights to geothermal fields(Harvey and GeothermEx Inc, 2013).

The preliminary study is a low cost phase, but the risktaking in the field of geothermal is is very high, see figure 4.1.

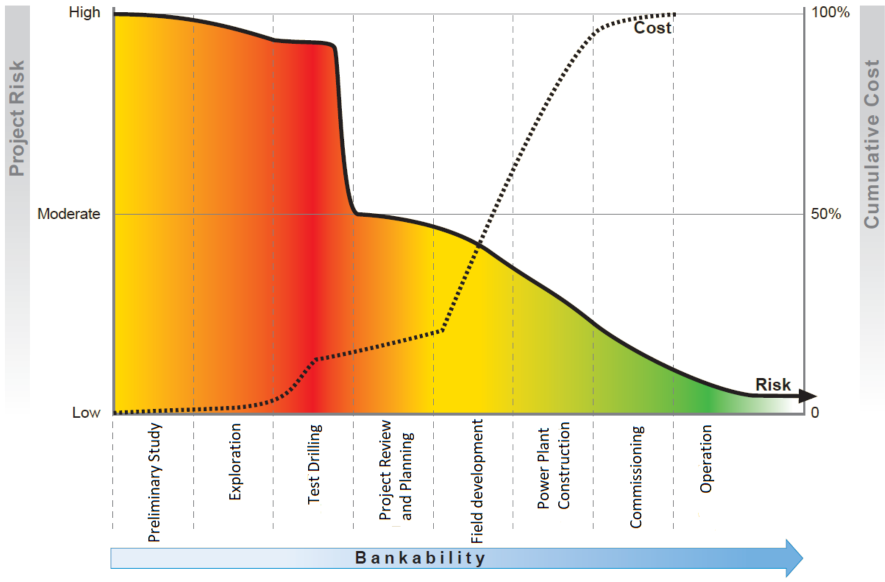

Figure 4.1: Risk and cost assessment for the different phases of a geothermal project (Gehringer and Loksha, 2012), adapted.

4.2 Phase 2 - Exploration

The exploration phase is carried out to minimize the risk in a cost effectively manner. Therefore most of the time simple methods are used for the exploration, these methods can be divided into three categorises *surface studies*, *geochemical surveying* and *geophysical surveying*, as seen in table 4.1 (Harvey and GeothermEx Inc, 2013).

The exploration data are gathered from existing wells or geothermal surface manifestations, such as hot springs or fumaroles. The studies of the environment in the well or the manifestations give a baseline of information on the geothermal field before wells are drilled which is a high cost in a geothermal project(Harvey and GeothermEx Inc, 2013). When the geoscience studies have been completed a conceptual model is made. The conceptual model represents the best understanding of the geothermal field at the moment. It is important to have this model, even though in the end it is shown to be very incomplete and often the model is very crude, as it is needed to start the drilling phase. The conceptional model should enlighten the properties and features in the wells. When the conceptional model is finished a numerical model is made to forecast the performance of the geothermal field in the future (Harvey and GeothermEx Inc, 2013).

4.3 Phase 3 - Test drilling

The test drilling phase is the phase where the first full size diameters are drilled, normally slim-holes, and is further described in chapter 5. The test drilling phase is where the risk is still very high and the cost is also increasing as the drilling is a high cost operation. Normally two or three wells are drilled to demonstrate the production of the wells in the geothermal field. The test wells should preferable demonstrate what can be expected of wells, such as an estimation of the heat source and determining the average well production. The test drilling phase can also disclose underground isotherms and thereby the locations of the production wells (Harvey and GeothermEx Inc, 2013).

Surveying techniques		
Surface studies	**Geochemical surveying**	**Geophysical surveying**
Gathering local knowledge	Geothermometry	Gravity
Locating active geothermal surface features	Electrical conductivity	Electrical ressistivity
Assessing surface geology	pH	Magnetotelluric
	Flow rate of fluids from active features	Temperature gradient drilling
	Soil sampling	2D and 3D seismics

Table 4.1: The surveying techniques used in the exploration phase (Harvey and GeothermEx Inc, 2013).

4.4 Phase 4 - Project review and feasibility

Once the test drilling has revealed that the wells has a productivity which can be used commercially, the risk falls drastically. In this phase of the geothermal project, the numerical model, developed in the second phase, is updated and a financial model is developed (Harvey and GeothermEx Inc, 2013). A report is normally made which states what has been found so far as wells as prospects for further development. This report is mainly made for investors. The report will obtain location of the drilling pads, the design of the production wells and number, forecast for production, power plant design etc. (Harvey and GeothermEx Inc, 2013).

This phase is not a phase that reduce risk much, and is not very costly either (Gehringer and Loksha, 2012).

4.5 Phase 5 - Field development

The field development can be described as a construction of the geothermal field. It includes drilling of production and re-injection wells, but also constructing the gathering system such as pipe network (Harvey and GeothermEx Inc, 2013). The production and re-injection wells are, in average, 2 km deep and have a drilling time of 40-50 days (Harvey and GeothermEx Inc, 2013), but this depends on the geothermal field as well as the diameter of the well (Thorhallsson, 2016). The ratio between production wells and re-injection wells is in the range 4:1 to 1:1 depending on the enthalpy, production fluid, fluid-steam ratio etc. (Harvey and GeothermEx Inc, 2013). The specific location and depth of the wells is predicted by the numerical model made earlier. The field development is a high cost in the geothermal project, but it also decreases the risk of failure as more and more wells are drilled, see figure 4.1.

4.6 Phase 6 - Power plant construction

The construction of the power plant requires civil works. The construction is based on the field review report. The power plant will consist of turbine buildings, auxiliary buildings, transformer stations, separators, cooling towers etc. See chapter 5 for an in-depth description of a power plant. The construction should also include transmission lines and roads to the geothermal field (Harvey and GeothermEx Inc, 2013).

4.7 Phase 7 - Commissioning and operation

When the field development and the construction of the power plant is finished the power plant can be commissioned. Since the energy source is at the field and the gathering system has been constructed it is not necessary to provide a energy source as in other power plants (Harvey and GeothermEx Inc, 2013). The main focus of this phase is to optimise the production and re-injection as well as manage the power plant successful so that there is a reliable delivery of geothermal power. Another focus is to minimise the operational cost, maximise the investments return (Harvey and GeothermEx Inc, 2013).

It may be necessary to drill new production and re-injection wells to make up for lost production over the time, therefore the cost will still increase a little over the years but the risk is at a minimum now, as seen in figure 4.1.

The cost for a geothermal power plant is 2-5 MUSD per MW installed, where the most costly phases are the test drilling, field development and of course the construction of the power plant (Jóhannesson, 2016).

CHAPTER 5

System presentation

The design of a geothermal power plant depends on different parameters. These parameters are mostly the temperature or enthalpy in the geothermal field. The temperature and mass flow of the geothermal fluid from the wells has a large impact on which type of power plant would be most optimal as described in chapter 1. Another parameter is the placement of the wells, as well as which climate the power plant is being build in. This is especially important for the cooling units for the condensers.

5.1 Geothermal field

The geothermal field will vary from country to country both in temperatures, the geothermal fluid composition and the placement of the wells. Wells located in mountain will have a different gathering system than wells located on a plane field (DiPippo, 2012a).

For this project a hypothetical geothermal field has been created based on Gunnarsson et al. (1992), Steingrímsson (2016) and Tolentino and Buñing (n. d.)[1]. This approach has been applied as it has not been possible to find a full set of data from one single geothermal field. Therefore the well data are both from the Philippines, the geothermal fields Leyte, Tiwi and Southern Negros, and from Iceland, from the geothermal fields Nesjavellir and Laugarnes. It has been necessary to use these data as the dataset was incomplete with either temperature or enthalpy not given and pressure was not given for any of the available data.

The hypothetical geothermal field is placed in mountains, as most of the data are from Nesjavellir which is in the Hengill mountains. Therefore the 26 drilled production wells are also placed in the Hengill mountains and are placed in different elevations, see figure 5.1, which will affect the piping network.

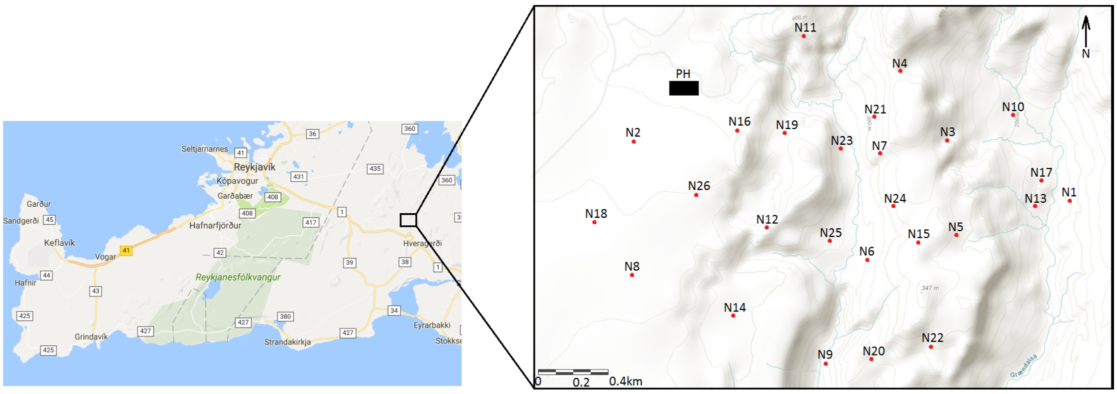

Figure 5.1: The geothermal field in Hengill mountains and the placement of the 26 production wells, the black box is the power house.

5.1.1 Wells

Geothermal wells can have different designs depending on the purpose of the well as well as the depth, but the main design is the same consisting of *conductor*, *surface casing*,

[1] No date available.

anchor casing, *production casing* and a *slotted liner*, see figure 5.2. The main reason to use casings in the wells is to support the drilled hole, as well as to seal unwanted aquifers from entering the well (Thorhallsson, 2016).

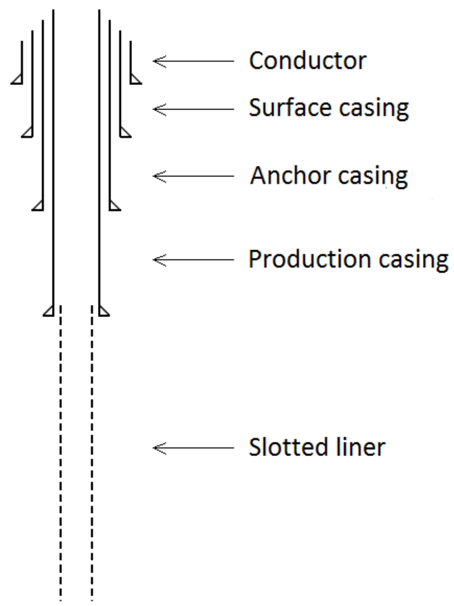

Figure 5.2: Standard design of a geothermal well (Thorhallsson, 2016).

The different casings have different features, the slotted line is the casing which allows the heated geothermal fluid into the well. The production casing is the casing which is the walls of the well and thereby where the geothermal fluid is; hence the name. The anchor casing is the casing which is used to anchor the wellhead to the well. The surface casing is to support the blow-out preventer, when drilling for the anchor casing. The conductor is inserted to the the drilling of the rest of the well (Thorhallsson, 2016).

The depth of the casings as well as the diameter depends on which type of well is drilled. There are general three types of wells, slimholes, regular holes, and large holes. The slimholes have a diameter of production casing of 117.8 mm and are often used as exploration wells, or shallow wells, the max depth is 1200 m, the advantages with slimholes is that it is a cheaper well to drill, but if the well has to be deeper than 1200 m, or there is much scaling in the geothermal fluid slimholes cannot be utilised (Thorhallsson, 2016). The regular, diameter of 244.5 mm, and large holes, diameter of 339.7 mm, are for deeper wells, from 1200 m and deeper. The large holes are more expensive than the regular holes, but if there is much scaling in the geothermal fluid or the flow rate is high the large hole is a better solution, as a larger hole will be able to produce more compared to the smaller regular hole. The regular hole is the most used as it is suitable for the most wells and it is relatively cheap compared to the output of the well (Thorhallsson, 2016).

The 26 wells which have been drilled, have a depth of 1027 m to 2743 m. From table 5.1 it is seen that there are four wells that could have been slimholes (well N2, N8, N16 and N24), however the flowrates are relatively high for all of these wells and therefore it has been deemed unsuitable to use the slimholes as it will prevent an optimal flow. Based on Gunnarsson et al. (1992) and Karlsdóttir (2012) it has been deemed that the scaling in the geothermal fluid does not pose a problem to use regular holes as the scaling in

Hengill mountains does not pose a big problem. Therefore, 22 regular hole wells will be drilled, the last four will be large hole wells as the flow in well N2, N5, N10 and N13, has a higher flow to justify the more expensive well. The re-injection wells will also be regular holes, the ratio of production wells and re-injection wells will be 4:1 as the enthalpy is relative high and in the Nesjavellir there are three re-injection wells and a geothermal waste disposal pool (Zarandi and Ivarsson, 2010), thereby there will be seven re-injection wells (Harvey and GeothermEx Inc, 2013). The total number of wells is therefore 33 wells.

Well	**Depth [m]**	**Temperature [°C]**	**Enthalpy [kJ/kg]**	**Mass flow [kg/s]**	**Temperature Classification**
N1	2001	295.7	1320	36	High temperature
N2	1124	106	444.4	50	Very low temperature
N3	1804	363.6	1800	10	Ultra high temperature
N4	1564	150	632.3	29	Low temperature
N5	1992	290	1289	70	High temperature
N6	2100	221.4	950	45	Moderate temperature
N7	1264	229	985.3	33	Moderate temperature
N8	1102	112	469.8	30	Very low temperature
N9	2743	174	736.8	37	Low temperature
N10	1798	301.1	1350	52	Ultra high temperature
N11	1276	130	546.4	14	Very low temperature
N12	1751	195	829.9	11	Moderate temperature
N13	1856	295.7	1320	57	High temperature
N14	1378	136	572.1	45	Very low temperature
N15	2361	265	1159	24	High temperature
N16	1027	123	516.5	37	Very low temperature
N17	1304	297.5	1330	28	High temperature
N18	1287	103	431.7	15	Very low temperature
N19	1739	148	623.7	25	Very low temperature
N20	1611	175	741.2	5	Low temperature
N21	1746	218.2	1450	47	Moderate temperature
N22	2598	187	794.2	22	Low temperature
N23	1603	206	879.5	26	Moderate temperature
N24	1173	241	1042	31	High temperature
N25	2136	221.4	950	35	Moderate temperature
N26	2108	113	474.1	21	Very low temperature

Table 5.1: The drilled wells in the geothermal field, based on data from Gunnarsson et al. (1992), Steingrímsson (2016) and Tolentino and Buñing (n. d.).

The well data has been computed with the program *Engineering Equation Solver* (EES) by making the assumption that the quality of the wells is 0, thereby liquid dominated (saturated). This assumptions has been made based on Gunnarsson et al. (1992), which states that most of the wells in Nesjavellir are liquid dominated, as well as Laugarnes (Harrison et al., 2013). The 26 production wells have been sorted into the classifications, *very low temperature*, *low temperature*, *moderate temperature*, *high temperature* and *ultra high temperature*. The data and classifications of the wells can be seen in table 5.1. There are eight very low temperature, four low temperature, six moderate temperatures, six high temperature and two ultra high temperature wells.

It has been decided that the wells with the temperature classification very low temperature will be directed to a BC unit, eight wells, the wells with the classification low and moderate temperature, ten wells, will be utilised in a SF unit and the wells with classification high and ultra high temperature, eight wells, will be utilised in a DF.

5.1.2 Piping network

The piping network can be designed in three different ways, depending on where the separators is placed. As there are three units, a BC, a SF and a DF, the piping network will have to be designed so that the right wells are combined to the right unit. The placement of the separators is rather important as the flow in from the wellheads to the separator will be two-phase and thereby an uphill flow is not a suitable solution. This is due to the fact that the geothermal fluid is flashed in the wellheads.

One way of designing the piping network is to place one separator at the power house, see figure 5.3 a. This solution is the best solution if the wells are placed in the same level. The design with only one separator is the cheapest as only one separator is, as mentioned needed, the steam will thereby enter the turbine shortly after the separator. This design is however only suitable in a relatively flat geothermal field (DiPippo, 2012a).

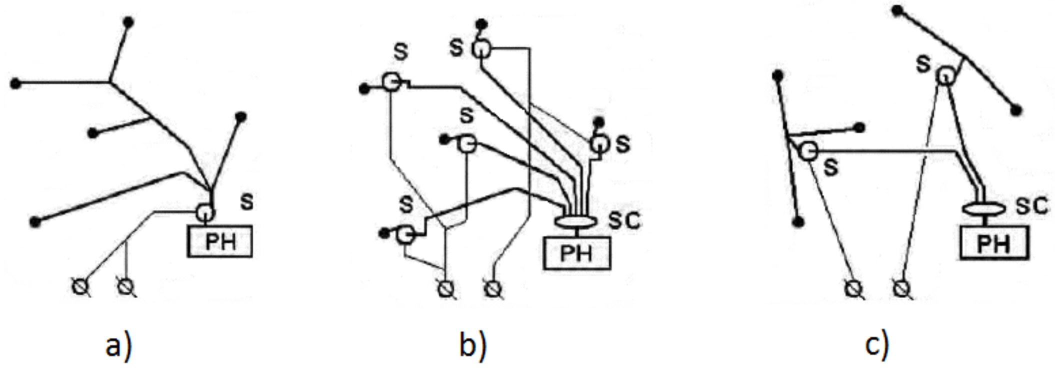

Figure 5.3: The three designs of piping network, one central separator, one separator for each production well and a satellite system. The filled circles are production wells and open circles re-injection wells. (DiPippo, 2012a).

The second design is to place a separator at each wellhead and a steam pipe will lead to a steam collector from the other wells, see figure 5.3 b. As there is a separator at each wellhead, re-injection pipes have to be made from each well to the re-injection well. This is very costly but can be necessary if the wells are placed in different valleys to prevent a two-phase flow flowing upwards which will cause problems (DiPippo, 2012a).

The last design is a hybrid of the two designs above, a so-called satellite system, see figure 5.3 c. Here there is a separator placed between the wells and the power house (PH). The benefit of such as system is it is cheaper than the system with one separator at each wellhead but still have the benefits of this type of system (DiPippo, 2012a).

As the wells are placed in Hengill mountains, it is seen that some of the wells lie in other valleys than the power house; therefore the first design with only one separator is not a suitable design. It will be possible for some of the wells to share a separator, see figure 5.1, therefore a satellite system will be implemented. On figure 5.4, the placement of the separators and which wells will be connected to the separator can be seen. The pipe line is not placed as it might be in reality, but is placed to show how the overall piping network could look like.

Therefore six separators and two steam collectors in this system, will be needed.

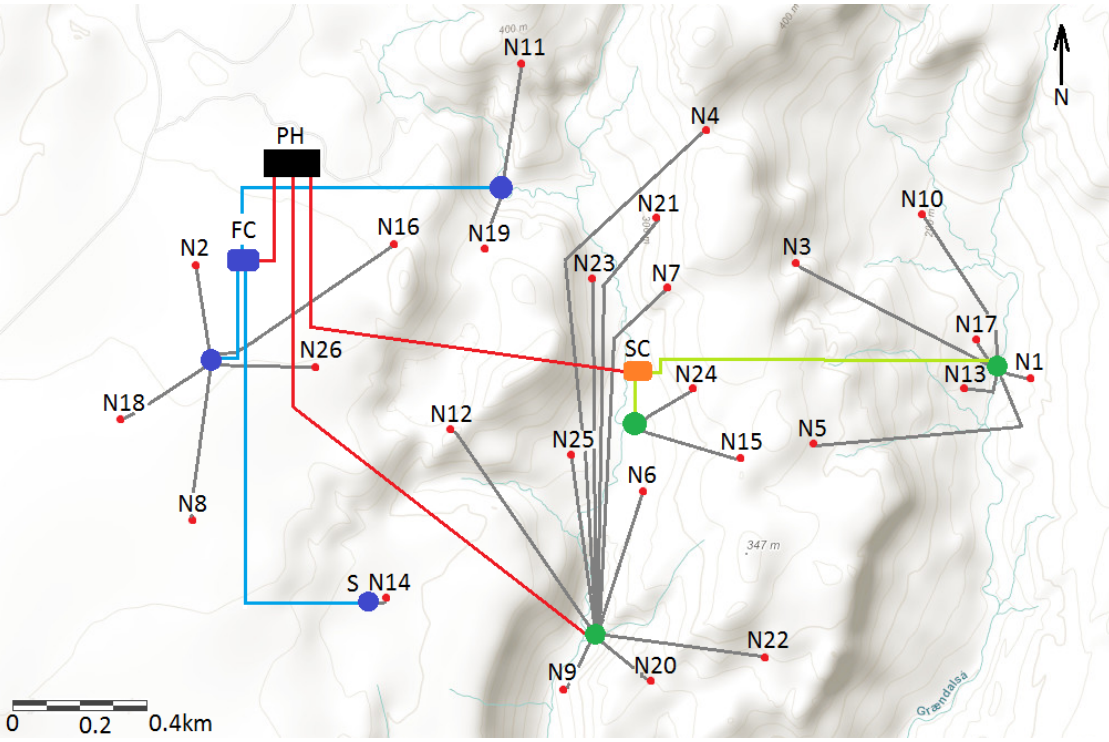

Figure 5.4: The piping network of the geothermal field, the grey lines are geothermal fluid lines, the light green lines are steam lines to steam collectors (SC), the light blue lines are fluid lines, the green rounds is separators, the orange square are steam collectors, the dark blue rounds are fluid collectors (FC) and the red lines are fluid or steam lines going to the three units, BC, SF and DF.

5.2 Energy conversion system

As described in chapter 1, different power plants are needed depending on the temperature of the geothermal fluid. As described in section 5.1, the systems in this study have temperatures ranging from 103°C - 363.6°C, which is within in the classifications of very low to ultra high, therefore both BC, SF and DF will be relevant in the power plant for this system.

5.2.1 Binary cycle

In a binary cycle plant the geothermal fluid does not come into contact with the turbine, but is used as a hot source in a heat exchanger. When the geothermal fluid has been through the heat exchanger the fluid is pumped down into a re-injection well (DiPippo, 2012a), see figure 5.5. When the geothermal fluid has to go through a heat exchanger it is important to ensure that the fluid stays in liquid form. This is achieved by using a pump, which is located under the flashing point down in the production wells (DiPippo, 2012a). The reason for keeping the fluid in a liquid state is that it has a potentially higher heat transfer rate and it is known from practical experience that having the fluid in a liquid state will reduce the risk of corrosion (Çengel et al., 2012). The geothermal fluid has to be kept at a pressure above the flash point at all times to prevent generation of steam and thereby the non-condensable gasses which could lead to corrosion (DiPippo, 2012a). The temperature of the fluid is not allowed to go below the point where silica or other scaling materials solidify (DiPippo, 2012a).

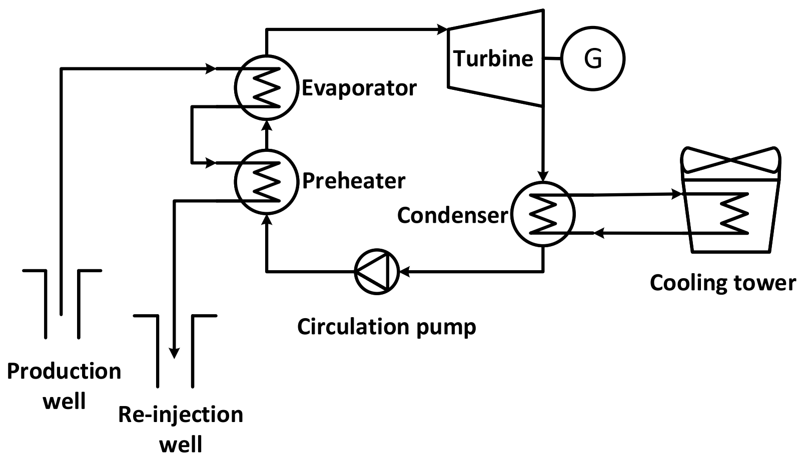

Figure 5.5: A simple and standard BC power plant. (DiPippo, 2012a).

The other part in the BC plant is the ORC system which consists of a preheater unit, where the working fluid in the ORC is brought to the boiling point. In the evaporator the working fluid is evaporated into saturated gas and then it enters the turbo generator, where it expands to the condenser pressure. The condenser, is condensing using cold water from a cooling tower. In the end a circulation pump ensures that the fluid is circulated in the ORC. The components that are used in the BC are described further in section 5.3.

One of the main things to consider is which fluid is to use in the ORC. There are some considerations that need to be taken into account, these are mainly the properties of the working fluid, the environmental and health aspects.

For a fluid to be attractive to utilise in a BC there are some features which would be favourable. These are the critical temperature, T_c, which should be low to ensure that the relatively low temperature from the wells can be used as a heat source and evaporate the working fluid. Another feature is if the fluid is a retrograde[2] or not, as it might be able to be pure gas if the fluid is are retrograde. The last considerations are the environmental and health properties for the staff working at the unit.

In Saleh et al. (2007), different working fluids have been tested to determine the best working fluid for a ORC in geothermal power plants. It was found that the best working fluid, for water temperatures under the critical temperature, is R152a. This is not a retrograde fluid, but the increase in temperature are more uniform than other working fluids (Saleh et al., 2007). The working fluid was looked up in the Environmental Protection Agency (EPA), which in corporation with the UN, lists of working fluids which has a low health and environmental risk (EPA, 2015). The working fluid, R152a, is listed by EPA (2015) as a working fluid that is acceptable for use with low risks for staff and the environment; therefore this has been chosen as the working fluid in the BC unit.

[2]This refers to a fluid which has a T-s curve that curves inwards on the steam side.

5.2.2 Single flash

In a single flash plant the water has been flashed once as the name suggest. The flash process is when the pressurised geothermal fluid is transformed to a mixture of both liquid and steam, which is done by lowering the pressure. The flashing of the fluid can take place in various places. It can happen in the reservoir as the fluid ascend to the surface which is accompanied by a pressure loss, as described in chapter 1; it can also happen at any place in the well, as a pressure loss can exist due to friction. The last place the fluid can flash is at the wellhead or just before entering the separator due to a controlled throttling valve (DiPippo, 2012a). In this project it has been assumed that the flashing is a controlled flashing which occurs in the wellhead.

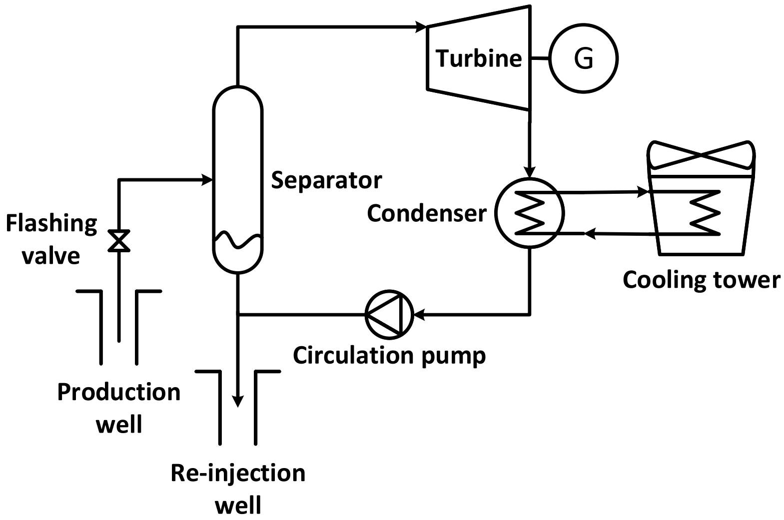

Figure 5.6: A simple and standard SF power plant. (DiPippo, 2012a).

The steam comes from the separator which has a moisture remover implemtet to remove the rest of moisture in the steam, this is done to ensure that the moisture content of the steam is less 0.01 % (Jóhannesson, 2016) (DiPippo, 2012a). When the moisture has been removed, the steam enters the turbine and power is generated, as seen in figure 5.6. After the turbine the expanded steam enters the condenser. In geothermal fluid there are gasses which are non-condensable (NCG) which will be removed by a steam ejector. The water after the condenser is then either used as feed water in a open cooling tower or re-injected if the cooling tower is closed , as in figure 5.6 DiPippo (2012a). The water from the separator is also re-injected.

5.2.3 Multiple flash

The multiple flash unit has several flashings, hence the name. At present there are double and triple flash power plants (DiPippo, 2012a), but there are research suggesting that at ultra high temperature geothermal fields, a quadruple flash might be possible (Bertani, 2015). In this report the multiple flash is a double flash as only two wells are in the classification ultra high. A simplified DF can be seen in figure 5.7.

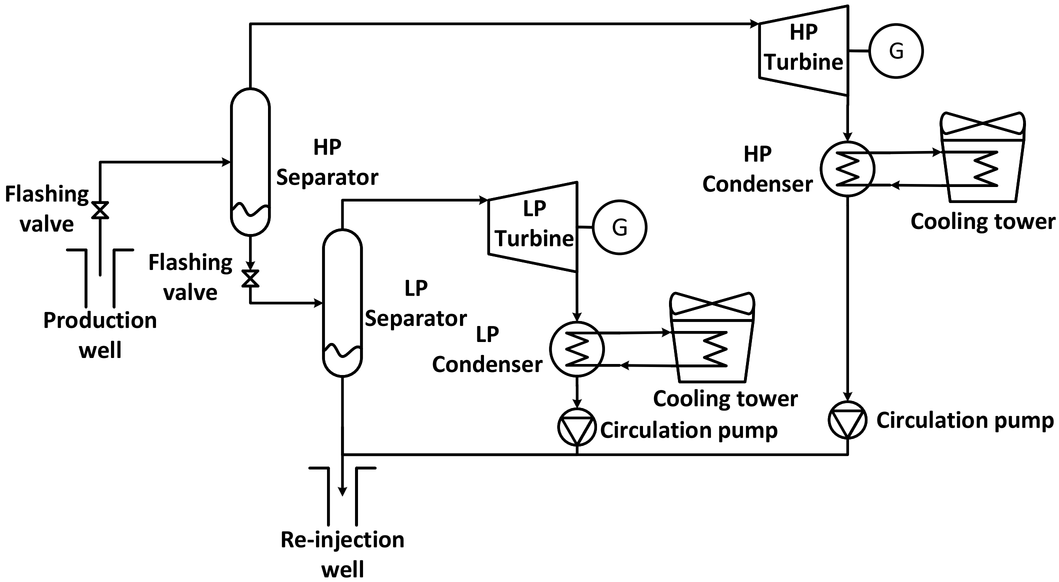

Figure 5.7: A simple and standard DF power plant with one turbine. (DiPippo, 2012a).

The design of a double flash is the same as a single flash. The steam from the separator enters the turbine followed the condenser and steam ejectors. The difference of the DF and the SF lies in the utilisation of the liquid phase from the separator. The liquid phase is flashed again, the steam from this second flash is thereby utilised in a LP turbine and goes through the same process as the steam from the first flash. The steam from the second flash can be utilised in different ways, it can be used in the same turbine or in a second turbine and thereby a second condenser is needed.

There are some environmental aspects that need to be taken into considerations when designing flashing units; mostly the risk of large air and water pollution. Unlike BC units flashings units emit some non-condensable gases such as H_2S and CO_2, these can give nuisances with regards to smells, which many areas with geothermal activities experience. Most of these gases will be treated before being let into the atmosphere but the smell will most likely still be present (DiPippo, 2012a). Water pollution is today easier to deal with as re-injection wells are more common than earlier. This means that the waste water pools are being phased out, but there can still pose problems with water pollution. The geothermal fluid often consist of different chemical elements that can contaminate the ground water if not treated carefully. These elements include:

- Arsenic
- Boron
- Calcium
- Chloride
- Fluoride
- Lithium
- Magnesium
- Potassium
- Silicon
- Sodium

If these elements enter the ground water it can be very dangerous, especially with the arsenic as this is a highly toxic element. Boron and lithium can, in pure form or in contact with water, also pose health risks (Lenntech, 2017). The main way to prevent water pollution is to re-inject the water instead of surface pools for the waste water (DiPippo, 2012a).

5.2.4 Hybrid

The plant types just described in the previous sections are only the simple versions of these plants. There are many different ways of designing a geothermal power plant. It has been found through literature studies that there are almost as many different designs as there are authors. The BC, SF and DF plants can be build in different ways. In ORC plant a recuperator can be used to preheat the fluid before enter the preheater and thereby the temperature of the geothermal fluid can be even lower and still be able to heat the working fluid to a gas.

The DF can also be designed in different ways, with a single or double flow turbine, this affects the number of components but also the reliability of the plant. A DF can also be designed with two turbines and only one condenser, so that the fluid mixture from the high pressure turbine connect with the low pressure steam and thereafter enters the low pressure turbine.

The single flash system has fewer ways to be designed as it is a more simple design. The biggest differences are the different ways to combine the components, for example using a backpressure turbine and thereby avoiding to have a condenser and steam ejectors as it is led directly out in the atmosphere.

To ensure to get the maximum energy out of the geothermal fluid a hybrid power plant can also be designed. A hybrid design can be made by using the flashing units as top units and the waste water, which is still relatively warm, to power an ORC unit. Another way could be to combine the waste water from the different units and then powering a ORC or other alternative uses. The hybrid design is also more suitable to utilise the plant for heat, as there will be multiple heat sources within the plant.

It has been chosen to design the simple unit for the universal power plant as this would be more applicable around world. The units will be combined for the final power plant design, and hybrid units, such as adding a bottom BC unit may be utilised if suitable.

5.3 Components

The components in the different designs of BC, SF, DF or a hybrid are the same components, but there are different types of these components and advantage and disadvantages for the different types as well.

5.3.1 Separator

The separator does, separate the fluid mixture into steam and water. There is two overall ways to design a separator, a cyclone separator, with either top and bottom outlet, and a gravity separator, which can be both horizontal and vertical. The cyclone separator is the separator which is oldest and therefore most used (Jóhannesson, 2016). Since the 1990 the gravity separators are more and more utilised.

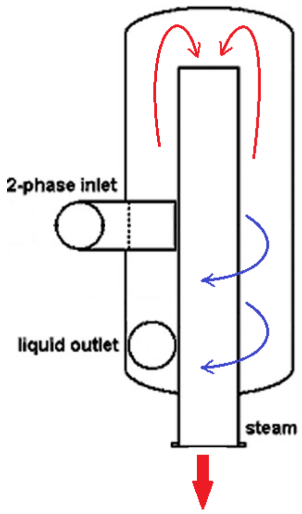

Figure 5.8: Illustration of a cyclone separator, blue indicates liquid and red indicates steam (DiPippo, 2012a).

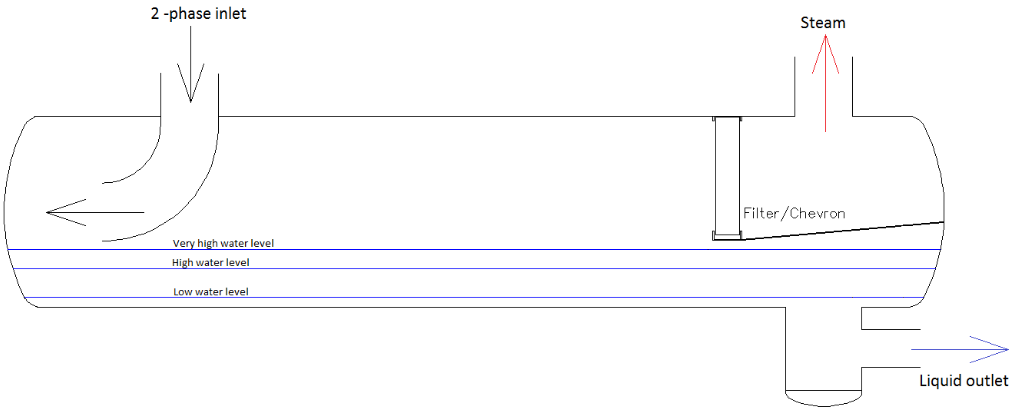

Figure 5.9: Illustration of a gravity separator, blue indicates liquid and red indicates steam (DiPippo, 2012a).

The cyclone separator uses the centrifugal force to separate the liquid and steam, see figure 5.8, the liquid with the highest density will be forced to the walls of the separator and the steam goes to the center and up. The gravity separator is using the gravity to separate the fluid, see figure 5.9, the liquid will be collected in the bottom of the separator and the steam will go out in the top (Jóhannesson, 2016).

The gravity separator has been chosen as separators as the mass flow range is larger, and the visual impact is lower and therefore it would be easier to build in most countries.

5.3.2 Turbine

There are some features that a geothermal turbine should be compared to a turbine in, say, a conventional power plant. These types of turbines need to be made of material that is corrosive resistant due to that chemical composition of the geothermal fluid, the main culprit here is the content of H_2S. Another thing to consider is that, unlike other power plants, the steam in a geothermal power plant is not superheated, this means that during the expansion of the steam droplets will form and this will cause damage to the turbine blades. This is especially a problem in the last stages of the turbine, therefore the blades in the last stages has to be reinforced (DiPippo, 2012a).

There are two types of turbines that can be used, these are the reaction turbine and the impulse turbine. There are advantages and disadvantages for both. The main difference is that in the impulse turbine the steam expands in the moving blade, while in a reaction turbine the steam expands in both the stationary and the moving blades, see figure 5.10 (Munson et al., 2013).

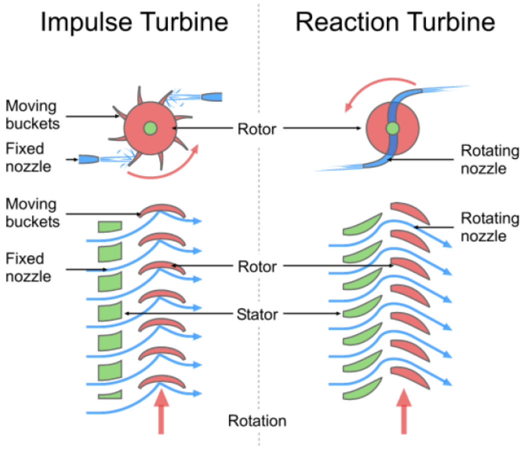

Figure 5.10: Illustration of a impulse and reaction turbine (Jóhannesson, 2016).

It has been decided to use an impulse turbine as this is the most used turbine in geothermal power plants (DiPippo, 2012a). The turbine used in Nesjavellir is also an impulse turbine (Jóhannesson, 2016). The impulse turbine can be a double or single flow turbine. It has been chosen to have a double flow as the blades can be smaller and thereby the corrosion is lower. This is important as there is already relative much corrosion in a geothermal power plant due to the chemical composition of the geothermal fluid (Jóhannesson, 2016). It was also found in the literature study that most of the turbines in geothermal power plants are double flow.

The temperature in a geothermal power plant is relatively low compared to others power plants such as conventional power plants. This means that during the expansion the quality of the steam will decrease, making the steam wet. The wetter the steam is the higher the erosion will be and thereby damaging the turbine. Another problem with this is that the efficiency is getting lower as well. The quality at the turbine outlet can therefore not be under 0.85 as the erosion will become to large and the efficiency to low (Haywood, 1975). Acording to Baumann (1921) the efficiency of the turbine will decrease 1% for each percentage the quality decrease.

5.3.3 Condenser

There are two types of condensers, surface-to-surface- and direct-contact condensers, see figure 5.11 for illustration. The condensers are used after the turbine to get the fluid to a liquid state again. The surface-to-surface is a heat exchanger in which the cooling water and steam is not in contact. There are different types of surface-to-surface heat exchanger, such as shell-and-tube and plate heat exchanger which is the most used in geothermal power plant (Çengel et al., 2012) (DiPippo, 2012a). In the direct contact heat exchanger the steam and water is in contact, which means these two are mixed and in that way the steam will condensate (DiPippo, 2012a).

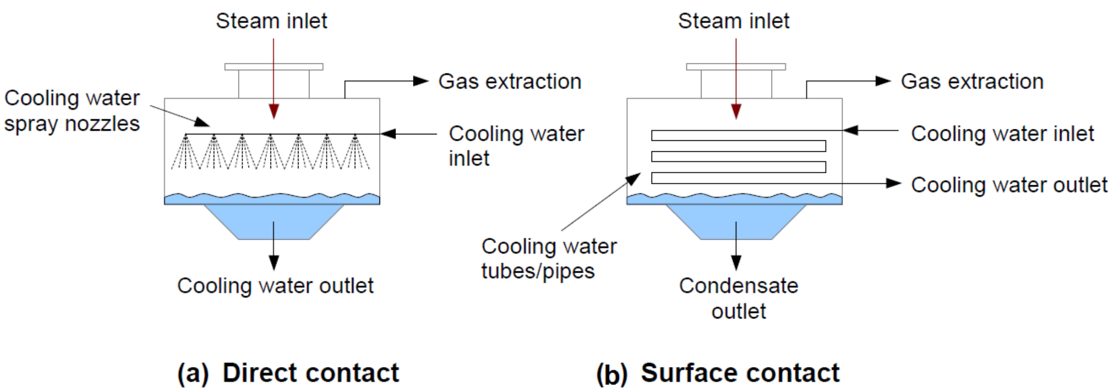

Figure 5.11: Illustration of a direct-contact heat exchanger heat exchanger (a) and a surface-to-surface (b) (Jóhannesson, 2016).

The surface-to-surface heat exchanger is a type of heat exchanger which is used in many different applications, but the basics is that the steam from the turbine and the cooling water are separated by either plates or pipes. In the geothermal area the surface-to-surface heat exchanger is always used as the boiler component in the BC unit (DiPippo, 2012a). The direct heat exchanger has advantages over the surface-to-surface, such as the heat transfer is better and the capital cost is lower (Jóhannesson, 2016). There are however more disadvantages, such as the cooling water is not suitable for district heating, and the condensate water can only be recovered in the cooling tower.

It has been decided to use a surface-to-surface heat exchanger. This has been chosen for the main reason to secure that the design can be changed easily to fit countries with district heating. It has been chosen to use a shell-and-tube heat exchanger, see figure 5.12, as this is the heat exchanger most used in the geothermal industry (DiPippo, 2012a).

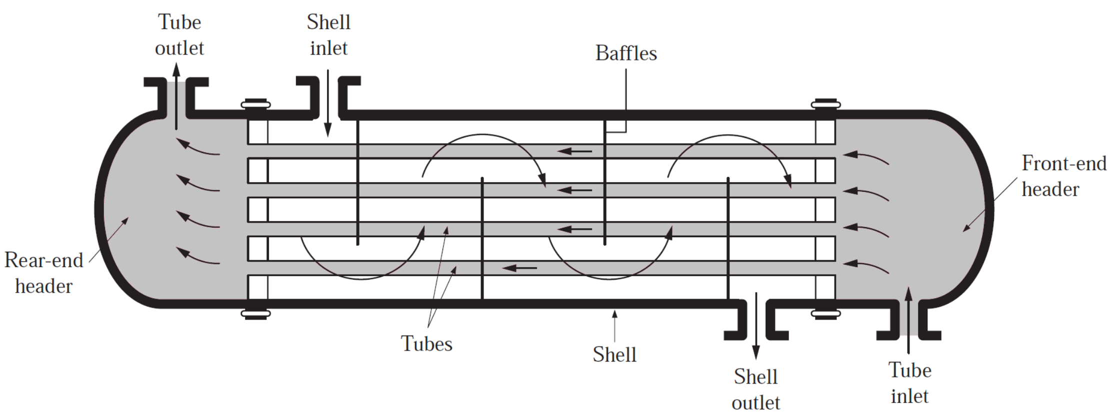

Figure 5.12: Shell-and-tube heat exchanger (Çengel et al., 2012).

In the condenser the NCG extraction also takes place. The gas extraction is necessary as the NCG needs to be excluded from the system, before the geothermal fluid is pumped back into the ground (DiPippo, 2012a). There are different ways to remove NCG, such as a vacuum pump, steam ejector or a compressor (Jóhannesson, 2016). A compressor has been chosen to remove the NCG. It has been assumed that the NCG are only CO_2, as this is the most common and the total NGC that represents the major part of the NGC (Pálsson, 2014). The NGC accounts for 1%-4% of the total mass flow (Jóhannesson, 2016). The gas extraction only takes place in flashing units, and if the unit is a DF the gas extraction would only be in the HP cycle.

5.3.4 Cooling tower

The cooling tower is connected to the condenser and the water is used as the cold side of the condenser. The cooling towers can be constructed in different ways. There are overall two types, the wet and dry cooling tower, see figure 5.13 and 5.14. Furthermore the flow in a cooling tower can be natural, induced, and forced draft. The most common type of cooling tower is the wet natural draft.

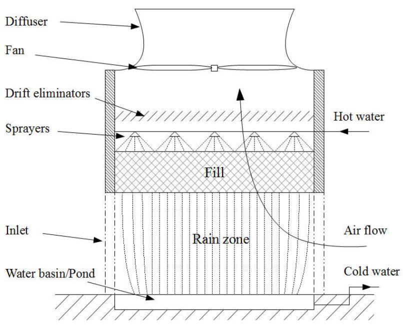

Figure 5.13: Wet cooling tower with induced draft (Jóhannesson, 2016).

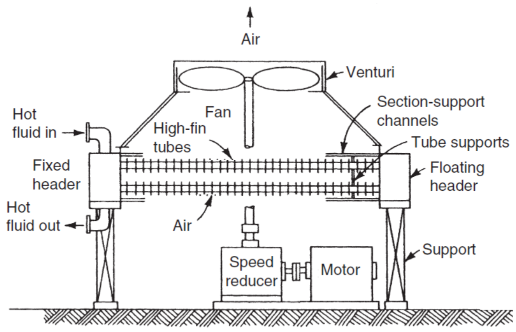

Figure 5.14: Dry cooling tower with induced draft (Serth and Lestina, 2014).

The wet cooling tower utilises the colder surrounding air by means of the air flows through the warmer water and thereby cools the water. The wet cooling tower is the most used cooling tower as it is very efficient. The problem with this cooling tower is the water can evaporate, therefore make-up water is an important source, and in areas with little water a wet cooling tower can pose a even bigger problem, as water can be scare (Jóhannesson, 2016).

The dry cooling tower was not as often used, but it is now used more and more because the visual impact has larger influence when designing geothermal power plants today, as the wet cooling tower emits more steam from the fans than the dry cooling tower (DiPippo, 2012a). Another advantages with the dry cooling tower is that the cooling water is a closed system, and thereby the water will not evaporate in hot climates or freeze in cold climates.

There are mainly three ways to create the draft for cooling as mentioned. The most normal is the induced draft (DiPippo, 2012a). The induced draft is utilised by means of a fan, the fan sucks the air through the water or water pipes, see figure 5.13 and 5.14. In the forced draft a centrifugal fan forces the air through the the water or water pipes, see figure 5.15, this type of draft is not often used in larger scales and thereby not much used in geothermal power plants. It is mostly used if there is a limited amount of space available (DiPippo, 2012a). The last draft way is the natural draft (Jóhannesson, 2016). The natural draft cooling towers is very large, see figure 5.16. The advantages with the natural draft is that there is little or no electricity needed in the cooling towers, on the other hand these types of cooling towers has a large visual impact and therefore these cooling towers not often used (DiPippo, 2012a) (Jóhannesson, 2016).

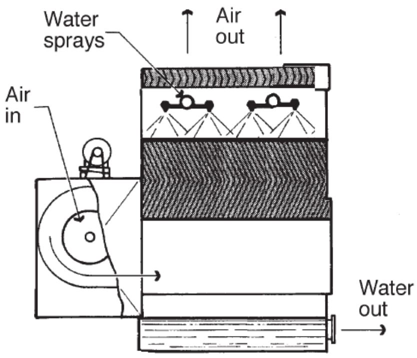

Figure 5.15: Illustration of wet cooling tower with forced draft (Jóhannesson, 2016).

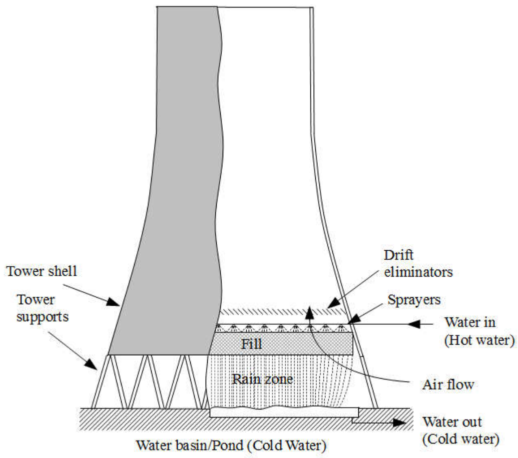

Figure 5.16: Illustration of wet cooling tower with natural draft (Jóhannesson, 2016).

It has been chosen to use dry induced draft cooling towers, so that the designed power plant can be utilised as many places as possible. By using the dry induced draft cooling tower, the climate is of less concern as the cooling water is in closed and therefore not at risk for evaporating in areas with scare water supply.

5.4 Final designs

To summarise the decisions made in this chapter in regards to the components and designs of the power plant.

The designed power plant will consist of three units, a binary cycle, a single flash and a double flash. The single flash and double flash unit each has a bottom binary unit to utilised the energy in the geothermal to the fullest. There is also included district heating as this is more and more widely utilised around the world (Bertani, 2015) The final system can be seen in figure 5.17.

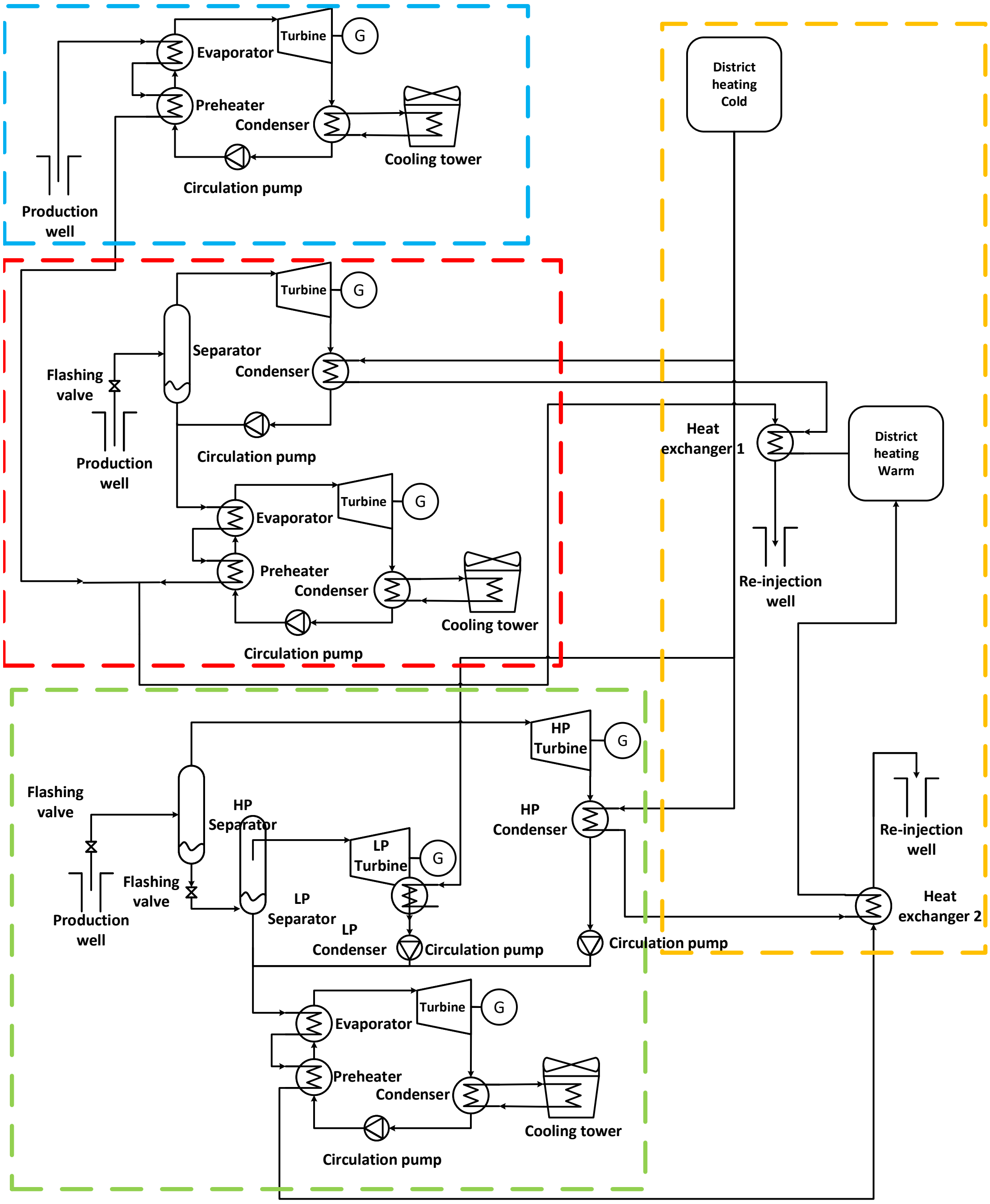

Figure 5.17: The final design of the model, the blue framed part is the BC unit, the red framed part is the SF unit, the green framed part is the DF and the orange framed part is the district heating

CHAPTER 6

Modelling of units

To model the total system the single units have to be modelled first. It has been assumed that there are three units, one BC unit, one SF unit and one DF unit. The final design consists of three BC, one SF and one DF, therefore these types of units has been modelled and optimised, to be used later in the final design.

There has been made some assumptions in regards to the components. The assumption made is that the heat loss due to radiation and spurious sources in the components can be neglected, as it is assumed to be relatively small in steam power plant, 1-2% (Condra, 2017). The pressure loss in the condensers has been assumed to be neglectable as well.

6.1 Component modelling

The components in the different units are modelled the same way, therefore there are eight different components that have been modelled.

Flashing process

For first process for the flashings units is the throttle valve. The valve is placed at the well head in this report. As is has been mentioned in chapter 5, the fluid from the well is at liquid state, therefore the flashing process also starts on the saturation line. The flashing process means that the pressure is decreased through the valve, see figure 6.2. It has been assumed that the process is a isenthalpic process as the flashing is spontaneous, steady and adiabatic (DiPippo, 2012a):

$$h_1 = h_2 \tag{6.1}$$

where:			
	h	Enthalpy	(J/kg)

The flashing process on a T-s diagram can be seen in figure 6.1.

It has been assumed the there is not losses in this process.

Separator

When the fluid has been flashed it enters the separator, which separates the liquid from the gas. It has been assumed that there is a pressure loss in the separator of 1 bar (DiPippo, 2012a). The separator will spilt the mass flow into two, the steam going into the turbine and the liquid going into a new flashing valve or a re-injection depending on the unit. The mass flows are modelled by equations 6.2 and 6.3 for the steam mass flow and the liquid mass flow respectively.

$$\dot{m}_2 = \dot{m}_1 \cdot x_1 \tag{6.2}$$

$$\dot{m}_3 = \dot{m}_1 \cdot (1 - x_1) \tag{6.3}$$

where:			
	ṁ	Mass flow	(kg/s)
	x	Steam quality	(kg/kg)

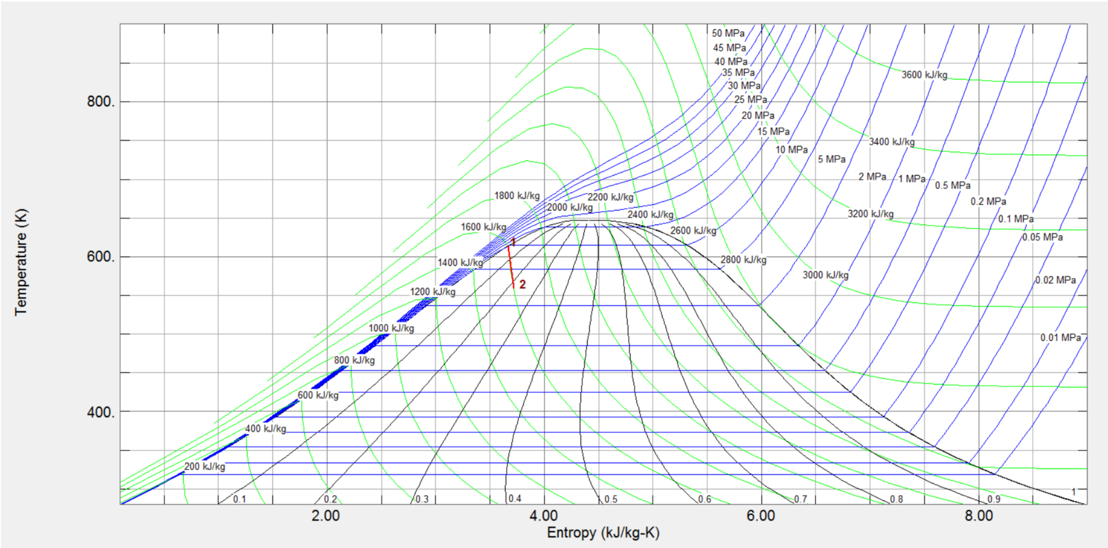

Figure 6.1: The flashing process in a T-s diagram with water as fluid.

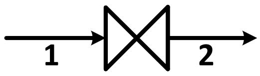

Figure 6.2: Throttle valve used for the flashing process.

An illustration of the separator can be seen in figure 6.3 with the subscripts used in the equation above. The corresponding T-s diagram for the separation process can be seen in figure 6.4.

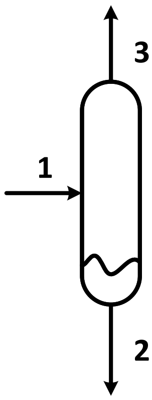

Figure 6.3: The separator.

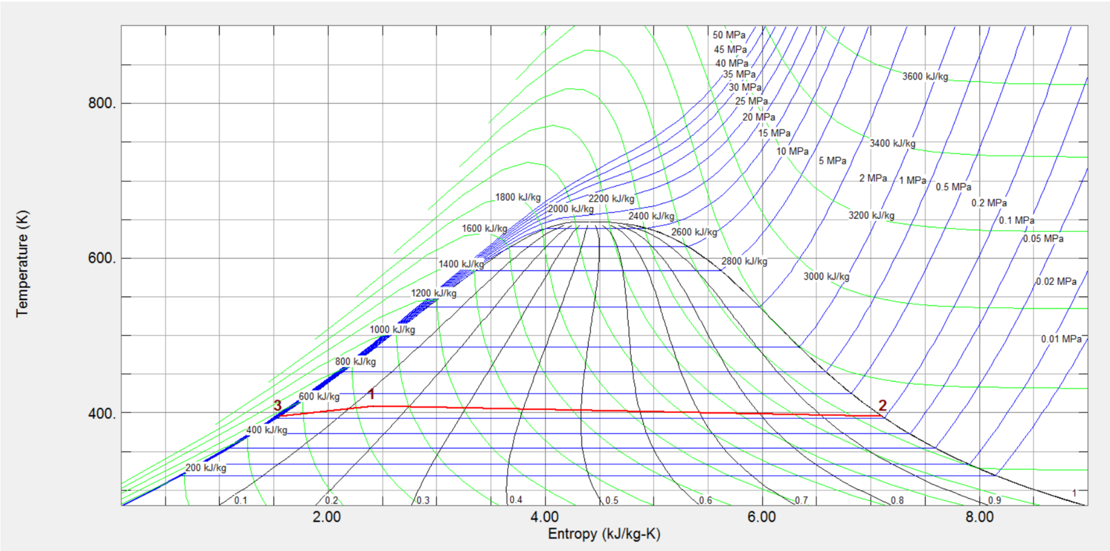

Figure 6.4: The separation process in a T-s diagram with water as fluid.

Evaporator and preheater

In a BC unit the fluid from the wells is not flashed and therefore a flashing valve and separator are not needed. Instead the fluid is lead through an evaporator and preheater to heat the working fluid in the ORC, see figure 6.5 for illustration and figure 6.6 for the process on a T-s diagram.

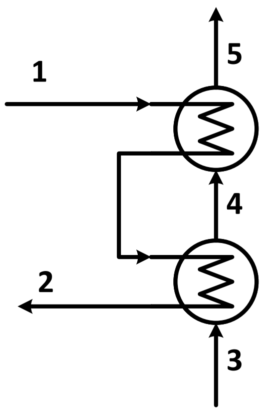

Figure 6.5: Illustration of a preheater (bottom heat exchanger) and a evaporator (top heat exchanger).

It has been assumed that there is no pressure loss in these components either, therefore:

$$P_1 = P_2 \tag{6.4}$$
$$P_3 = P_4 = P_5 \tag{6.5}$$

where: P | Pressure (Pa)

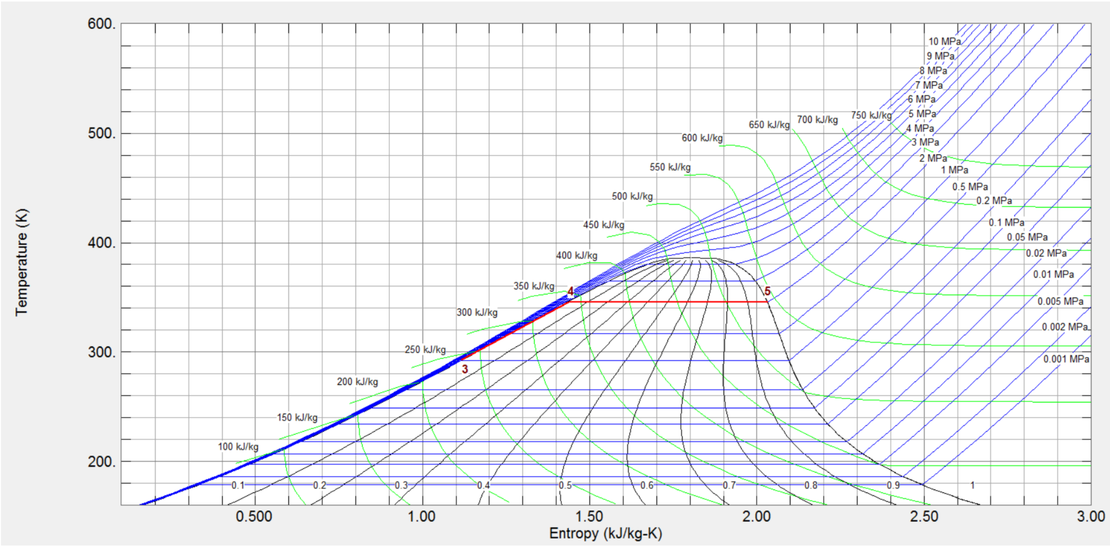

Figure 6.6: The preheater and evaporator process in a T-s diagram with R152a as fluid.

It has been assumed that all the heat transferred from the fluid, see equation 6.6, is absorbed by the working fluid, thereby the heat transferred to the working fluid can be written as equation 6.7.

$$\dot{Q}_f = \dot{m}_1 \cdot (h_1 - h_2) \tag{6.6}$$

$$\dot{Q}_f = \dot{m}_{R152a} \cdot (h_5 - h_4) + \dot{m}_{R152a} \cdot (h_4 - h_3) \tag{6.7}$$

where: $\dot{Q}$ | Heat transfer rate (W)

Equation 6.7, is used to determine the mass flow for the working fluid.

Turbine

After the separator or the evaporator the steam is entering the turbine, it is assumed that the steam entering has a quality of 1, i.e. x = 1, and is thereby pure steam. The steam is not superheated in any of the processes. As the steam is not superheated the outlet steam will be wet, therefore the efficiency for the turbine will decrease as well. An illustration of the turbine model can be seen in figure 6.7 and the T-s diagram for the process can be seen in figure 6.8.

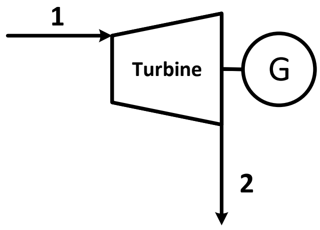

Figure 6.7: A turbine.

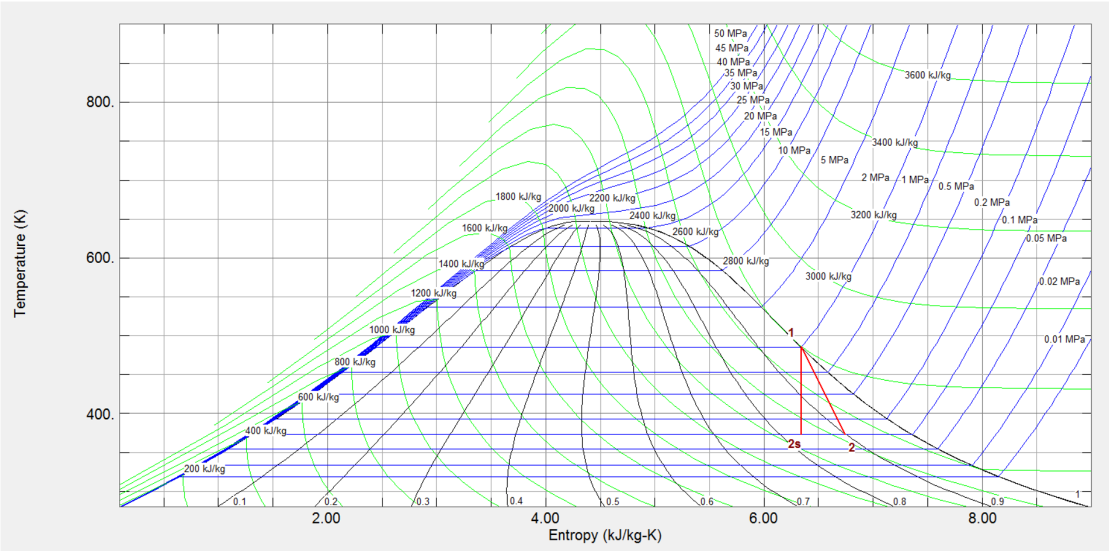

Figure 6.8: The steam expansions process in a T-s diagram with water as fluid. The "s" indicates an isentropic process.

The turbine has been modelled as a real process and not an isentropic, i.e. $s_1 \neq s_2$. When the steam expands the wetness of the steam (1-x) increases through the turbine and therefore the efficiency decreases. The Baumann rule (Baumann, 1921), equation 6.8 represent the phenomena which and states a direct relation between steam wetness and turbine efficiency, also known as wet turbine efficiency.

$$\eta = \eta_0 - \frac{1 - x_2}{2} \tag{6.8}$$

where:			
	η	Efficiency	(-)
	η_0	Dry turbine efficiency	(-)

The dry turbine efficiency has assumed to be 85%, based on DiPippo (2012a).

The Baumann rule can be rewritten to define the real quality of the steam at the turbine outlet, by using the definitions of the enthalpy of steam at turbine outlet. The steam quality at the turbine outlet can be found by equation 6.9.

$$x_2 = \frac{h_1^g - h_2^l - (\eta_0 - \frac{1}{2})(h_1^g - h_2s)}{h_2^g - h_2^l + \frac{h_1^l - h_2s}{2}} \tag{6.9}$$

By using equation 6.9, the real process is calculated, this is shown as (2) in the T-s diagram in figure 6.8. The turbine power output is defined by the mass flow through the turbine multiplied by the enthalpy difference, as in equation 6.10, where it is assumed that the mass flow through the turbine is constant, $\dot{m}_1 = \dot{m}_2$.

$$W_t = \frac{\dot{m}_1 \cdot (h_1 - h_2)}{\eta_t} \tag{6.10}$$

where:			
	W	Power	(W)
	η_t	(-)	

The turbine power output is not the total power plant output, as it has to cover the power losses from pumps and cooling fans motors etc.

Condenser

The condensers are located after the turbine in each unit. The condensers used are a surface-to-surface heat exchangers as described in chapter 5. It has been assumed that there is no pressure loss in the condensers $P_1 = P_3$ and $P_2 = P_4$; see figure 6.9 for the subscripts. As it is a condenser the temperature of the steam will not change either, see figure 6.10.

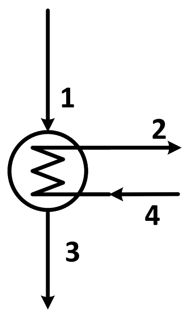

Figure 6.9: A condenser.

A pinch temperature difference of 5 K has been set based on a qualified estimation by the author. The energy balance for the condenser is given as equation 6.11 and constant mass flow on both side of the condenser has been assumed.

$$\dot{m}_1 \cdot (h_1 - h_3) = \dot{m}_2 \cdot (h_2 - h_3) \tag{6.11}$$

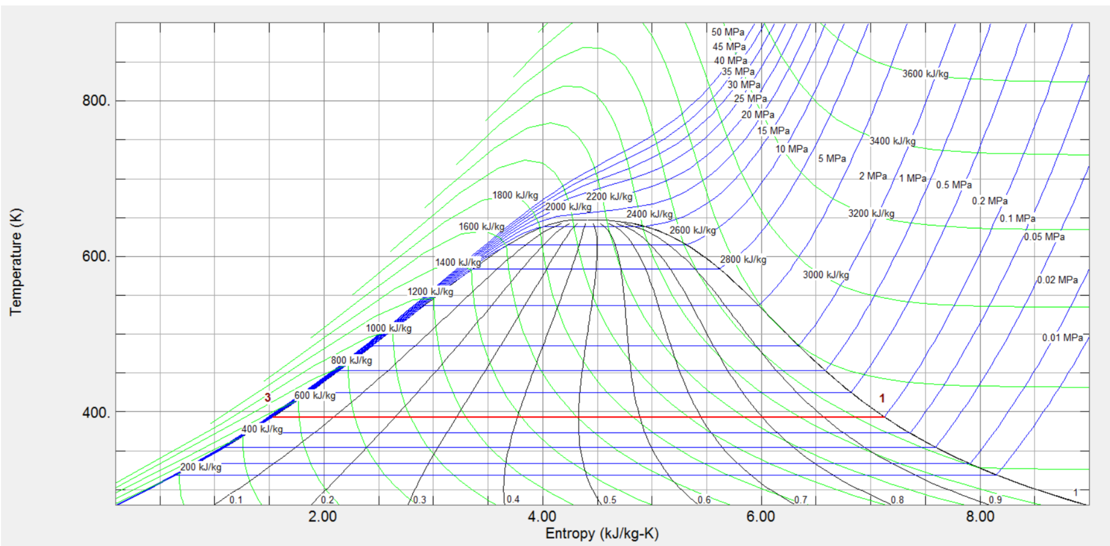

Figure 6.10: The condensation process on the steam side.

Cooling tower

The cooling tower is an air cooling tower as described in chapter 5. The cooling tower is essential an air-cooled heat exchanger. It has been assumed that the ambient temperature is 5°C and there is a pinch temperature of 5 K as well. This means that the cooling water into the condenser is $T_2 = T_{amb} + 5$ K and the temperature after the fans has been set as $T_4 = T_1 - 5$ K, see figure 6.11. The cooling tower is a counter flow, see figure 6.11.

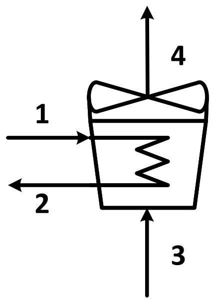

Figure 6.11: Illustration of a dry induced cooling tower .

The needed fan power is found by equation 6.12. Further detail for the power consumption can be seen in appendix C, where the dimensions for the cooling tower is also calculated.

$$W_{fan} = \frac{\Delta P \cdot \dot{V}_{fan}}{\eta_{fan}} \cdot N_{CT} \tag{6.12}$$

where:			
	$\dot{V}$	Volumetric flow rate	(m^3/s)
	N_{CT}	Number of cooling fans	(-)

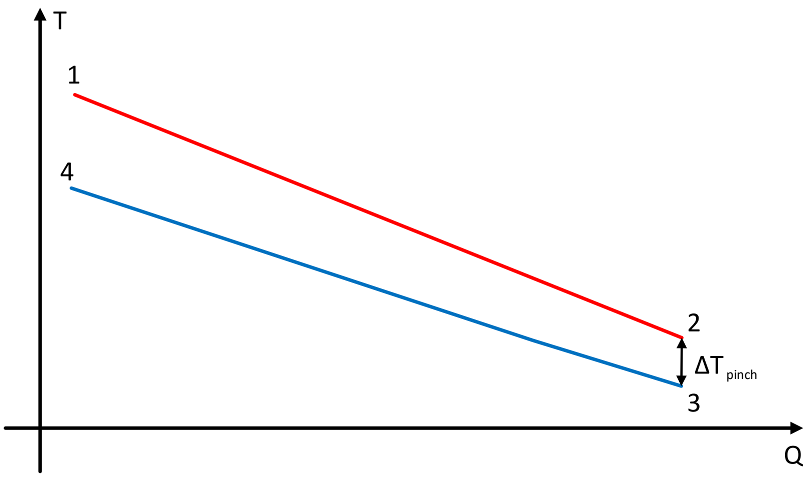

Figure 6.12: The T-Q diagram for the cooling tower.

Pumps

In the BC unit a circulation pump is installed, to circulate the working fluid. In the flashing units pumps are installed after the condenser to pump the water back in the re-injection wells. In figure 6.13 and 6.14, an illustration of the pump and the process in a T-s digram is seen respectively.

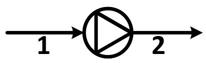

Figure 6.13: Illustration of a pump.

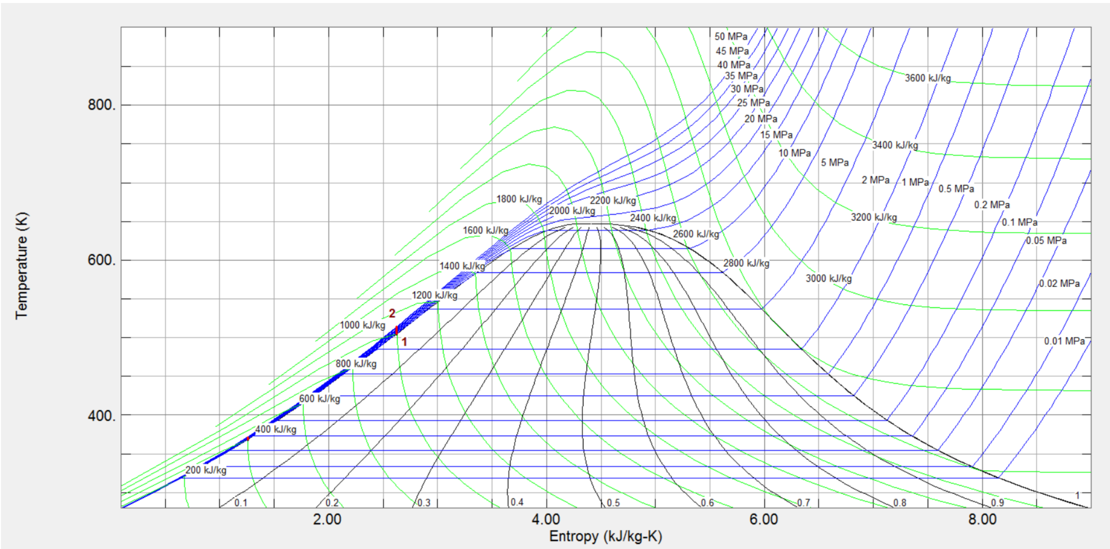

Figure 6.14: The T-s diagram for the pumping process.

The power consumption of the circulation pump and re-injection pump is found as equation 6.13

$$W_p = \frac{\dot{m}_1 \cdot (h_2 - h_1)}{\eta_p} \tag{6.13}$$

To circulate the cooling water a circulation pump is used. The power consumption for the cooling water pump is calculated using equation 6.14.

$$W_{p,CW} = \Delta P \cdot \dot{V}_{CW} \tag{6.14}$$

The pressure loss in the cooling water circuit has been estimated to be 1 bar (DiPippo, 2012a).

Power

The total power output is the turbine power with the electricity required to operate the power plant subtracted.

$$W_{tot} = W_t - W_{req} \tag{6.15}$$

The required power to operate the power plant is the power used by the pumps, the fans etc.

The efficiency of a geothermal power plant can not be found with the thermal efficiency as it is not a closed system. To find the efficiency of a geothermal power plant the second law of efficiency is used (DiPippo, 2012a). The second low of efficiency describes how well a systems preform in respect to the theoretical maximum performance. The second law of efficiency is described as equation 6.16.

$$\eta_{II} = \frac{W_t}{\dot{m}_1 \cdot (h_1 - h_0 - T_0 \cdot (s_1 - s_0))} \tag{6.16}$$

Where the subscript 0 denotes the geothermal fluid properties in the well and the subscript 1 denotes the cooling water properties into the condenser.

6.2 Unit models

The units that are modelled is a BC, SF and DF unit. The input, temperature, pressure and mass flow, to the units have been assumed constant all year around as the changes is no larger than 2% throughout the year (Jóhannesson, 2016). The models have undergone a parameter optimisation to find the best design parameters.

6.2.1 Binary cycle model

The binary cycle has been modelled with the components described i section 6.1. The binary unit is designed as in figure 6.15.

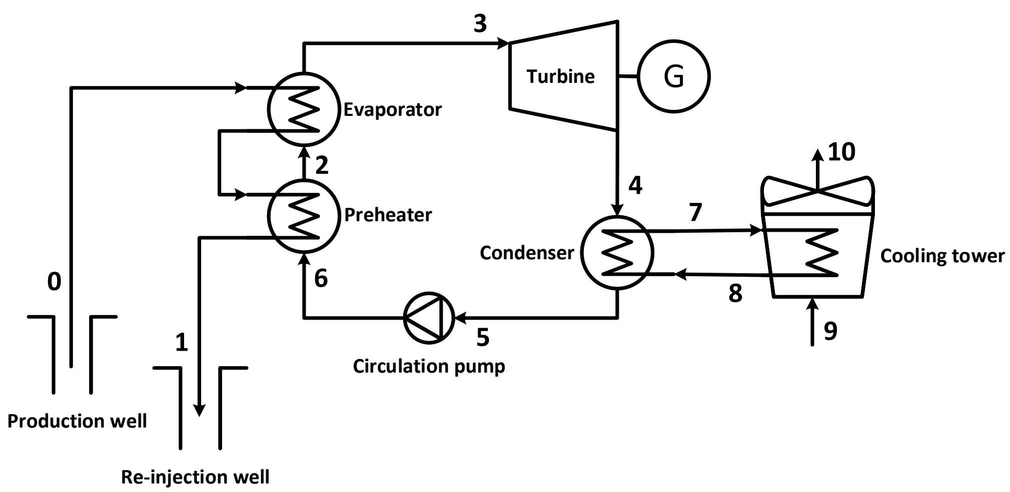

Figure 6.15: The model BC unit.

A parameter optimisation is conducted to find the largest power output, the design parameter which is varied is the pressure in the evaporator (P_2) and turbine outlet (P_4). The temperature from the BC wells, subscribed 0, has a temperature of 121.5°C, a pressure of 2.08 bar, and a mass flow of 237 kg/s. The working fluid in the BC unit is R152a as described in chapter 5.

In the parameter optimisation the pressure into the turbine (P_3) is varied between 4.6 bar and 20 bar. The maximum pressure at 20 bar has been based on DiPippo (2012a), the lowest pressure at 4.6 bar has been chosen to ensure that there is a pressure difference though the turbine so an expansion of the steam can occur. There have been 200 optimisation point generated between these two pressures which is estimated to be sufficient to calculate the largest power output.

The pressure in the condenser (P_4) is varied from 4.5 bar to 0.1 bar lower than the turbine pressure (P_3), this is therefore at the highest 19.9 bar for the parameter optimisation. This is done to ensure that the steam is actually able to expand even at the higher pressure. The pressure of 4.5 bar in the condenser, is the lowest the pressure can be, if the pressure was lower the temperature of the cooling water out of the condenser would be under 5°C and thereby the cooling water would transfer heat to the working fluid instead of absorbing it.

To summarise the parameter optimisation:

$$
\begin{aligned}
4.6\,\text{bar} \leq & P_3 \leq 20\,\text{bar} \\
4.5\,\text{bar} \leq & P_4 \leq (P_3 - 0.1)\,\text{bar}
\end{aligned}
$$

Another consideration was the quality of the steam after expansion, this could not be lower than 0.85. This was not found, however it was found that at many condenser pressures the quality was 1 or above according to the model. As this is not physically possible it was decided that qualities of 1 and above, after the steam expansion would not be taken into considerations. This is done based on the fact that the working fluid is not a retrograde and therefore it is assumed that the quality of the steam would be under 1 after the expansion.

The parameter optimisation was conducted and the pressure for the inlet to the turbine (P_3) and the condenser pressure (P_4) which gave the highest total power output was found. This is shown in figure 6.16.

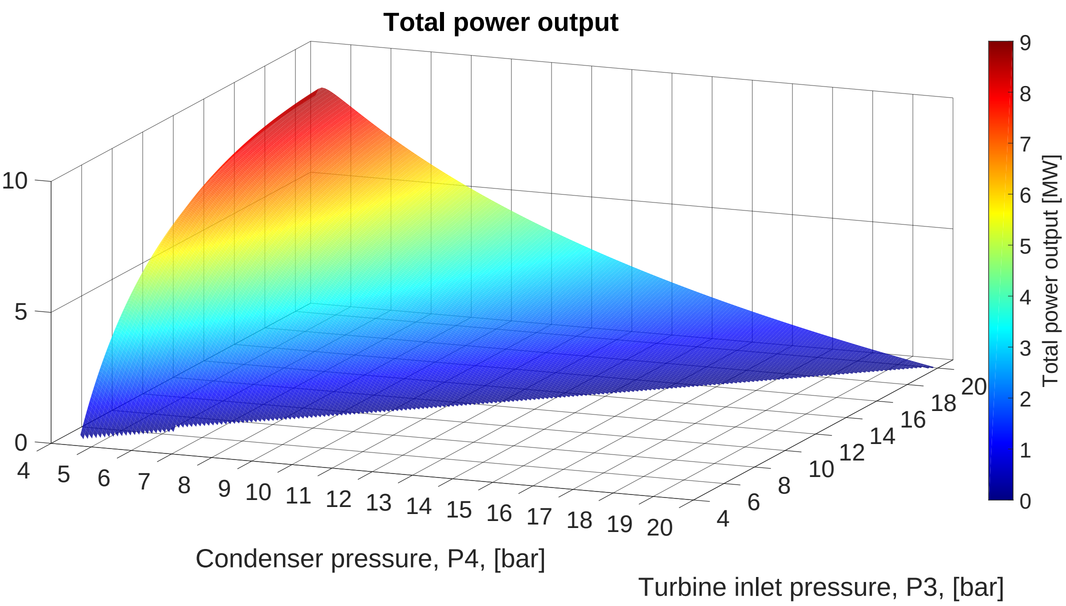

Figure 6.16: The parameter optimisation of P_3 and P_4.

It was found that the highest total power output is 8.64 MW_e, with an inlet turbine pressure of 20 bar, i.e. the highest possible pressure. The condenser pressure was 4.65 bar, not the lowest pressure. The reason for this is due to the cooling tower. When the pressure in the condenser is to low the temperature difference between the T_9 and T_{10} is very low, due to the pinch temperature between T_7 and T_{10} (T_{10} = T_7 - 5 K). This causes a high mass flow of the air and thereby the power needed to drive the fans to be equally high.

The pressure found is used to find the final design of the BC unit. The fluid properties at the different stages can be seen in figure 6.17.

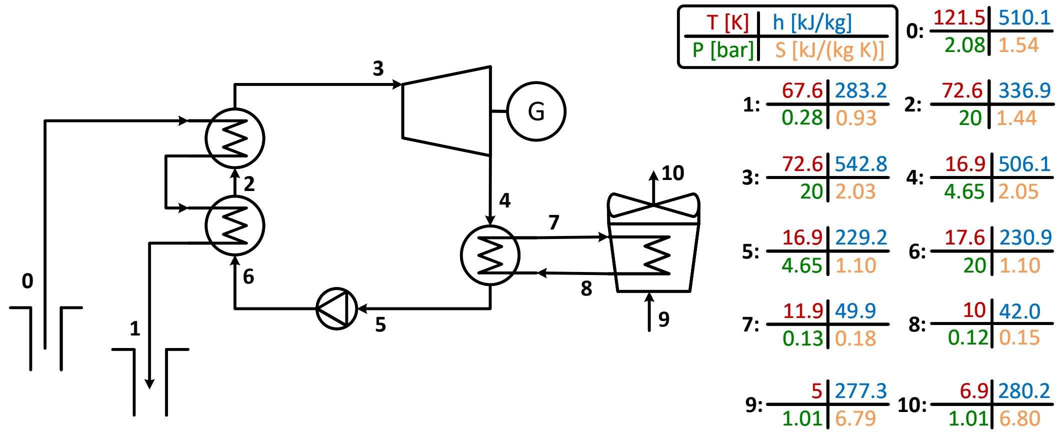

Figure 6.17: The final BC unit and its properties.

As power plants vary from plant to plant this model is difficult the validate. To validate the model the components has been looked at to investigate whether the results seem reasonable. A T-s diagram has been plotted to give a overview of the process, see figure 6.18.

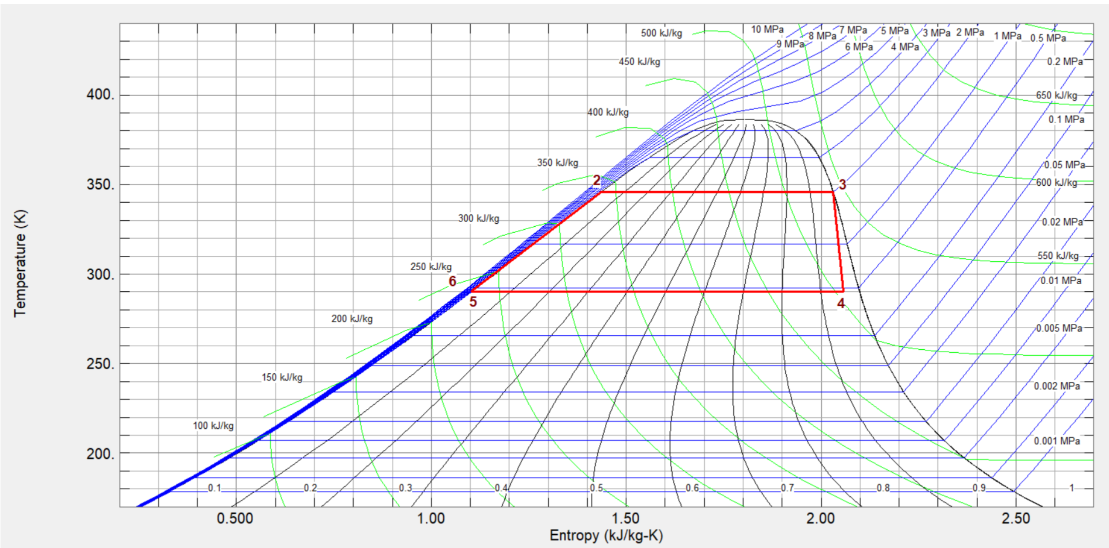

Figure 6.18: The T-s diagram for the BC process, the number indicates the subscribes at figure 6.17.

Figure 6.19 show that the preheater heats the fluid from 11.9°C to the saturation temperature at 72.6°C at 20 bar, from where it is evaporated in the evaporator. The preheater and evaporator cools the geothermal fluid from 121.5°C to 67.6°C. This process is seen in figure 6.19 and as the process from 6 to 3 in the T-s diagram at figure 6.18.

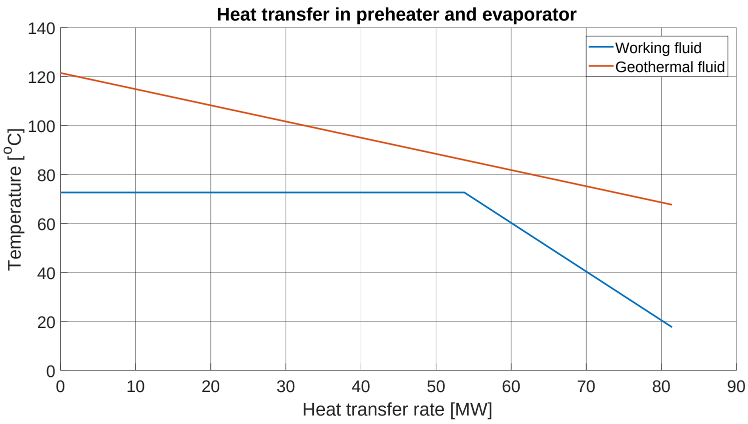

Figure 6.19: T-Q diagram for the process taking place in preheater and evaporator.

At the inlet to the evaporator it is seen in figure 6.19, that the pinch temperature is 5 K. Which was to be expected.

The temperature in the condenser and cooling tower does not change as much as in the preheater and evaporator, mainly due to the surrounding temperature which is estimated to be 5°C. The temperatures in the condenser and the cooling tower can be seen in figure 6.20 and 6.21 respectively. From figure 6.20 it is seen that the pinch temperature is at the inlet of the condenser on the steam side (T_4) and at the outlet temperature for the cooling water T_7.

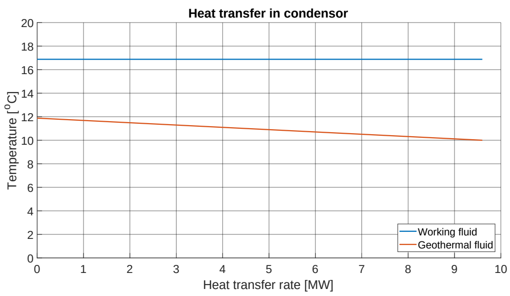

Figure 6.20: T-Q diagram for the process taking place in condenser.

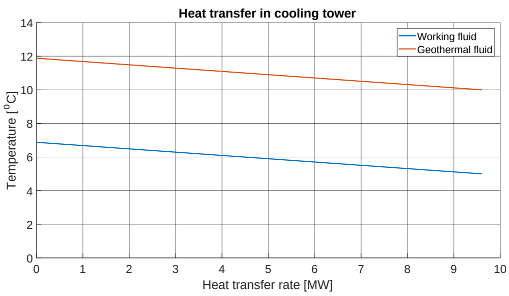

Figure 6.21: T-Q diagram for the process taking place in cooling tower.

For the cooling tower it is seen that the temperature difference is constant, this is due to the assumption that the air after the fans is 5°C lower than the water coming from the condenser (T_7) and that the cooling water into the condenser is 5°C higher than the ambient temperature. The main results of the unit is summarised in table 6.1. When investigating the results nothing seems to be unreasonable. The power output and the second efficiency is also within normal ranges for a BC system. The second law of efficiency for a BC should be between 15%-45%, (DiPippo, 2012b). For this model it is 45% and it makes sense it is in the high end as the model has been optimised to

Results for the optimised BC unit		
Temperature from the well	T_0	121.5 °C
Pressure from the well	P_0	2.08 bar
Evaporator temperature	T_2	72.6 °C
Evaporator pressure	P_2	20 bar
Condenser temperature	T_4	16.9 °C
Condenser pressure	P_4	4.65 bar
Quality of the steam after turbine	x_4	95.8%
Turbine power output	W_t	9.6 MW
The total required pump power	W_p	579.9 kW
Required power to drive the fans	W_{fan}	385.1 kW
Total power output	W_{tot}	8.64 MW
Plant efficiency	η_{II}	45%

Table 6.1: The main results from the optimised BC unit.

generated as much power as possible. The cooling tower has a size of 22.8 meters wide and 68.4 m in length. This seems very reasonable for a power plant placed in Iceland based on the authors experience, where only one cooling tower was needed for this unit.

When the model was optimised it was investigated whether there was certain mass flow which resulted in larger power output. This was done to see if there was a potential to have multiple units of the same type as the power output would increase. It was however found that the mass flow and the power output was proportional and the higher the mass flow was the higher the power output would be, therefore it was chosen to have one unit with the full mass flow through, to ensure the cost to be lower.

The maximum output as mentioned earlier is 8.64 MW_e. This is within the range of the BC power plants units around the world, however in the higher end, as the BC units are mostly used in geothermal fields which is of low temperatures. This combined with the results above it is deemed reasonable that the output is 8.64 MW_e.

6.2.2 Single flash model

The single flash model which has been modelled can be seen in figure 6.22. A parameter optimisation was also conducted on the this model. The parameters that was optimised was the pressure in the separator, i.e. the pressure which the fluid is flashed to (P_1). The other pressure optimised is the condenser pressure (P_3). The pressure from the SF wells are 16.70 bar, the temperature are 203.4°C and the mass flow is 290 kg/s, these are subscripted with 0.

The separator pressure (P_1) are varied from 1.2 bar to 16.6 bar and the condenser pressure are varied from 0.1 bar to 1 bar. The high pressure in the turbine is 0.1 bar under the pressure from the wells to ensure a two-phase mixture in the separator. The low pressure in parameter variable P_1 at 1.2 bar as there is a preesure loss of 1 bar in the separator and to ensure that the steam through the turbine are able to expand even at the lowest turbine pressure and the highest condenser pressure. The condenser pressure (P_3) is varied from 0.1 bar to 1 bar, the pressure at 0.1 bar are set based on Thorolfsson (2005), who says that a lower pressure would result in a too large cooling tower as the mass flow of the air would be very large.

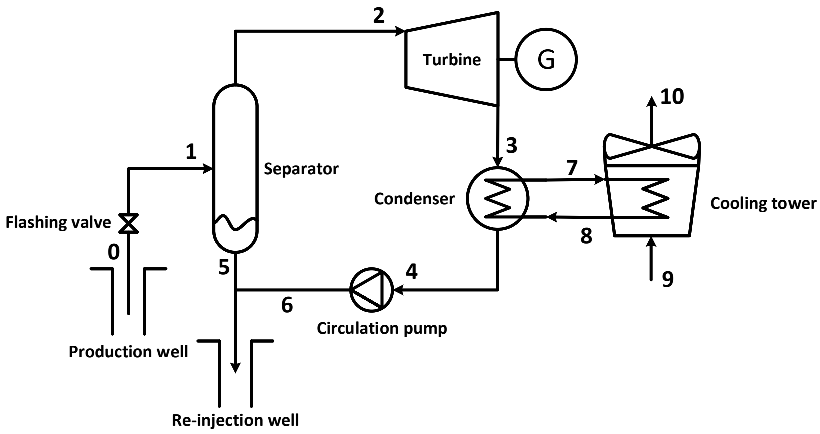

Figure 6.22: The model SF unit.

The quality of the steam at the turbine outlet (x_3) was also considered as a constrained parameter. The quality of the steam was not to be under 0.85, if the quality of the steam was under 0.85 the entry was not used for further calculations.

To summarise the design parameters:

$$1.2 \text{ bar} \leq P_2 \leq (P_0 - 10) \text{ bar}$$
$$0.1 \text{ bar} \leq P_3 \leq 1 \text{ bar}$$

The parameter optimisation was conducted and the separator pressure and the condenser pressure was found, the results is seen in figure 6.23.

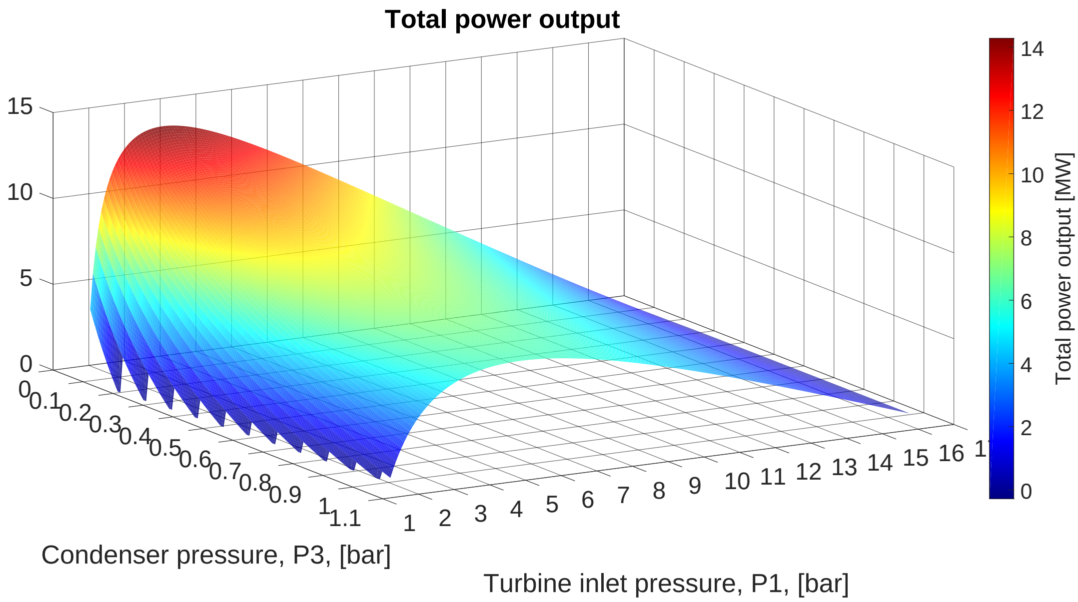

Figure 6.23: The parameter optimisation of P_1 and P_3.

The parameter optimisation gave a maximum power output of 14.3MW$_e$ at a separator pressure for 3.21 bar and a condenser pressure of 0.1 bar. It is seen that the condenser pressure is the lowest possible pressure. This could indicate that there is a lower pressure for the condenser which will give a higher input. This was investigated by varying the condenser pressure from 0.02 bar, which was the lowest possible to ensure values for the properties which made physically sense, and it was found that there was a lower pressure where total output was higher. This was at 0.04 bar for the condenser and 2.67 bar for the turbine pressure with a total power output of 18.4 MW_e, but the cooling tower would be very large (71 m x 213 m) as Thorolfsson (2005) predicted, therefore it was chosen to keep the minimum condenser pressure at 0.1 bar.

The peak in the separator pressure is due to turbine power output increasing slower the higher the pressure is, compared to the faster increase in the total required power to operate the pumps, fans, etc.

The found pressures in the parameter optimisation is now used to determine the optimised model. The optimised model process can be seen in the T-s diagram in figure 6.24 and the fluid properties at the different stages can be seen in figure 6.25.

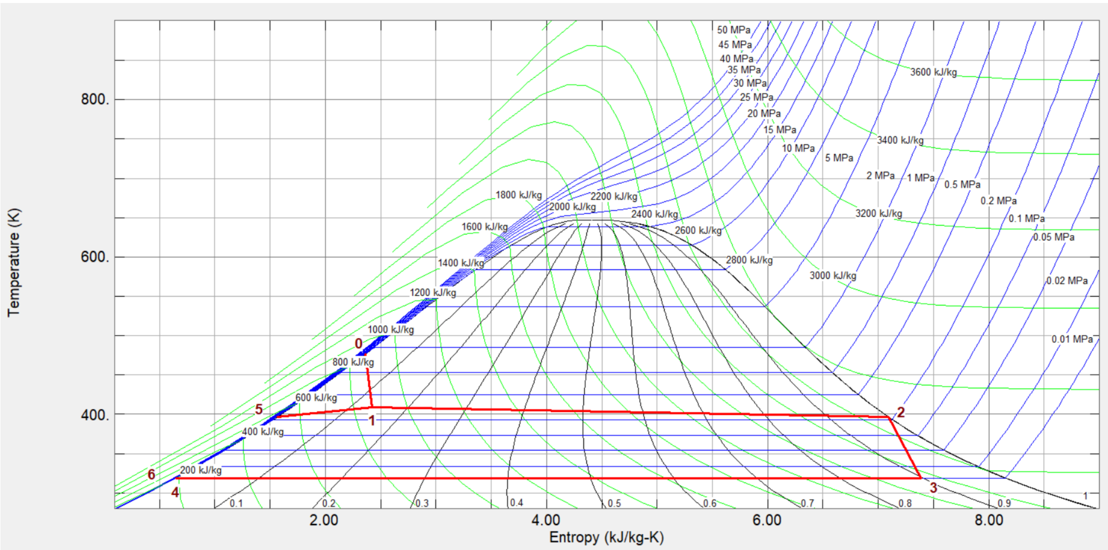

Figure 6.24: The T-s diagram for the BC process, the number indicates the subscribes at figure 6.22.

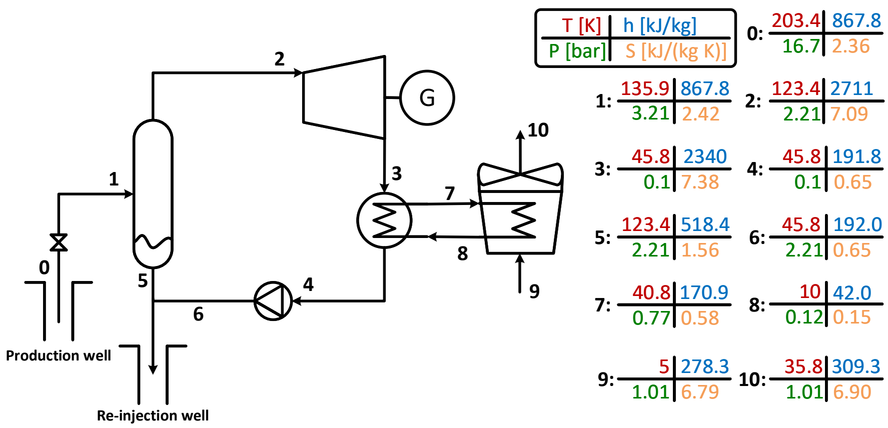

Figure 6.25: The final SF unit and its properties.

The same problem regarding validation in the BC model is present in this model, therefore the results is overlooked to see if they seem reasonable. The temperature change in the condenser and cooling tower are investigated in a T-Q diagram. The temperature change can be seen in figure 6.26 and 6.27 for the condenser and the cooling tower respectively.

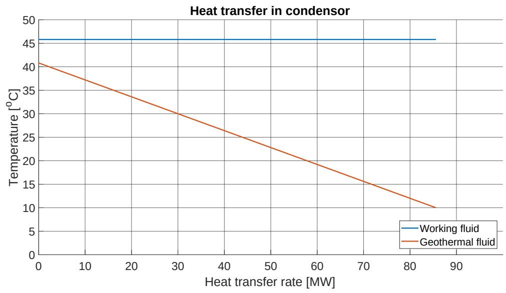

Figure 6.26: T-Q diagram for the process taking place in the condenser.

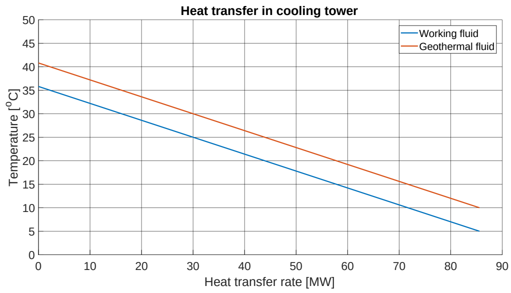

Figure 6.27: T-Q diagram for the process taking place in the cooling tower.

The condenser and the cooling tower is modelled in the same way as the BC model, in regards to the inlet temperature for both the cooling water and the air. However due to a different input and working fluid, the outlet temperatures are different. The SF models temperature are higher, mainly due to the fact that the steam is not R152a, but water and thereby the temperature is higher, as described earlier. The cooling water decreases in temperature by 30.8°C in the condenser, the air which goes through the fans are heated with 30.8°C as well. This is expected as the pinch temperature between T_7 and T_{10}, and T_8 and T_9 are both 5 K. The second efficiency is 24.7 %, this is in the middle of the range for a SF which should be between 20%-30%, and is therefore within the expected range. The cooling tower has a reasonable size of 17.2 m wide and 51.6 m, this is even smaller than the BC unit. Only one cooling tower was needed for this unit.

Is was investigated as well for the SF if there was a specific mass flow into the unit that would give a maximum power output, therefore the mass flow was varied to see what influence it had on the power output. Again it was found that the mass flow and the power output was proportional, and therefore is was decided to have only one SF unit to keep the costs down.

The main result for the optimised SF unit can be seen in 6.2.

The maximum power output for the optimised model gave a total power output of 14.3 MW, this is within the range of the SF unit around the world. It is however in the lower end compared to average, this is because of the fact that SF is used at almost all moderate to ultra high temperature classification as a test plant before the more expensive and complex DF is build (DiPippo, 2012a). Based on the results the model is deemed to be reasonable, even though the required power to the cooling tower seems very high compared to the total power output.

6.2.3 Double flash model

The DF model is very similar to the SF but with an extra separation, therefore the parameter optimisation was also conducted with twice as many pressures, these pressures are the HP separator pressure (P_1), the HP condenser pressure (P_3), the LP separator

Results for the optimised SF unit		
Temperature from the well	T_0	203.6 °C
Pressure from the well	P_0	16.7 bar
Separator temperature	T_1	135.9°C
Separator pressure	P_1	3.21 bar
Condenser temperature	T_3	45.8°C
Condenser pressure	P_3	0.1 bar
Separator temperature of liquid state	T_5	123.4°C
Quality of the steam after turbine	x_3	89.8%
Turbine power output	W_t	14.8 MW
The total required pump power	W_p	211.8 kW
Required power to drive the fans	W_{fan}	271.2 MW
Total power output	W_{tot}	14.3 MW
Plant efficiency	η_{II}	24.7%

Table 6.2: The main results from the optimised SF unit.

pressure (P_7) and the LP condenser pressure (P_9). Each pressure was model with 100 data points, it was not possible to model with 200 points as the other models as the computational time would be very long. The design of the model for the DF unit can be seen in figure 6.28. The inlet conditions, from the well, for this unit is a pressure of 81.3 bar, a temperature of 296.1°C and a mass flow of 308 kg/s.

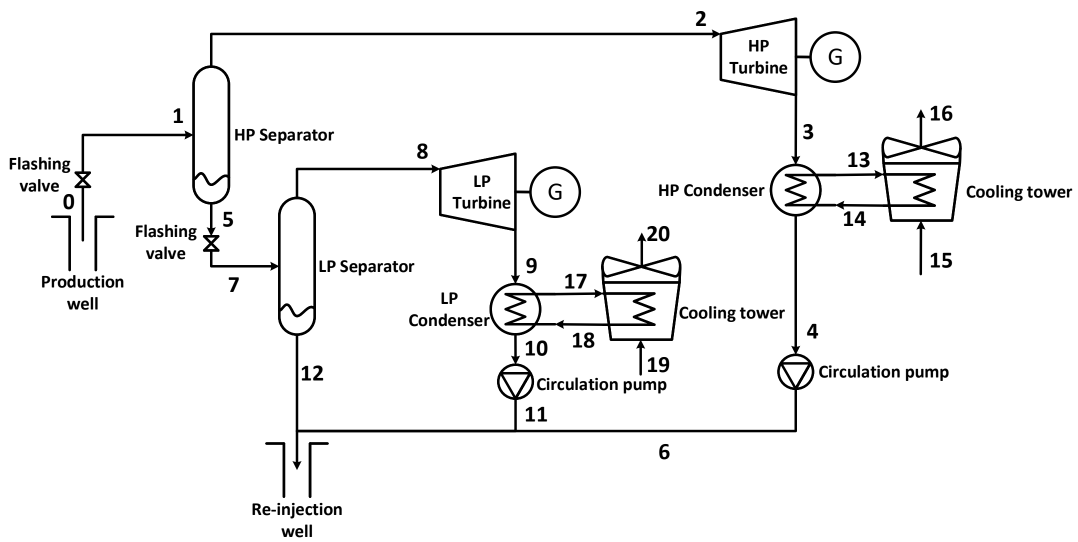

Figure 6.28: The model BC unit.

The HP separator pressure (P_1) was varied from 1.2 bar to 0.1 bar under the pressure from the wells i.e. 81.2 bar. The lowest pressure of 2.3 bar is to ensure that the steam will be able to expand through the LP turbine when the pressure in the LP condenser is at the lowest possible, 0.1 bar. The HP condenser pressure (P_3) has been varied from 0.1 bar to 1 bar, this is based on DiPippo (2012a), for the same reasons as the SF. The LP separator pressure (P_7) was varied from 1.2 bar to 0.1 bar under the HP separator pressure. The highest pressure was modelled this way to ensure that the pressure in the LP separator never exceeded or was equal to the HP separator pressure. The LP condenser pressure (P_9) was as well varied from 0.1 bar to 1 bar.

When varying these pressures the quality of the steam after the HP and LP turbine has to be over 0.85 otherwise it would cause to much damage in the turbines. To ensure that the quality of the steam is above 0.85 it has been modelled in such a way that if the quality x_3 and x_9 was under the optimisation point it was not used further in the optimisation.

To summarise the parameter variable for the parameter optimisation:

$$\begin{aligned} 2.3\,\text{bar} < P_1 &< P_0 - 0.1\,\text{bar} \\ 0.1\,\text{bar} < P_3 &< 1\,\text{bar} \\ 1.2\,\text{bar} < P_7 &< P_1 - 0.1\,\text{bar} \\ 0.1\,\text{bar} < P_9 &< 1\,\text{bar} \end{aligned}$$

The results of the parameter optimisation resulted in a 4D matrix which is not possible to display. It was found that both of the condenser pressures was the lowest at 0.1 bar. In figure 6.29, the parameter optimisation of the two separator pressures can be seen.

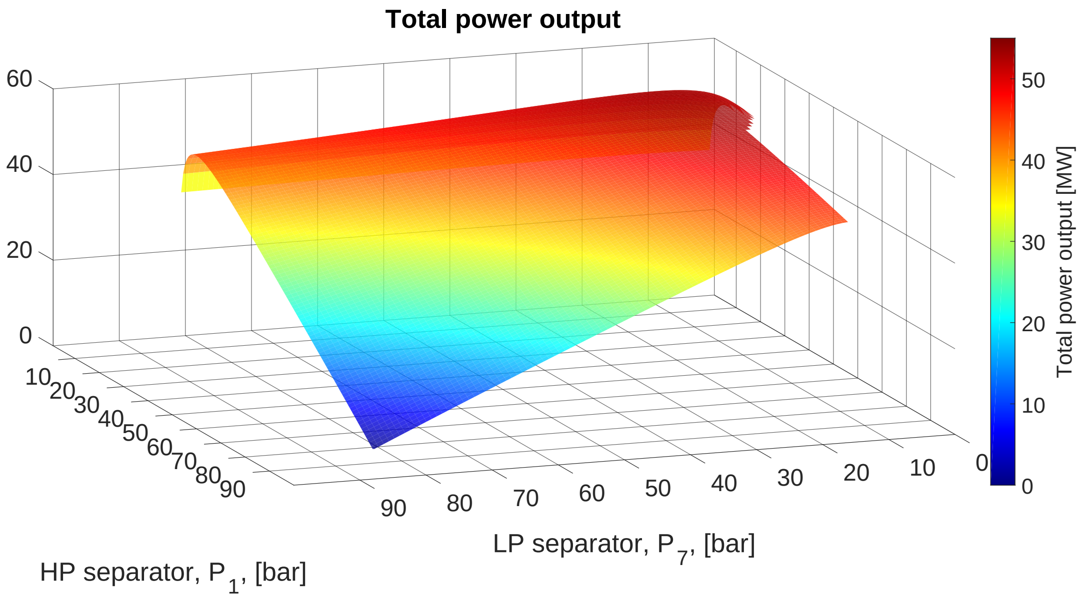

Figure 6.29: The parameter optimisation of P_1 and P_7.

The parameter optimisation gave a maximum power output at 52.4 MW_e at the pressures seen in table 6.3.

Optimised pressures	
P_1	12.7 bar
P_3	0.1 bar
P_7	1.68 bar
P_9	0.1 bar

Table 6.3: Optimised pressure from the parameter optimisation for the DF unit.

As said earlier the peak at the condenser pressure is the lowest possible pressure in the parameter optimisation. The peaks in the separator pressure however is not in the lowest or the highest possible pressure parameter. The reason for this is the same as for the SF model. This power output increases slower than the required power to operate the power plant increases.

The optimised model can be seen in figure 6.31, with the values for the state points. The T-s diagram with the same subscripts can be seen in figure 6.30

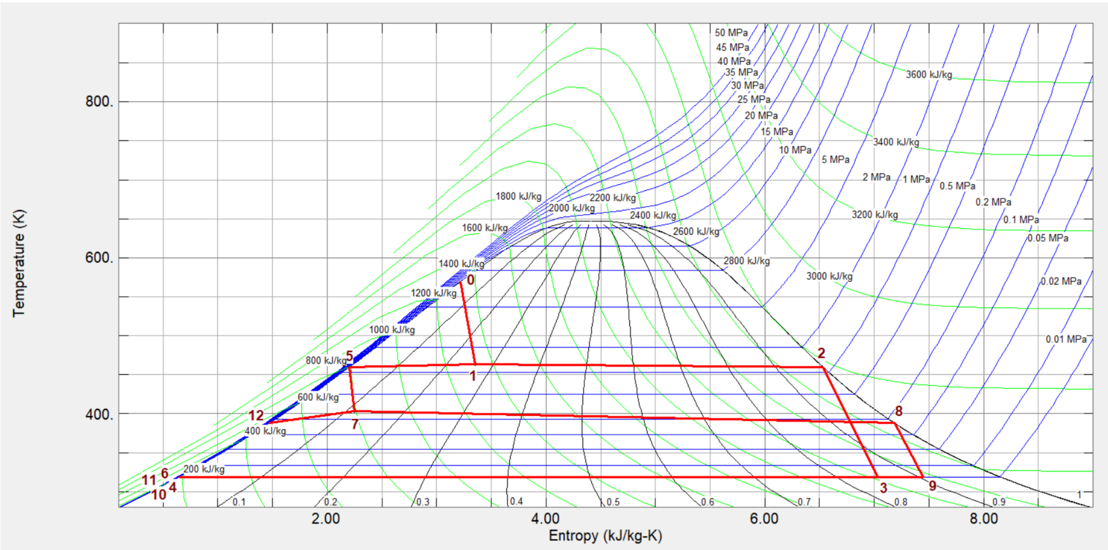

Figure 6.30: The T-s diagram for the DF process, the number indicates the subscribes at figure 6.22.

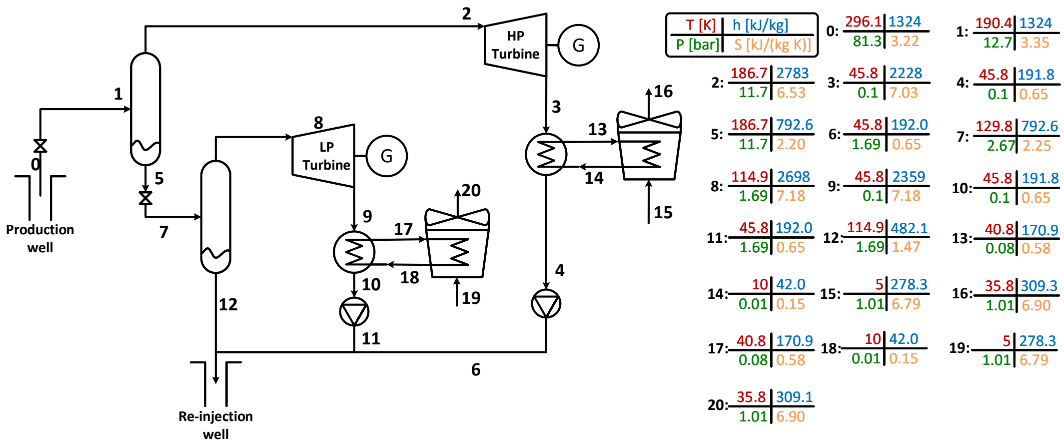

Figure 6.31: The final DF unit and its properties.

Validating this model is difficult as well if not more, due to the many possible configurations. Therefore the heat transfer in the two condensers and cooling tower is investigated. The HP condenser and cooling tower can be seen in figure 6.32 and 6.33, while the LP condenser and cooling tower can be seen in figure 6.34 and 6.35

It is seen, from figure 6.33, that the HP condenser cooling water is decreasing 30.8°C and the air at the cooling tower in increasing with the same amount, this is due to the way the definition of the pinch temperature in both the condenser and the cooling tower.

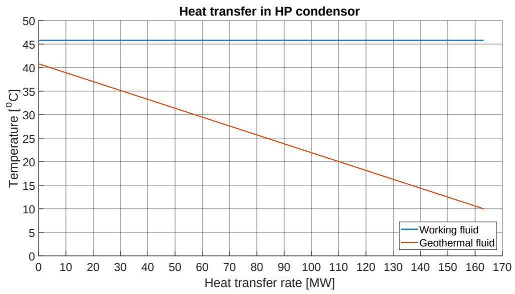

Figure 6.32: T-Q diagram for the process taking place in HP condenser.

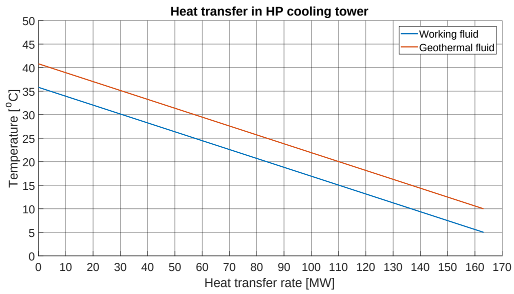

Figure 6.33: T-Q diagram for the process taking place in HP cooling tower.

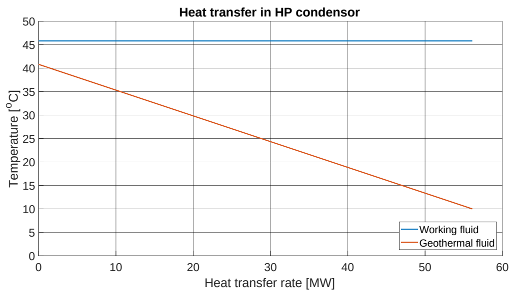

Figure 6.34: T-Q diagram for the process taking place in LP condenser.

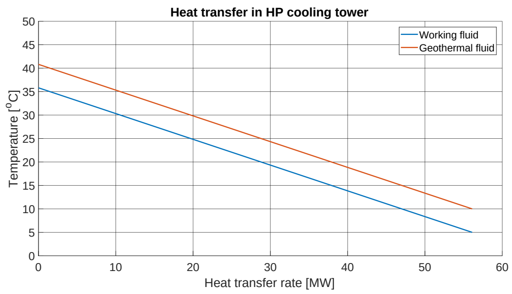

Figure 6.35: T-Q diagram for the process taking place in LP cooling tower.

The LP condenser and cooling tower has the same temperature difference, this is due to the fact that the condenser pressure is the same in both the HP and LP. It is also seen that the DF model has the same temperature differences as the SF, this is due to the condenser pressure being 0.1 bar in both unit. The second efficiency for this model is at 41.1%. This is within the range for DF models, which is between 35% and 45% (DiPippo, 2012b). It is therefore in the higher end of this range, which was desired for as an optimisation has been conducted. With the optimised pressures from table 6.3, it was found that the cooling towers was not of the same size. The HP cooling tower has a width of 23.8 m and a length of 71.4 m, the LP cooling tower was however smaller with a width of only 13.9 m and a length of 41.8 m. The optimised model was also investigated to see if there was a mass flow which would give a maximum output in the same manner as the two previous models. Again it was found that there was a proportionality between the power output and the mass flow. Therefore it was for this model also chosen to have only one unit for the high and ultra high temperature wells.

The main results from the DF model can be seen in table 6.4.

Results for the optimised DF unit		
Temperature from the well	T_0	296.1°C
Pressure from the well	P_0	81.3 bar
HP separator temperature	T_1	190.4°C
HP separator pressure	P_1	12.7 bar
LP separator temperature	T_7	129.8°C
LP separator pressure	P_7	2.67 bar
HP condenser temperature	T_3	45.8°C
HP condenser pressure	P_3	0.1 bar
LP condenser temperature	T_9	45.8°C
LP condenser pressure	P_9	0.1 bar
Separator temperature of liquid state	T_{12}	114.9°C
Quality of the steam after HP turbine	x_4	85.14%
Quality of the steam after LP turbine	x_4	90.61%
HP turbine power output	$W_{t,HP}$	44.4 MW
LP turbine power output	$W_{t,LP}$	8.8 MW
The total required pump power	W_p	446 kW
Required power to drive the fans	W_{fan}	541 MW
Total power output	W_{tot}	52.4 MW
Plant efficiency	η_{II}	41.1%

Table 6.4: The main results from the optimised DF unit.

The maximum power output of the DF model was 52.4 MW_e, this is within the range of the power output of operational DF unit, however it is in the lower end. This could be because of the way the industry uses the SF units. The DF units is not utilised unless there is a high certainty that the temperature of the geothermal fluid is very high, therefore there might be some SF units that would go under this reports definition of the temperature for the DF unit.

CHAPTER 7

Modelling of power plant

The final system that has been modelled is the system described in chapter 5. The final system is combined with the optimised units modelled in chapter 6. In the final model of the entire power plant it has been assumed that the optimised units are in the best possible configuration. The final model consist of one BC unit, one SF unit with a bottom BC unit and one DF unit also with a bottom BC unit, see figure 7.1.

The assumptions made in chapter 6, are preserved in this model. It has been assumed that the optimised pressures for the three types of units are the best configuration, even after the units are combined. Therefore the configurations for each units is used in the model of the entire power plant. The pressures can be seen in table 7.1. It has been possible to utilise the bottom binary units as the temperature from the SF separator and from the DF LP separator has a high enough temperature to be utilised in a BC unit. The temperature of the SF unit is 112.9°C and the temperature out of the DF unit is 100.2°C.

Pressure used in the final model		
BC well pressure	P_{BC}	2.08 bar
BC evaporator pressure	P_2	20 bar
BC condenser pressure	P_4	4.65 bar
SF well pressure	P_{SF}	16.70 bar
SF separator pressure	P_{11}	3.21 bar
SF condenser pressure	P_{13}	0.1 bar
SF bottom BC unit evaporator pressure	P_{19}	20 bar
SF bottom BC unit condenser pressure	P_{21}	4.65 bar
DF well pressure	P_{DF}	81.3 bar
DF HP separator pressure	P_{29}	12.66 bar
DF HP turbine condenser pressure	P_{31}	0.1 bar
DF LP separator pressure	P_{35}	2.68 bar
DF LP condenser pressure	P_{37}	0.1 bar
DF bottom BC unit evaporator pressure	P_{44}	20 bar
DF bottom BC unit condenser pressure	P_{46}	4.65 bar

Table 7.1: The fixed pressures used in the final model which is optimised in chapter 6.

For the SF and DF unit the cooling towers has been replaced with district heating. This means that there are only three cooling towers attached to the BC units. There are no district heating on the BC as the temperature in the condenser is 10°C and therefore the BC units would not be able to contribute with heat to the district heating network. The heat transfer in the BC units are very similar, see figure 7.2. However the heat transfer in the DF bottom BC unit is smaller, due to the inlet temperature to this unit is lower than to the others BC units.

The district heating is heated from 5°C to 67.2°C, at this temperature is can be used to both heating houses and domestic water for shower and cooking (Jóhannesson, 2016). The temperature for the domestic water can not be under 60°C to ensure that Legionella pneumophila is not able to live in the water. The district heating water is heated at

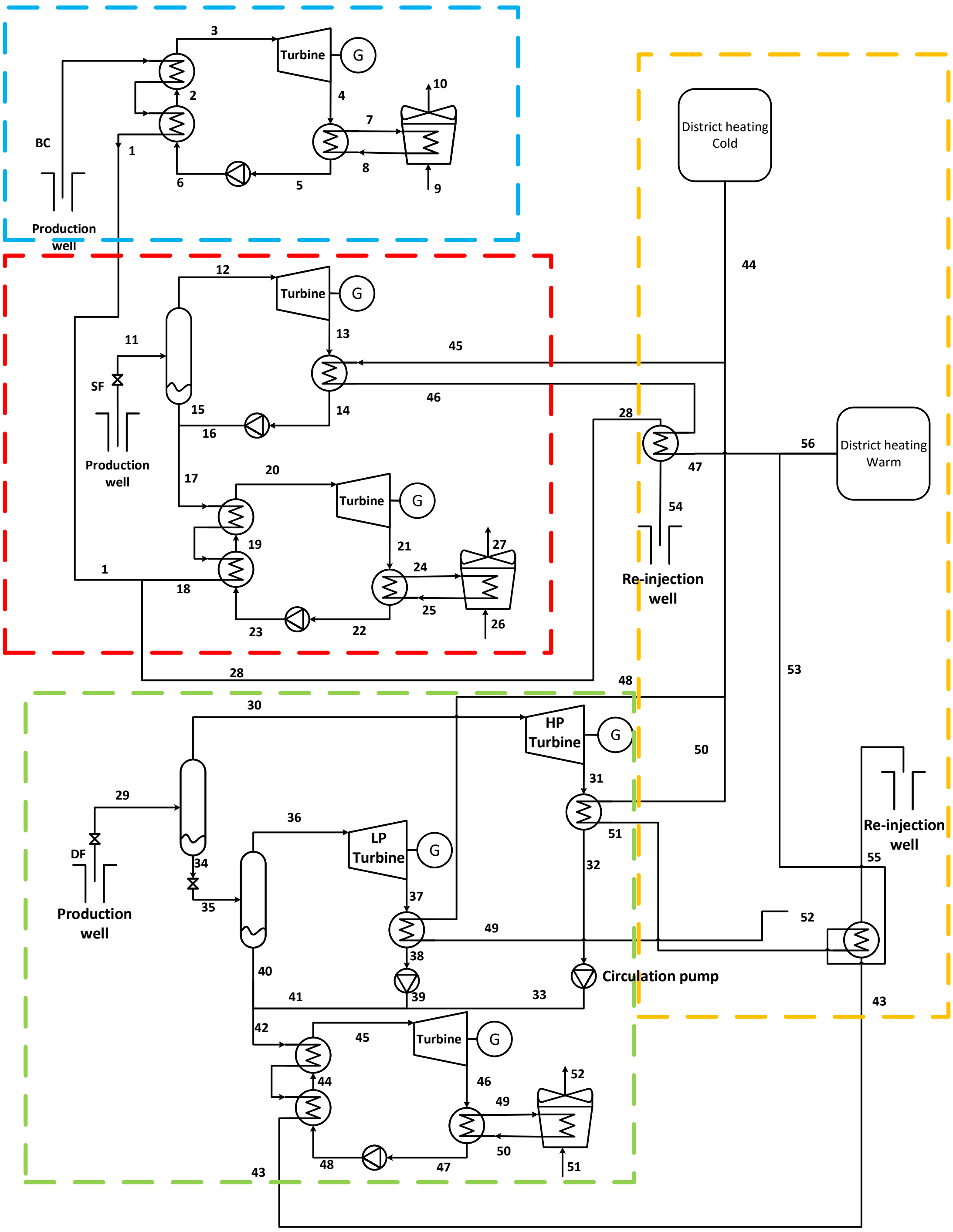

Figure 7.1: The final design of the model,the blue framed part is the BC unit, the red framed part is the SF unit, the green framed part is the DF and the orange framed part is the district heating.

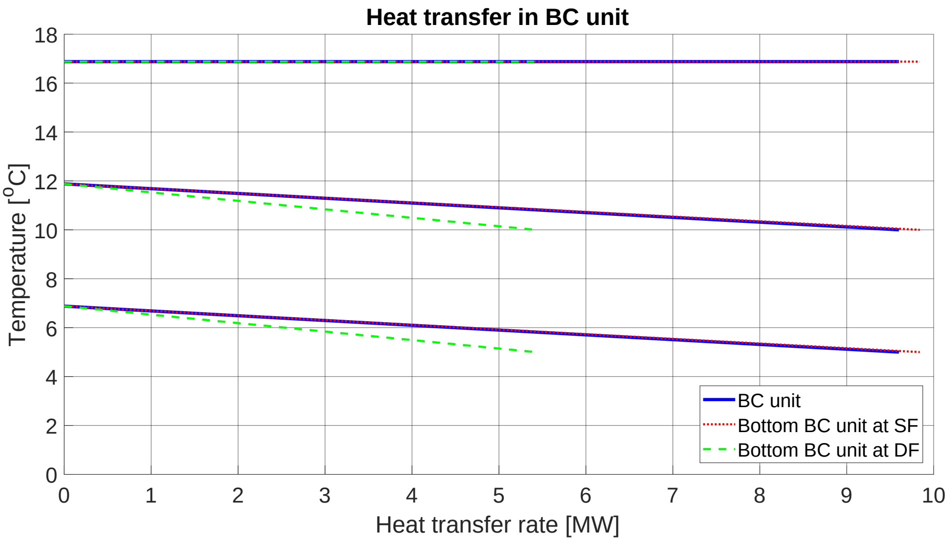

Figure 7.2: T-Q diagram for the three BC units with cooling towers. The top line indicated temperature difference in the condensers, the middle line indicates the temperature difference in the cooling water and the bottom line indicates the temperature difference on the air side in the cooling tower.

the condensers on the SF and DF unit, further more two heat exchangers is placed to boost the temperature of the district heating even more. The heat transfer to the district heating water can be seen in figure 7.3 and 7.4 for heat exchanger 1 and for heat exchanger 2 respectively. It is seen the heat transfer in the DF condenser to the district heating water is higher than in the SF condenser, this is due to the fact that the temperature difference for the district heating water through the condenser is almost the same The SF temperature is a bit higher, however the mass flow of the district heating water through the DF condenser is almost twice as high, and therefore the heat transfer becomes larger in the DF condenser compared to the SF condenser. The heat transfer in the heat exchanger is higher in the SF unit, due to the mass flow of the district heating water being higher (526.5 kg/s) in heat exchanger 1 than in the heat exchanger 2 (307.5 kg/s).

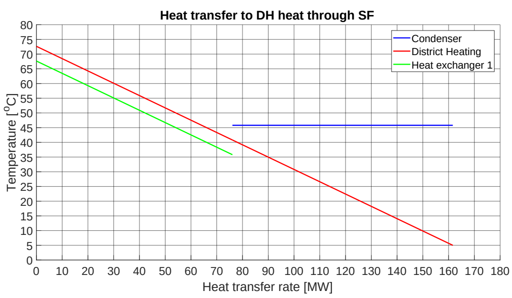

Figure 7.3: T-Q diagram for the heat transfer for the district heating water going through SF and heat exchanger 1.

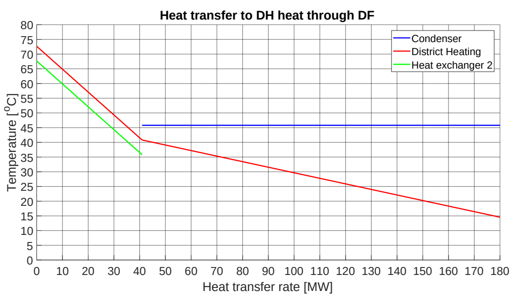

Figure 7.4: T-Q diagram for the heat transfer for the district heating water going through DF and heat exchanger 2.

7.1 Results

The total power output from the power plant is 91.8 MW_e and 610 MW_{th}. The reason for the large thermal power is due to the large mass flow that is needed for this power plant, which is 2,527 kg/s. This seems very high as the Nesjavellir power plant utilises around 1,100 kg/s (Gunnarsson et al., 1992), however the total mass flow into the power plant is also larger than it is into the Nesjavellir power plant, so the thermal power seems reasonable in that sense.

The main results for the full geothermal power plant can be seen in table 7.2.

Main results for the power plant		
Temperature from BC wells	T_{BC}	121.5°C
Temperature from SF wells	T_{SF}	203.5°C
Temperature from DF wells	T_{DF}	296.1°C
Temperature from BC preheater	T_1	67.6°C
SF separator temperature	T_{11}	135.86°C
Temperature into SF bottom BC evaporator	T_{17}	112.9°C
DF HP separator temperature	T_{29}	190.4°C
DF LP separator temperature	T_{35}	129.8°C
Temperature into DF bottom BC evaporator	T_{42}	100.2°C
Temperature of cold district heating	T_{44}	72.6°C
Temperature of warm district heating	T_{56}	67.3°C
Power output from BC turbine	$W_{t,BC}$	9.6 MW_e
Power output from SF turbine	$W_{t,SF}$	14.8 MW_e
Power output from SF bottom BC turbine	$W_{t,SF\text{-}BC}$	9.8 MW_e
Power output from DF HP turbine	$W_{t,HP}$	44.4 MW_e
Power output from DF LP turbine	$W_{t,LP}$	8.8 MW_e
Power outpur from DF bottom BC turbine	$W_{t,DF\text{-}BC}$	7.4 MW_e
Total required power	W_{req}	3.07 MW_e
Total power output	W_{tot}	91.78 MW_e

Table 7.2: The main result for the final power plant.

If the total power plant power output compared to the total power out for the stand alone units added together which is found from the results from chapter 6; so three BC units, one SF unit and one DF unit, it is seen that power plant power output is higher with 91.8 MW_e compared to 71.4 MW_e for the stand alone units. The reason for the higher power output can be due to the fact that the cooling towers for the SF and DF now does not require any power, as this has been assumed that the district heating company is paying to pump the district heating water around. The power plant does now also utilise district heat and this gives an additional thermal power of 610 MW_{th}. For a system which is able to utilise a DF unit, the total output is a bit low, however it is not outside of the range for simple power plants as this (DiPippo, 2012a).

CHAPTER 8

Geothermal energy in Denmark

Denmark is one of the countries that do not utilise geothermal energy for power generation, however there is three plants in Denmark, in Thisted, Margretheholm in Copenhagen and Sønderborg, which utilises geothermal energy through absorptions heat pumps. Thisted geothermal power plant produces 7 MW_{th}, Margretheholm geothermal power plant has a capacity of 14 MW_{th} and Sønderborg has a capacity of 12 MW_{th}. The temperatures from the wells is 43°C, 74°C and 48°C respectively (Røgen et al., 2015). These temperatures are under the classification *Non electrical*, and is therefore most suitable for direct use with a heat pump as it is utilised in Denmark.

8.1 Danish reservoirs

In Denmark there are no temperature anomalies such as volcano activity, therefore the temperature gradient in Denmark is the same most of the places at a temperature of 22-28°C/km (Røgen et al., 2015). The wells drilled in Denmark which is used for the geothermal power plants depends on the geology as there has to be a reservoir. The reservoir which is used in the Danish geothermal power program is the Gassum reservoir. For Thisted geothermal power plant this reservoir is shown as light pink in figure 8.1. As the depth of the wells are 1.25 km deep, the Haldager and Skagerak reservoir lays above the Gassum reservoir (Røgen et al., 2015). The geothermal power plant in Sønderborg is also at the Gassum reservoir. This is also seen as the depths of the wells are almost the same in the depth of 1.2 km. The Bunter Sandstone reservoir lays underneath the Gassum reservoir. Margretheholm geothermal power plant utilises the Bunter Sandstone reservoir and has the deepest wells at 2.6 km. It is also the power plant which has the highest temperature, the Gassum reservoir lays above the Bunter Sandstone reservoir as well.

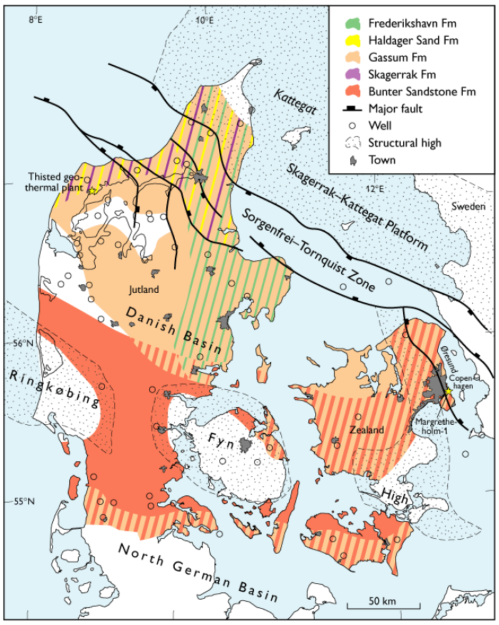

Figure 8.1: The different potential geothermal reserviors in Denmark (Nielsen et al., 2004).

As the temperature gradient in the Danish underground is 22-28°C/km. The boreholes has to be at least between 3.5 and 4.5 km to get a geothermal power production with a BC unit, which is fairly deep. However in the Copenhagen area there is a known higher potential. This is also seen at Magretheholm power plant which has a temperature of 74°C and therefore the Danish government and the national district heating organisation, Dansk Fjernvarme, see the highest potential in this area. De Nationale Geologiske Undersøgelser for Danmark og Grønland (GEUS) has investigated the Danish underground and it is found that the reservoir that Margretheholm power plant utilise is max 3.5 km deep. The maximum temperature is just around 100°C, which is just enough to utilise the geothermal energy for power generation.

The Gassum reservoir in Sønderborg is shallower than the Bunter Sandstone reservoir at Margretheholm power plant, this is only 1.2 km, so the boreholes in Sønderborg is as deep as possible, however the Bunter sandstone reservoir is placed deeper with a bottom depth of 2.2 km. This is however not deep enough to produced geothermal electrical power.

The power plant in Thisted utilise the Gassum reservoir. In this part of Denmark the reservoir has a bottom depth of 3.8 km. This gives a temperature of 136 °C which can be utilised in a BC unit for geothermal power production. However if the the boreholes was placed closer to Nykøbning Mors the bottom depth would be 4.7 km which would give a temperature of around 168°C assuming the temperature gradient does not change the deeper one goes. This would be suitable for power production, and a SF might even be utilised. The Bunter Sandstone reservoir is placed even deeper with around 4.7 km as a top depth and a bottom depth of 7.2 km. This reservoir would give a minimum temperature of 168 °C which would be classified as a low temperature reservoir. The bottom temperature would be 258°C which is classified as high temperatures and therefore suitable for geothermal power production (Sanyal, 2005).

The Bunter Sandstone reservoir is the reservoir which is deepest with 6.5 km as a top depth and a bottom depth of 9.2 km at Hornum in Northern Jutland. This reservoir would give a minimum temperature of 232 °C which would be classified as a high temperature reservoir. The bottom temperature would be 329°C which is classified as Ultra high temperatures (Sanyal, 2005).

8.2 Possibilities of geothermal energy in Denmark

There are three main problems with geothermal energy in Denmark, the permeability of the reservoirs at large depths, the cost of drilling and building against the power output and lack of experience among professionals working with geothermal energy in Denmark. The permeability of the reservoirs becomes lower the deeper the boreholes are, as the rocks are less porous and therefore not suitable for geothermal energy, see chapter 1 (Mathiesen et al., 2009). It should be mentioned that this is an assumption made but not tested, and this leads to the second problem which is that the initial price for a geothermal power plant is very high. This is due to the boreholes which has to be drilled very very deep to get a temperature which would be suitable for power production. The price for drilling this deep is very high and the risk is also high, due to the fact there is no natural heat source such as a volcano and therefore the borehole might not be able to produce enough hot water to make the power plant profitable (Ravn, 2017). The last problem is that the professionals lack experience in the geothermal field in Denmark as other renewable energy sources are easier to get license to utilise (Ravn, 2017). The

Danish government does not have a subsidy scheme for geothermal energy, as to other renewable energy sources, therefore these are more often chosen to be utilised (Ravn, 2017).

The Danish government did include money for geothermal energy research in the proposal for the national budget 2015 cf § 29.24.17. This was later rewritten where there was less money for geothermal energy research. In January 2017 the Danish Energy-, Supply- and Climate minister said that geothermal energy should be a part of the Danish district heat system in the future (Folketinget, 2017).

CHAPTER 9

Discussion

This chapter contains a discussion of results obtained in the project, the working procedure, methods and assumptions, that could be a source of errors for the project in general, will also be discussed.

9.1 Discussion of the models and results

The models constructed has been chosen to be modelled as the simplest models possible. This results in a power output, for both the units individually but also for the power plant, which is lower than the average power plant with well properties as for this project, the second efficiency is however in the higher end for all the units. This means that the units are utilising the energy input in a acceptable matter compared to real power plants. It could be argued that if the units has a more complex design for example with recuperators, or other means of heat exchanger to heat the water, the power output would be higher as it might be possible to increase the total power output. Another option for increasing the power output would be to design hybrid plants. This has been done to some extend in the power plant model. However the more complex the designs become the less applicable are they for a universal system. The reason for this is that the more complex systems normally are designed more specific to a certain geothermal field. The simple system is also a cheaper system, as there is a minimum of components and the components has to be placed in a certain order for the power plant to operate. If the power plant is complex the number of components would most likely increase and thereby the power plant becomes more expensive (Jóhannesson, 2016). The complex system might be very suitable for some mass flows or temperatures but it is not certain this is the case for other geothermal fields, therefore it was chosen to design simple units.

The cooling tower used in this model are air cooled cooling tower. This has be chosen to secure the applicability of the plant around the world. It should however be noticed that air cooled towers is not as efficient as the water cooled cooling towers as the overall heat transfer coefficient for water are higher in the range of 850–1700 $W/(m^2 \cdot K)$ (Çengel et al., 2012). This would give a higher heat transfer rate, and thereby a lower flow rate of the cooling water which would result in a less power required for pumps. If water cooled cooling towers was utilised the condenser pressure might be able to be lowered a bit, as the heat transfer area would be lower due to the higher heat transfer. By lowering the condenser pressure the total power output would be higher as it was found in the parameter analysis in chapter 6. Therefore it should be considered to design two cooling towers, as if the power plants are placed near a lake or ocean this would be a better solution.

Another factor to consider in the final model is that the units are optimised in regards to electrical power and not thermal power. This means the condenser pressure is as low as possible (0.1 bar) to increase the electrical power output as much as possible. However the low condenser pressure results in a equally low outlet temperature of the cooling water. The low temperature of the cooling water means that district heating water, which give the thermal power, will not be able to be heated very much. If the optimisation was done in accordance to both electrical power and thermal power the condenser pressure was most likely not the lowest possible condenser pressure.

9.2 Discussion of methods and assumptions

The parameter optimisation is a more simple way to optimise a complex system like the models. A more suitable optimisation might be a genetic algorithm as this will explore more solutions. In a genetic algorithm the spacing between the data points would not be spaced in an equally manner as it is in the parameter optimisation (Jónsson, 2016). When spacing in an equally manner, the optimum might be missed, however with 200 data points, for each pressure, for the BC and SF units this will result in a minor difference. The DF has however only 100 data points, for each different pressure, this means that there is a possibility of the maximum not being found. The reason for choosing only 100 data point is the computational time which with 100 data point all ready was quiet extensive.

Another thing that has to be considered regarding the optimisation of the units is that they are done individually, which means that the configuration is good when the unit stand alone. However it has not been investigated whether the optimisation gives the highest electrical power output for the entire power plant, especially in regards to the bottom BC units on the SF unit and the DF unit, as the input temperature and mass flow is different than the stand alone BC unit, which is the optimised unit.

It has been assumed that there are no supercritical conditions, this is however not true in reality, especially not in geothermal field which are placed in areas with volcanoes and such. If the supercritical region was taken into account it would be possible to have a larger electrical power output, however the power plant would have to be reinforced to deal with the high pressures as the plant would be a steam plant and not a plant which utilised fluid mixtures (DiPippo, 2012b). When discussing the fluid properties is should also be mentioned that it was assumed that the wells was liquid dominated based on Gunnarsson et al. (1992) but also assumed as well data was very scare and therefore not possible to find all the fluid properties, this is not the case for all wells. If the well is not liquid dominated the flashing throttle valve would be unnecessary.

Steady state was assumed in the model, this was done as the flow, temperature and pressure from the wells vary very little (1%-2%). Therefore is was deemed not necessary to model the system dynamic. It was also found in the literature study that most authors in the geothermal area model in steady state.

CHAPTER 10

Conclusion

The overall purpose of the project was to design a power plant which could be used at different geothermal fields around the world without having to change much. Furthermore it should be able to take the different temperatures into considerations and thereby not mixing high and low temperatures.

Three unit models was formulated, to ensure that there was units for the different temperature classifications. The three models formulated was a binary cycle model, a single flash model and a double flash model.

As data for real geothermal fields was difficult to get hands on a hypothetical geothermal was designed with 26 wells. There was eight wells which was utilised in the BC unit with a temperature of 122.5°C and a mass flow of 237 kg/s. Ten of the units was utilised in the SF unit, the temperature of the wells was 203.4°C and a mass flow of 290 kg/s. The last eight wells was utilised in a DF unit, the temperature of the wells was 296.1°C and a mass flow of 308 kg/s. The models was formulated to be simple to ensure that the units could be used all over the world and be combined as necessary for the geothermal field and thereby securing the model to be more universal.

The unit models was optimised, using a parameter optimisation, to find the pressures for which the electrical power output was largest. It was found that the BC unit had the largest power output, at 8.63 MWe with a condenser pressure at 4.65 bar and a evaporator pressure at 20 bar. The optimisation showed that the largest power ouput was at the maximum evaporator pressure possible, however the condenser pressure was not the lowest. It was found that this was due to the required power to the cooling tower was high at lower pressures as the mass flow of the air would increase.

The SF unit was optimised in the same manner. It was found that the largest power output at 14.3 MW_e was found at a separator pressure at 3.21 bar and a condenser pressure at 0.1 bar. The condenser pressure was the lowest possible pressure. It was investigated if the power output would be higher if the condenser pressure was lower, this was found to be true, however the cooling towers would have to be very large, therefore it was chosen to keep the condenser pressure at 0.1 bar. The separator pressure had a maximum where the power output was largest. It was found that this peak was due the fact that even though turbine output was increasing and the power output was increasing the required power for the fans, pumps, etc. would increase faster and thereby this peak as created.

The last unit model was the DF model. This model was also optimised. Here is was found that the largest power output was 52.4 MW_e at the HP pressure of 12.7 bar, the LP separator pressure at 2.67 bar and the HP and LP condenser pressure was 0.1 bar. The condenser pressures was therefore again the lowest possible and the separator pressures has a maximum, it was found that the reason for this was from the same causes as in the SF unit.

The optimised units was combined to a power plant using the optimised configurations. The power plant utilised district heating, this meant that the cooling towers for the SF condenser, the DF HP condenser and the DF LP condenser was replaced with district heating instead. It was found that the total power output was 91.8 MWe and 610 MW_{th}. This is higher than if the units stood alone and was not combined. If the units stood alone the total power for three BC units, one SF unit and one DF unit was 71.4 MWe.

It should however be noticed that in the power plant model the required power for the three cooling towers was left out as the cooling towers is replaced by district heating.

The model has been formulated for the units in such a way that if the model was utilised on a different geothermal field only the ambient temperatures and the wells properties should be changed. If the geothermal field only has temperatures which classifies for one or two types of the units, the model is altered in such a way that only these units is utilised.

CHAPTER 11

Future Work

In terms of future work several suggestions, for further development of the project, will be made in relation to relevant and unexplored aspects of the current project subject.

11.1 Modelling reflections

The models for the units has been modelled very simple. The model for the power plant could be expanded with more complex units and district heating network. As the model is constructed at the moment, the district heating is only utilised in the condensers. It could be interesting to investigate a more complex district heating, such as using the water from the separators to heat the district heating as this water normally has a rather high temperature.

The power plant model is formulated using optimised configurations for the different units. This means that the thermal power was not variable in the optimisation, but in the power plant model district heating is one of the main results, therefore for future works the optimisation could be included if district heating is a parameter of interest. The power plant model could also be optimised by it self instead of optimising the units first, this will however mean that another optimisation method is needed or a larger computer as the computational time would be very large as the optimisation is conducted now.

The model is formulated with ideal components or components with a fixed loss, to get a more realistic model, losses could also be modelled and that way get a more precise model. This is especially in the condenser and separator. The separator was assumed to have a constant pressure loss of 1 bar based on DiPippo (2012b), this is however a crude assumptions as the pressure loss would be highly depended on the mass flow through the separator, and as the model is formulated to be a universal model, the mass flow would change from geothermal field to geothermal field. The condenser is modelled with no pressure loss. This is not realistic as there would be a pressure loss, this would also depend on the mass flow through the condenser (Çengel et al., 2012).

11.2 Very low temperature reservoirs

This paper only focus on power plant which can utilised enough energy for electrical production. However geothermal energy can be utilised as heat all over the world (Dickson and Fanelli, 2003). Therefore for a future project the focus could be one utilising geothermal reservoirs which is not suitable for electrical power generation. In chapter 8 it was found that in Denmark geothermal energy is utilised for heating purposes. The technology for this kind of power plants is very different from power plants generating electricity. The way to utilised this energy is normally with heat pumps or a direct system (Dickson and Fanelli, 2003) (DiPippo, 2012a). The direct systems is using the geothermal fluid in heat exchangers to heat a system which can be used for for example district heating.

11.3 Cost of a power plant

In the future an economic perspective on the geothermal power plant could be investigated. When designing a geothermal power plant it is possible to extract as much energy out of the geothermal fluid as possible, but to do this, more units and components is needed and the price of the power plant would increase. It could therefore be interesting to see at what point it is no longer profitable to extract extra energy from the geothermal fluid by hybrid power plants.

Bibliography

A history of geothermal energy in america, 2014. URL `https://energy.gov/eere/geothermal/history-geothermal-energy-america`.

K. Baumann. Some recent developments in large steam turbine practice. Journal of the Institution of Electrical Engineers, 59:565 – 623, 1921.

R. Bertani. Geothermal power generation in the world 2005-2010 updated report. Geothermics, 2011.

R. Bertani. Geothermal power generation in the world 2010-2014 update report. World Geothermal Congress, 2015.

Y. A. Çengel, J. M. Cimbala, R. H. Turner, and M. K. ğ lu. Thermal - Fluid Sciences. McGraw Hill, 2012.

T. Condra. Conversation. 2017.

M. H. Dickson and M. Fanelli. Geothermal electric power in the world from 1980 to the year 2000. Geothermics, 22(3):215–228, 1993.

M. H. Dickson and M. Fanelli. Geothermal Energy - Utilization and Technology. United Nations Educational, Scientific and Cultural Organzation, 2003.

R. DiPippo. Geothermal power plants of italy: A technical survey of existing installations, 1978.

R. Dipippo. Geothermal electric power, the state of the world - 1985. Geotherm. Resour. Counc., 14, 1985.

R. DiPippo. Geothermal Power Plants: Principles, Applications, Case Studies and Environmental Impact. Elsevier, 3rd edition, 2012a.

R. DiPippo. Comprehensive Renewable Energy. Elsevier, 1st edition, 2012b.

M. A. Einarsson. Climate of iceland, 2008. URL `http://en.vedur.is/media/loftslag/myndasafn/frodleikur/Einarsson.pdf`.

EPA. Federal register, 2015.

Folketinget. 20-spørgsmål s 546 om geotermisk energi i fjernvarmeforsyningen., 2017. URL `http://www.ft.dk/samling/20161/spoergsmaal/s546/index.htm`.

A. Garcia-Gutierrez, J. I. Martinez-Estrella, R. Ovando-Castelar, I. Canchola-Felix, and P. Jacobo-Galvan. Energy recovery in the cerro prieto geothermal field fluid transportation network. World Geothermal Congress 2015, 2015.

M. Gehringer and V. Loksha. Geothermal handbook: Planning and financing power generation, 2012.

A. Gunnarsson, B. S. Steingrimsson, E. Gunnlaugsson, J. Magnusson, and R. Maack. Nesjavellir geothermal co-generation power plant. Geothermics, 21(4):559–583, 1992.

R. Harrison, N. D. Mortimer, and O. B. Smarason. Geothermal Heating - A Handbook of Engineering Economics. Pergamon Press, 1st edition, 2013.

C. Harvey and GeothermEx Inc. Geothermal exploation best practice : A guide to resource data collection analysis and presentation for geothermal projects, 2013.

R. W. Haywood. Analysis of Engineering Cycles. Pergamon Press, 2nd edition, 1975.

G. W. Huttrer. The status of world geothermal power production 1990-1994. Geothermics, 25(2):165–187, 1995.

G. W. Huttrer. The status of the geothermal power generation 1995-2000. Geothermics, 30:1–27, 2001.

IDDP. Icelandic deep drilling project, 2000.

International Energy Agency. Key world energy statistics, 2016. URL http://www.iea.org/publications/freepublications/publication/KeyWorld2016.pdf.

T. Jóhannesson. Geothermal power plant course. Course offered at the University of Iceland, 2016.

M. T. Jónsson. Design optimisation course. Course offered at the University of Iceland, 2016.

L. B. Jørgensen. Private photos. 2016.

S. N. Karlsdóttir. Comprehensive Renewable Energy. Elsevier, 1st edition, 2012.

Lenntech. Health risk of elements, 2017. URL http://www.lenntech.com/periodic/periodic-chart.htm.

J. W. Lund and T. L. Boyd. Direct utilization of geothermal energy 2015 worldwide review. Geothermics, 60:66–93, 2016.

E. Marinot. Renewables - global futures report, 2013. URL http://www.ren21.net/Portals/0/documents/activities/gfr/REN21_GFR_2013.pdf.

S. Marshak. Earth - Portrait of a planet. W. W. Norton and Company, 4th edition, 2012.

A. Mathiesen, L. Kristensen, T. Bidstrup, and L. H. Nielsen. Vurdering af det geotermiske potentiale i danmark. Danmarks og Grønslands Geologiske undersøgelses rapport, 2009.

A. J. Menzies, L. B. V. n or, and E. G. Sunio. Tiwi geothermal field, philippines: 30 years of commercial operation. World Geothermal Congress 2010, 2010.

B. R. Munson, T. H. Okiishi, W. W. Huebsch, and A. P. Rothmayer. Fluid Mechanics. Wiley, 7th edition, 2013.

H. Murakami. Wayang windu geothermal power plant. Fuji Electric Review, 47(4), 2001.

L. H. Nielsen, A. Mathiesen, and T. Bidstrup. Geothermal energy in denmark. Geological Survey of Denmark and Greenland Bulletin, 4:17–20, 2004.

H. Pálsson. Utilization of geothermal energy for power production - lecture notes, 2014.

H. Quick, J. Michael, H. Huber, and U. Arslan. History of international geothermal power plants and geothermal projects in germany. World Geothermal Congress 2010, 2010.

K. B. Ravn. Dansk geotermi mangler erfaring. Ingeniøren, 2017.

REN21. Renewables 2016 - global status report, 2016. URL http://www.ren21.net/wp-content/uploads/2016/10/REN21_GSR2016_FullReport_en_11.pdf.

B. Røgen, C. Ditlefsen, T. Vangkilde-Pedersen, L. H. Nielsen, and A. Mahler. Geothermal energy use, 2015 country update for denmark. World Geothermal Congress, 2015.

B. Saleh, G. Kogelbauer, M. Wendland, and J. Fischer. Working fluids for low-temperature organic rankine cycles. Energy, 32:1210–1221, 2007.

S. K. Sanyal. Classification of geothermal systems - a possible scheme. Thirtieth Workshop on Geothermal Reservoir Engineering, 2005.

S. K. Sanyal and S. L. Enedy. Fifty years of power generation at the geyser geothermal field, california - the lessons learned. Thirty-Sixth Workshop on Geothermal Reservoir Engineering, 2011.

R. W. Serth and T. Lestina. Process Heat Transfer. Elsevier, 2nd edition, 2014.

B. Steingrímsson. Geothermal wells course. 2016.

I. A. Thain and B. Carey. Fifty years of geothermal power generation atwairakei. Geothermics, 38:48–63, 2009.

S. Thorhallsson. Geothermal wells course. Course offered at the University of Iceland, 2016.

G. Thorolfsson. Maintenance history of a geothermal plant: Svartsengi iceland. World Geothermal Congress 2005, 2005.

B. S. Tolentino and B. C. Buñing. Geothermal development in the philippines, update and program, n. d.

H. Wesula. Olkaria i geothermal power station operation challenges. Kenya Geothermal Conference 2011, 2011.

S. S. M. M. Zarandi and G. Ivarsson. A review on waste water disposal at the nesjavellir geothermal power plant. World Goethermal Congress, 2010.

J. Zhu, K. Hu, X. Lu, X. Huang, K. Liu, and X. Wu. A review of geothermal energy resources, development, and applications in china: Current status and prospects. Energy, 93:466–483, 2015.

APPENDIX A

Worldwide geothermal power production

The installed capacity of geothermal power for larger areas in the period 1980-2015.

Total worldwide geothermal electrical power generation [MW_e]								
Area	1980	1985	1990	1995	2000	2005	2010	2015
Europe	267.7	537	631	722	1019	1124	1643	2133
Africa	-	45	45	45	52	136	209	601
America	1170	2577.1	3605	3800	3390	3911	4565	5089
Asia	612.3	1155.7	1271.3	1980	3075	3290	3661	3756
Oceania	189.6	189.6	283.2	286	437	441	818	1056
Total	2239.6	4504.4	5835.5	6833	7973	8902	10896	12635

Table A.1: Total worldwide geothermal electrical power generation (Dickson and Fanelli, 1993), (Huttrer, 1995), (Huttrer, 2001), (Bertani, 2011), (Bertani, 2015).

Installed capacity for each country which utilise geothermal power, in the period 1995-2015, can be seen in table A.2 and figure A.1.

Country	**1995** [MW_e]	**2000** [MW_e]	**2005** [MW_e]	**2010** [MW_e]	**2015** [MW_e]
Argentina	0.67	0	0	0	0
Australia	0.17	0.17	0.2	1.1	1.1
Austria	0	0	1.1	1.4	1.2
China	28.78	29.17	28	24	27
Costa Rica	55	142.5	163	166	207
El Salvador	105	161	151	204	204
Ethiopia	0	8.52	7.3	7.3	7.3
France	4.2	4.2	15	16	16
Germany	0	0	0.2	7.1	27
Guatemala	0	33.4	33	52	52
Iceland	50	170	202	575	665
Indonesia	309.75	589.5	797	1,197	1,340
Italy	631.7	785	791	843	916
Japan	413.7	546.9	535	535	519
Kenya	45	45	129	202	594
Mexico	753	755	953	958	1,017
New Zealand	286	437	435	762	1,005
Nicaragua	70	70	77	88	159
Papua New Guinea	0	0	6	56	50
Philippines	1,227	1,909	1,930	1,904	1,870
Portugal	5	16	16	29	29
Romania	0	0	0	0	0.1
Russia	11	23	79	82	82
Taiwan	0	0	0	0	0.1
Thailand	0.3	0,3	0.3	0.3	0.3
Turkey	20.4	20.4	20	91	397
USA	2,816.7	2,228	2,534	3,098	3,450

Table A.2: Worldwide power production from 1995 to 2015 (Huttrer, 2001) (Bertani, 2011) (Bertani, 2015).

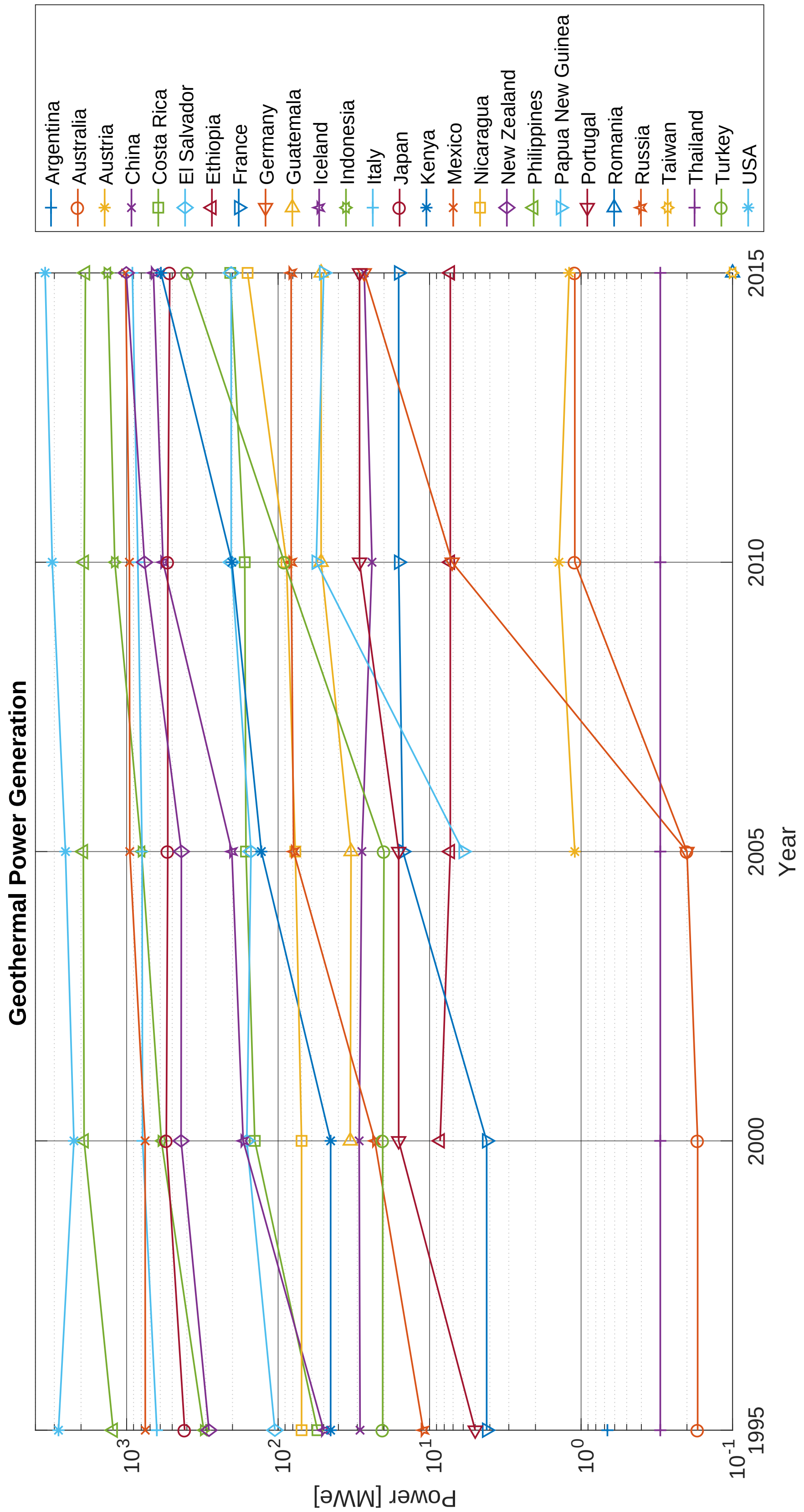

Figure A.1: Geothermal power per country from year 1995 to 2015 (Huttrer, 2001) (Bertani, 2011) (Bertani, 2015).

APPENDIX B

Timeline for a geothermal project

There is several phases in a geothermal development from preliminary survey to a operating power plant. The steps can be seen in figure B.1.

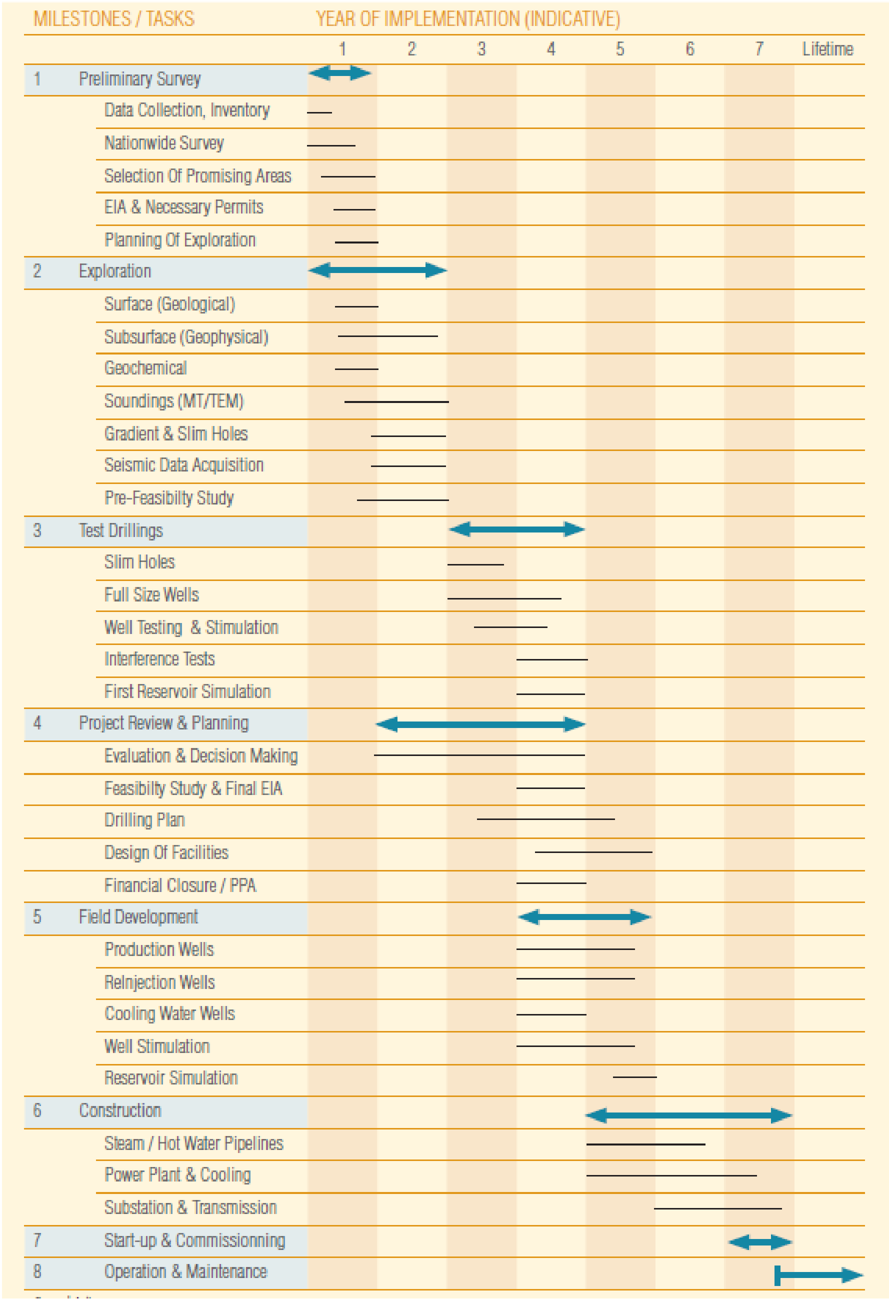

Figure B.1: Timeline for a geothermal project for a unit of 50 MW_e (Gehringer and Loksha, 2012).

Cooling tower model

The cooling tower model is based on an air cooled cooling tower as mentioned in chapter 5 and 6, and is based on Serth and Lestina (2014) if nothing else is mentioned. The cooling tower model is modelled as in figure C.1.

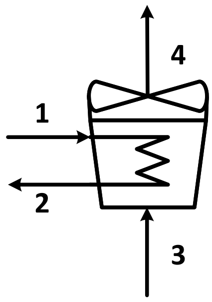

Figure C.1: Illustration of a dry induced cooling tower .

The input parameter there is fixed in every cooling tower as given in table C.1.

C.1 Cooling tower dimensions

The temperature on the air side is the ambient temperature, which is set to 5°C which is the average temperature of Iceland (Einarsson, 2008). The temperature in and out on the water side has been found in the model for the condenser and the temperature after the fans is determined to be 5°C lower than the inlet temperature of the the cooling water (Serth and Lestina, 2014), therefore:

$$T_1 = T_{cond,o} \tag{C.1}$$
$$T_2 = T_{cond,i} \tag{C.2}$$
$$T_3 = T_{amb} = 5°\mathrm{C} \tag{C.3}$$
$$T_4 = T_1 - 5°\mathrm{C} \tag{C.4}$$

The first step in the model is to find the total mass flow of the air through the fans. Here

Fixed input		
Outer diameter of of tubes	$\mathrm{d_o}$	51 mm
Distance to edge of cooling tower	$\mathrm{D_{edge}}$	0.5 mm
Tube pitch ($\mathrm{D_o} \cdot 4$)	p	85 mm
Fin height	b	16 mm
Number of fins per meter	$\mathrm{N_{fin}}$	400
Fin thickness	τ_{fin}	0.3 mm
Overall heat transfer coefficient	U	36.88 W/(m^2· K)
Fan efficiency	η_{fan}	0.7

Table C.1: The parameter which is fixed in very cooling tower it has been assumed that the heat transferred from the cooling water is absorbed by the air and the mass flow can thereby be found by equation C.6.

$$\dot{Q} = \dot{m}_1 \cdot c_{p,CW} \cdot (T_1 - T_2) \tag{C.5}$$

$$\dot{m}_3 = \frac{\dot{Q}}{c_{p,air} \cdot (T_4 - T_3)} \tag{C.6}$$

To find the required power to the fans the pressure drop across the fans has to be determined. To determine the pressure drop the area which the air has to go through is found by equation C.7.

$$A_{face} = \frac{\dot{V}}{v_{std}} \tag{C.7}$$

where:			
	A_{face}	Face area of the cooling tower	(m^2)
	$\dot{V}$	Volumetric flow	(m^3/s)
	v_{std}	Standard velocity	(m/s)

The standard velocity is estimated to be 3 m/s based on Serth and Lestina (2014). The face area is also defined as the width of the tube bundle multiplied by the length of the tubes, equation C.8. The length of the tubes is established to be 3 times the width of the tube bundle.

$$A_{face} = L \cdot B = 3 \cdot B^2 \tag{C.8}$$

where:			
	B	Width of the tube bundle	(m)
	L	Length of the tubes	(m)

The number of tubes beside each other in one row can now be determined:

$$N_{t/r} = B/p \tag{C.9}$$

where:			
	$N_{t/r}$	Number of tubes per row	(-)

In the cooling tower the tubes are placed in layers, there will be 6 layers as suggested in Serth and Lestina (2014). Therefore the total heat transfer area is as given in equation C.10

$$A_{tot,tubes} = N_{rows} \cdot N_{t/r} \cdot L \cdot A_{spec} \tag{C.10}$$

where:			
	N_{rows}	Number of rows	(-)
	A_{spec}	Specific area of the tubes	(m^2/m)

As the pressure drop highly depend on the velocity though the smallest gap between the tubes, this is found by equation C.12 and will have the highest velocity in the cooling tower.

$$A_{small} = L \cdot N_{t/r} \cdot (p - (d_o + 2 \cdot \tau_{fin}) \tag{C.11}$$

$$v_{air} = \frac{\dot{V}}{A_{small}} \tag{C.12}$$

where:	τ_{fin}	Fin height	(m)
	A_{small}	Free gas area	(m^2)

C.2 Pressure drop and power

Now the pressure drop can be determine with equation C.13

$$\Delta P = \frac{v_{air}^2}{2} \cdot \rho_{air} \cdot f \cdot N_{rows} \tag{C.13}$$

where the friction factor f, is based on Ganguli as in equation C.14

$$f = \left(1 + \frac{2e^{-a/4}}{1+a}\right) \cdot \left(0.021 + \frac{27.2}{Re_{eff}} + \frac{0.29}{Re_{eff}^{0.2}}\right) \tag{C.14}$$

where:

$$a = \frac{p - (d_o + 2 \cdot \tau_{fin})}{d_o} \tag{C.15}$$

$$Re_{eff} = Re \cdot \frac{\ell}{b} \tag{C.16}$$

where:	Re_{eff}	Effective Reynolds number	(-)
	ℓ	Fin spacing	(m)
	b	Fin height	(m)

When the pressure drop is found for a cooling tower the dimensions of the cooling tower is found to validate whether this seems reasonable. The velocity and pressure drop is known however the total number of tubes is unknown. The total number of tubes depends on the width of the cooling tower and the pitch of the tubes. The width and the length of the tube bundle can be redefined as equation C.17 and C.18 respectively.

$$W = (N_{t/r} - 1) \cdot p + 2 \cdot d_{edge} \tag{C.17}$$

$$L = 3 \cdot B = 3 \cdot ((N_{t/r} - 1) \cdot p + 2 \cdot d_{edge}) \tag{C.18}$$

To find the total number of tubes per row the total area between the tubes needs to be calculated. This is done by the velocity through the cooling tower which will be where there are no tubes, equation C.19. To find this area the mass flow of the air needs to be determined, this is done with equation C.6.

$$A_{free} = \frac{\dot{m}_3}{\rho_{air} \cdot v_{air}} \tag{C.19}$$

Another way of writing the total area between the tubes are

$$A_{free} = A_{face} - A_{tubes} \tag{C.20}$$

These two areas are depending on the width and the length of the tubes by eqaution C.21 and C.22 respectively.

$$A_{face} = B \cdot L = 3B^2 \tag{C.21}$$
$$A_{tubes} = N_{t/r} \cdot L \cdot p \cdot 1.1 \tag{C.22}$$

Combining equation C.17, C.18, C.21 and C.22, the total number of tubes can be found. When the total number of tubes is found the width and thereby also the length of the cooling tower can be determine:

$$W = N_{t/r} \cdot p \tag{C.23}$$
$$L = 3 \cdot B \tag{C.24}$$

When the dimensions of the the cooling tower is found the number of cooling towers can be determined by finding the required area for the heat transfer by using equation C.25, while the heat transfer area in one cooling tower (A_{CT}) is found by equation C.26.

$$A_{req} = \frac{\dot{Q}}{U \cdot \Delta T_{LMTD}} \tag{C.25}$$
$$A_{CT} = N_{t/r} \cdot L \cdot N_{rows} \cdot A_{spec} \tag{C.26}$$

where:			
	A_{CT}	Area of one cooling tower	(m^2)

The overall heat transfer coefficient (U) has been set to 36.88 W/($m^2 \cdot$ K), based on Serth and Lestina (2014), it has been assumed that the overall heat transfer coefficient does not change. The number of cooling tower is found by dividing the required area with the area for one cooling tower.

The total power required for a cooling tower is thereby found with equation C.27

$$W_{fan} = \frac{\Delta P \cdot \dot{V}_{fan}}{\eta_{fan}} \cdot N_{CT} \tag{C.27}$$